NASA TECHNICAL TRANSLATION

NASA TT F-786

NASA TT F-786

(NASA-TT-F-786) METEOROLOGICAL INTERPRETATION OF SPACE PHOTOGRAPHS OF THE EARTH (QUANTITATIVE METHODS) (Linguistic Systems, Inc., Cambridge, Mass.) 143 p HC $5.75 CSCL 04B H1/47

N75-18849

Unclas 12356

METEOROLOGICAL INTERPRETATION OF SPACE PHOTOGRAPHS OF THE EARTH (QUANTITATIVE METHODS)

D. M. Sonechkin

Hydrometeorological Press
Leningrad, 1972

NATIONAL AERONAUTICS AND SPACE ADMINISTRATION • WASHINGTON, D. C. • FEBRUARY 1975

1. Report No.	2. Government Accession No.	3. Recipient's Catalog No.
NASA TT F- 786		

4. Title and Subtitle	5. Report Date
METEOROLOGICAL INTERPRETATION OF SPACE PHOTOGRAPHS OF THE EARTH (QUANTITATIVE METHODS)	February 1975
	6. Performing Organization Code
7. Author(s)	8. Performing Organization Report No.
D.M. Sonechkin	
	10. Work Unit No.
9. Performing Organization Name and Address	11. Contract or Grant No.
LINGUISTIC SYSTEMS, INC. 116 AUSTIN STREET CAMBRIDGE, MASSACHUSETTS 02139	NASW-2482
	13. Type of Report & Period Covered
	TRANSLATION
12. Sponsoring Agency Name and Address	
NATIONAL AERONAUTICS AND SPACE ADMINISTRATION WASHINGTON, D.C. 20546	14. Sponsoring Agency Code

15. Supplementary Notes

Translation of: "Meteorologicheskoye Deshifrirovaniye kosmicheskikh Snimkov Zemli (Kolichestvennyye Metody), Leningrad, Hydrometeorological Press, 1972, pp 1-130.

16. Abstract

The work is devoted to a systematic exposition of the procedures and results of meteorological interpretation of television and infra-red images of the earth, obtained with the aid of satellites. Main attention is devoted to quantitative methods. Modern techniques of patter recognition as the methodical basis of quantitative interpretation of earth photographs are surveyed. A considerable portion of the monograph is based on the author's own investigations. Other Soviet and foreign acheivements in the considered field of satellite meteorology are also systemized.

The work is intended for specialists in the field of satellite meteorology, as well as all those who are interested in the applications of static methods in meteorology.

17. Key Words (Selected by Author(s))	18. Distribution Statement
	UNCLASSIFIED - UNLIMITED STAR Category 20

19. Security Classif. (of this report)	20. Security Classif. (of this page)	21. No. of Pages	22. Price
UNCLASSIFIED	UNCLASSIFIED	142	$5.75*

*For sale by the National Technical Information Service, Springfield, Virginia 22151

TABLE OF CONTENTS

Introduction

The main means of obtaining meteorological data with the aid /3
of artificial earth satellites is presently television (TV) surveying carried out in the visible and infrared (IR) regions. In meteorological interpretation of TV and IR images, it is possible to obtain data on the nature of the cloud cover in various geographical regions, and, indirectly, taking into account that cloud cover is a unique indicator of the state of the atmosphere, it is also possible to obtain an idea on the type of synoptic processes for the corresponding sections of the atmosphere and even values of individual meteorological elements (wind, atmospheric humidity, etc.).

The main stage of meteorological interpretation of TV and IR images is recognizing clouds and open sections of the earth's surface on photographs with subsequent determination of cloud cover characteristics: their number, predominant forms, and meso- and macrostructures. The interpretation procedure includes the technical operations of sorting the photographs, time and geographic control matching of them, as well as mapping the results of interpretation in the form of charts (nephanalysis).

Nephanalysis is presently carried out manually. Automated elements are encountered only when performing the technical operations indicated above. With respect to the main operation—recognition of cloud cover—it is accomplished by visual inspection of the TV and IR photographs by a meteorologist interpreter. The enormous and continuously increasing volume of incoming meteorological satellite TV and IR photographs, with the necessity of processing them within extremely compressed deadlines, leads to a reduction in the quality of visual nephanalysis. Its subjectivism is great. Nephanalyses performed by different meteorologist interpreters are hard to compare. The presence of appreciable errors in nephanalysis due to slips of the pen, etc., is typical.

In this regard, objectification and automation of all processing and interpretation of photographs to reduce the number of personnel engaged in this work, to reduce processing time, to eliminate the gross errors of nephanalysis, and to standardize its results are of interest. In posing this problem, one should take into ac- /4
count that the mechanism of visual perception and recognition of patterns by man is extremely complicated and has been barely studied. It is presently difficult to count on modelling of this mechanism in its entirety with the aid of some technical facilities. During the first stage it is feasible to investigate the theoretical possibilities of creating an automated system for processing and analysis of TV and IR photographs coming from meteorological satellites. Proof of the possibility of even partial solution of this

problem would be a major achievement, because the "objectivity" of machine nephanalysis and the fact that cover data are immediately distributed in the computer storage in an ordered form in a specific manner indicate that the main beneficiary of such nephanalysis would be numerical analysis schemes and weather forecasting. With respect to synoptic methods, especially for purposes of regional and local weather forecasting, machine nephanalysis can probably compete with visual analysis in this field to a limited extent.

The given paper summarizes four years of research into the possibilities of utilizing satellite TV photographs of the earth for tracking cloud cover. These investigations included the following main stages:

- study of the space-time variability of cloud cover to determine the requirements on the satellite system for tracking the earth's cloud cover and for analyzing the quality of satellite data on cloud cover;

- analysis of TV equipment as a means of tracking cloud cover from space;

- development of techniques for visual interpretation of cloud cover from TV and IR photographs of the earth;

- investigation of the possibilities of automated processing and analysis of TV and IR photographs.

The main method of investigation was mathematical-statistical. The abundant experience accumulated in aerial surveying was used in developing techniques of visual interpretation. New mathematical equipment for pattern recognition was employed to solve the problem of automating interpretation.

Besides the author, I. S. Solov'yeva, L. M. Soskin, and V. V. Rožanov, colleagues of the Department of Investigations on Satellite Meteorology of the Hydrometcenter of the USSR, participated in the investigation. Results obtained by colleagues of the Hydrometcenter of the USSR L. G. Mizina, M. G. Nayshuler, V. I. Solov'yev, I. S. Khandurova, and T. A. Yakovleva, as well as my students of the Department of Meteorology and Climatology of the Faculty of Geography of Moscow State University, were used in some sections of the investigation. The author expresses deep gratitude to all of them.

Chapter 1
TELEVISION SURVEYING OF THE EARTH'S CLOUD COVER FROM SPACE

1. The Television Equipment of Meteorological Satellites /5*

The sources of meteorological data of observation of the earth from space are spatial, temporal, and angular variations of radiation intensity, reflected or emitted by the earth-atmosphere system in different regions of the electromagnetic spectrum. Technically, the simplest and most physically descriptive method of using these data is tracking of cloud cover by qualitative recording of the spatial variations of reflected solar radiation intensity in the visible region of the spectrum, where the amount of radiation energy is sufficiently great to record comparatively small-scale inhomogeneities of the radiation field with an acceptable signal-to-noise ratio. The possibility itself of detecting cloud cover is related in this case to the fact that the more significant brightness contrasts in the reflected radiation field are usually related to the edges of clouds and the open sections of the earth's surface.[1] Of course, brightness differentiation of the clouds themselves, and in particular of the open sections of the earth's surface, may be just as great, and sometimes even greater. Therefore, reliable recognition of clouds on the background of the earth's surface is related to use of the structure (pattern) of the brightness homogeneities of the reflected radiation field as a recognition feature. Hence, the desire to track as many as possible of the small details of the radiation field is understandable.

In order to track cloud cover on the earth's night side, it is preferable to employ measurements of the earth's thermal radiation intensity in those spectral ranges where the cloudless atmosphere has a comparatively negligible effect in transforming the radiation traveling upward from the earth's surface and cloud tops. /6 Since the amount of energy in this case is much less than when using the visible portion of the daytime spectrum, small-scale details of the radiation field are lost in noise and only sufficiently large cloud formations can be successfully recorded.

Unlike the case of daytime cloud surveying in the visible range, the possibility of detecting clouds in thermal surveying is

---

*Numbers in the righthand margin indicate pagination of foreign text.

[1]Here and henceforth, when speaking about the "edge of clouds and open sections of the earth's surface", we will have in mind the boundary between the images of these objects on the photograph.

related to the fact that comparitively large thermal contrasts are associated with the boundary between a cloud and the earth's open surface [28,34].

Radiometers, photographic cameras, and television cameras are suitable as instruments for recording the variation of the reflected radiation field. The cloud cover pattern may be inspected directly by the observer meteorologist onboard the spacecraft or orbital station. Since daily tracking of cloud cover over large areas is required for operational purposes, and since these data also should be delivered to the forecasting centers within short deadlines, the most suitable of the enumerated observation facilities are radiometers and television cameras. Photographic surveying of clouds from space may be exceptionally useful for scientific research purposes, since the number of space photographic images of the earth is practically limited, and those which are obtained are not of operational use when delivered to the forecasting centers.

Attempts to track cloud cover were the first meteorological experiments conducted in space [112,116,128,132]. However, substantial results were obtained only after launching of the Tiros satellite in 1960 [121] which carried two transmitting TV cameras. Subsequently, onboard television cameras for daytime cloud surveying became standard equipment on meteorological satellites. The technical parameters of the camera itself and its optical system naturally changed as experience was accumulated in meteorological interpretation of the images obtained and in development of space television techniques (Table 1). Thus, now with the transmitting TV cameras, which perform continuous tracking of cloud cover over large areas (the world's first experiment of this type was carried out in 1966 on the Molniya-1 satellite [11,73]), mechanical television systems are employed on satellites, i.e., those devices in which a photomultiplier having a small angle of view corresponding to a single element of the photograph is used instead of a transmitting TV camera, and a complete photograph is obtained by mechanical shifting of the photomultiplier with respect to the observed region of the earth (image scanning) [169].

Mechanically scanning television systems are also used in Soviet and U.S. meteorological satellites to track cloud cover on the earth's night side by its thermal emission in the infrared region of the spectrum [10,21,22].

The Soviet Union and United States now regularly launch mete- /7
orological satellites for operative tracking of cloud cover with the aid of television surveying in the visible and infrared regions (the Meteor, ESSA, and NOAA systems). The Cosmos and Nimbus meteorological satellites, designed for scientific research purposes, are also equipped with television cameras. A list of all satellites

launched up to the present and equipped with television systems for tracking cloud cover is presented in Tables 1 and 2.

Let us consider those characteristics of the television systems of meteorological satellites which determine the quality of the cloud cover images obtained. The main parts of such systems are: the onboard equipment, including the optical head, the photoelectric converter (photomultiplier, bolometer, or transmitting TV camera), devices for amplification and conversion of the electrical signal, often but not compulsory a block for intermediate collection of data onboard the satellite, a radio transmitter, a ground system including a radio receiver, devices for amplification and conversion of the electrical signal, a photorecorder, and facilities for photochemical processing of the results of recording the television pictures. In addition, the ground portion includes equipment for storage of the electrical signal on magnetic tape, video monitoring devices, and facilities for the main parts of the ground television equipment (Fig. 1).

The luminous flux impinging from the observed object on the receiver portion of the photoelectric converter is projected with the aid of the optical head; in this case two essentially different approaches to solution of this problem may be distinguished: frame-by-frame and element-by-element projection.

In the first case (Fig. 2) an objective with an angle of view sufficient for simultaneous projection of an image of a rather large section of the earth's cloud cover onto the photoelectric converter is used as the optical head. The shape and dimensions of the section may be different depending on what kind of cloud formations (large- or small-scale) are being studied on the photograph; for operational purposes an attempt is usually made to increase the area of this section to thousands of kilometers in cross-section, and its shape is assumed to be square for optimum use of the capabilities of the photoelectric converter, which in frame-by-frame projection is a transmitting television camera having a circular receiving part. The set of sequential frames provides a representation of the cloud cover distribution along the flight path of the satellite.

In the second case (Fig. 3) the objective or the device replacing it has such a small angle of view (usually about 1° or less) that at each moment of time the photoelectric converter, which is a photomultiplier or bolometer, can respond only to medium radiation intensity within the range of the angle of view of the optical /9
head. The image of the entire observed section of cloud cover is formed by visual inspection of it during scanning.

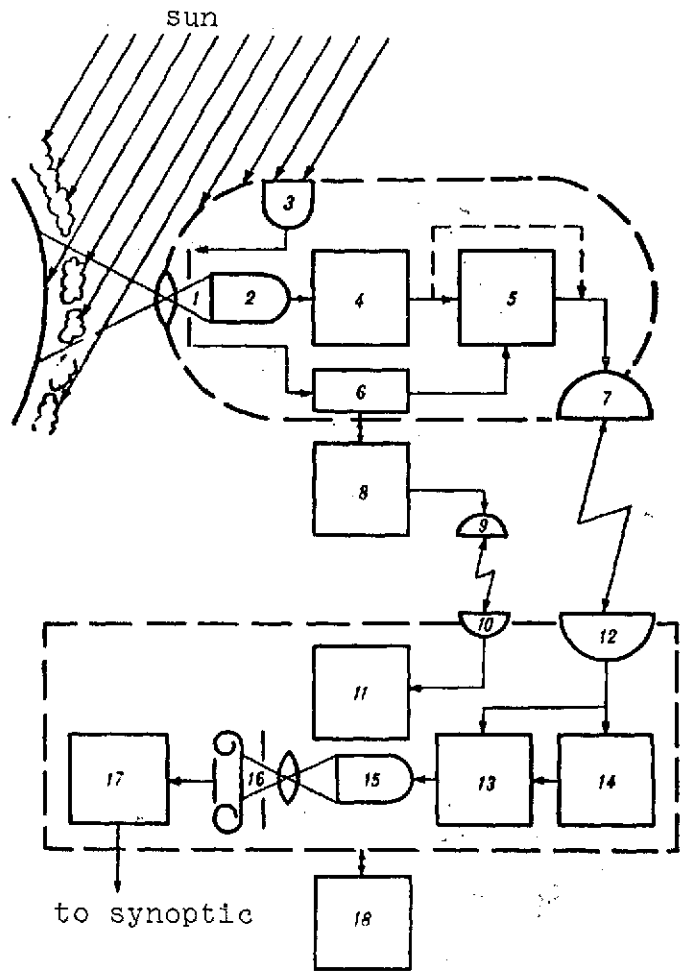

Fig. 1. Schematic block diagram of a television system designed for tracking cloud cover from a meteorological satellite.

Onboard equipment: 1- optical head, 2- photoelectric converter, 3- solar elevation and satellite space orientation sensor, 4- devices for amplification and conversion of the TV signal, 5- device for intermediate storage of data onboard the satellite, 6- device for recording the times of surveying and functioning of the onboard TV equipment, 7- radio transmitter, 8- device for control and monitoring of onboard equipment operation, 9- radio transceiver. Group equipment: 10- radio transceiver, 11- device for monitoring and programming the operation of the onboard TV equipment, 12- radio receiver, 13- devices for amplification and conversion of the TV signal, 14- device for intermediate storage of data, 15- photoelectric converter, 16- photorecorder, 17- photochemical processor, 18- devices for monitoring and adjusting of ground TV equipment.

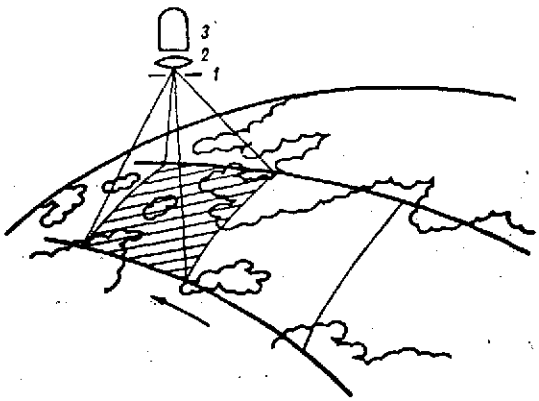

Fig. 2. Diagram of television tracking of cloud cover in frame-by-frame surveying.

1- shutter, 2- objective, 3- transmitting TV camera.

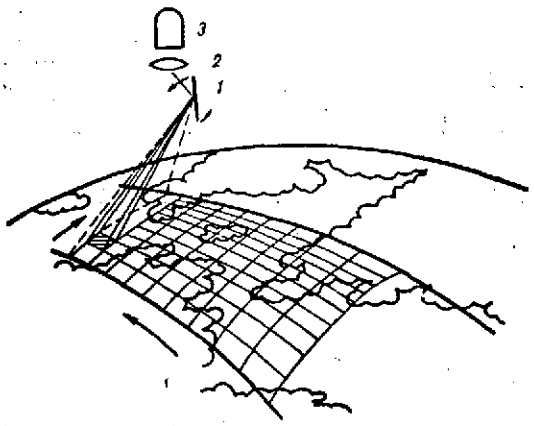

Fig. 3. Diagram of television tracking of cloud cover in element-by-element surveying.

1- tilting (rotating) mirror, 2- objective, 3- photomultiplier (bolometer).

The photoelectric converter (transmitting television camera, photomultiplier, or bolometer) is the most important integral part of the television system, which determines to a great extent the qualitative indices of the photographs obtained. If a television camera is used, the process of generating the electrical signal, /20 characterizing the image (the video signal), consists of the following stages [10,55].

Table 1. U.S. satellites launched to track cloud cover with the aid of television systems.

Name of satellite	Launch date	Altitude, km		Orbital inclination, deg.	Orbiting period, min.	Spectral sensitivity, μm
		apogee	perigee			
Vanguard-II	17 Feb. 1959	3380	628	32	-	-
... The Tiros scientific research series ...						
Tiros-1	1 April 1960	740	695	48.4	99.0	0.5-0.75
Tiros-2	23 Nov. 1960	730	628	48.5	98.0	0.5-0.75
Tiros-3	12 July 1961	817	740	47.9	100.0	0.5-0.75

Table 1 (continued)

Type of sensor	Television system parameters: terrain resolution in scheduled surveying, km^2	terrain coverage in scheduled surveying, km^2	total width of terrain coverage strip in scheduled surveying, km	operating mode (direct transmission - DT, with storage - ST)	Remarks
2 photo-elements	-	-	-	DT	Scanning was achieved by rotating the satellite around one axis. The actual orientation of the satellite differed from the calculated orientation; therefore it was impossible to reproduce the cloud cover pattern on the basis of the measurements.
... The Tiros scientific research series ...					
1 vidicon	3x3	1800x1800	1800	DT-ST	The satellite was oriented by rotation around a single axis, which was directed along the earth's radius, when the satellite is passing over at 30° north latitude. The optical axes of the cameras are aligned along the rotational axis, due to which surveying at the nadir was carried out in the region of 30° north latitude and was perspective to the north and south. Some of the frames showed the earth's horizon. Surveying was carried out in a series of 32 frames each by only one camera or alternately by both cameras.
1 vidicon	0.3x0.3	180x180	180	DT-ST	
1 vidicon	3x3	1800x1800	1800	DT-ST	
1 vidicon	0.3x0.3	180x180	180	DT-ST	
1 vidicon	3x3	1800x1800	1800	DT-ST	The satellite was designed for detection of tropical cyclones; therefore, it was equipped with two identical TV cameras to increase the operational lifetime. Surveying was conducted in a series of 48 frames each.
1 vidicon	3x3	1800x1800	1800	DT-ST	

Table 1 (continued)

Name of satellite	Launch date	Altitude, km		Orbital inclination, deg.	Orbiting period, min.	Spectral sensitivity, μm
		apogee	perigee			
Tiros-4	8 Feb. 1962	844	710	48.3	100.0	0.5-0.75
Tiros-5	19 June 1962	970	592	58.1	100.0	0.5-0.75
Tiros-6	18 Sept. 1962	710	685	58.3	99.0	0.5-0.75
Tiros-7	19 July 1963	647	621	58.2	97.0	0.5-0.75
Tiros-8	21 Dec. 1963	750	703	58.5	99.0	0.5-0.75
Tiros-9	22 Jan. 1965	2579	701	96.4	119.0	0.5-0.75

Table 1 (continued)

Television system parameters					
Type of sensor	terrain resolution in scheduled surveying, km^2	terrain coverage in scheduled surveying, km^2	total width of terrain coverage strip in scheduled surveying, km	operating mode (direct transmission - DT, with storage - ST)	Remarks
1 vidicon	3x3	1800x1800	1800	DT-ST	A camera with intermediate terrain coverage was designed to solve the problem of selecting the optimum parameters of the television equipment for meteorological satellites.
1 vidicon	1.6x1.6	900	900	DT-ST	
1 vidicon	3x3	1800x1800	1800	DT-ST	
1 vidicon	1.6x1.6	900	900	DT-ST	
1 vidicon	3x3	1800x1800	1800	DT-ST	
1 vidicon	1.6x1.6	900	900	DT-ST	
1 vidicon	3x3	1800x1800	1800	DT-ST	
1 vidicon	3x3	1800x1800	1800	DT-ST	
1 vidicon	3x3	1800x1800	1800	ST	Tests of the TV equipment for direct transmission of photographs to simplified ground receiving terminals (APT).
1 vidicon	2x2	1100x1100	1100	DT	
1 vidicon	3x3	1800x1800	1800	ST	Testing of a new system of orientation of rotation around an axis directed perpendicular to the orbital plane. The axes of the TV cameras were directed perpendicular to the rotational axis, so that the scheduled photographs of the cloud could be made alternately. The satellite's orbit was heliosynchronous, i.e., the satellite passes over every point on the earth at the same time of day. Tiros-9 was the prototype of the operational ESSA satellites. The orbit is uncalculated.
1 vidicon	3x3	1800x1800	1800	ST	

Table 1 (continued)

Name of satellite	Launch date	Altitude, km		Orbital inclination, degree	Orbiting period, min.	Spectral sensitivity, μm
		apogee	perigee			
Tiros-10	1 July 1965	834	739	98.6	101.0	0.5-0.75
... ESSA operational series ...						
ESSA-1	3 Feb. 1966	838	699	97.9	100.2	0.5-0.75
ESSA-2	28 Feb. 1966	1411	1353	101.4	113.5	0.5-0.75
ESSA-3	2 Oct. 1966	1485	1383	101.1	114.6	0.5-0.75
ESSA-4	26 Jan. 1967	1439	1323	102.0	113.4	0.5-0.75

Table 1 (continued)

Television system parameters					
Type of sensor	terrain resolution in scheduled surveying, km^2	terrain coverage in scheduled surveying, km^2	total width of terrain coverage strip in scheduled surveying, km	operating mode (direct transmission - DT, with storage - ST)	Remarks
1 vidicon	3x3	1800x1800	1800	ST	Launching of the ESSA prototype into the calculated orbit
1 vidicon	3x3	1800x1800	1800	ST	
	... ESSA operational series ...				
2 vidicons	3.5x3.5	2800x2800	2800	ST	The axes of the alternately operating (every 260 s) TV cameras are aligned at an angle of 26.5° from the nadir to the right and left of the flight path of the satellite at the moment of surveying. The satellite is heliosynchronous and was designed for collection of global data on cloud cover. 12 photos are taken per orbit.
2 vidicons	4.0x4.0	3350x3350	3350	DT	A satellite for direct transmission of cloud cover photographs to simplified receiving stations located at any point on earth. Alternately operating TV cameras (at an interval of 352 s) provide overlapping surveying which permits stereoscopic processing. Each ground station may receive 3 sequential photos during 1 revolution. Photos may be received from 3 sequential revolutions in mean latitudes.
2 vidicons	2.4x2.4	1900x1900	3300	ST	
2 vidicons	4x4	3350x3350	3350	DT	

Table 1 (continued)

Name of satellite	Launch date	Altitude, km		Orbital inclination, deg.	Orbiting period, min.	Spectral sensitivity, μm
		apogee	perigee			
ESSA-5	20 April 1967	1475	1382	101.9	113.5	0.5-0.75
ESSA-6	10 Nov. 1967	1484	1406	102.0	114.8	0.5-0.75
ESSA-7	16 Aug. 1968	1470	1430	101.7	114.9	0.5-0.75
ESSA-8	5 Jan. 1968	1461	1413	101.9	114.6	0.5-0.75
ESSA-9	26 Feb. 1969	1506	1421	101.8	115.2	0.5-0.75
... Nimbus scientific research series ...						
Nimbus-1	28 Aug. 1964	933	430	98.3	98.6	0.5-0.75 0.5-0.75 3.7-4.2
Nimbus-2	15 May 1966	1113	1108	98.0	108.1	0.5-0.75 0.5-0.75 3.7-4.20
Nimbus-3	14 April 1969	1113	1108	99.9	107.4	0.5-0.75 0.5-0.75 3.7-4.20
Nimbus-4	8 April 1970	1108	1092	99.9	107.2	0.5-0.75 0.5-0.75 3.7-4.20

Table 1 (continued)

Television system parameters					
Type of sensor	terrain resolution in scheduled surveying, km	terrain coverage in scheduled surveying, km^2	total width of terrain coverage strip in scheduled surveying, km	operating mode (direct transmission--DT, with storage--ST)	Remarks
2 vidicons	2.4x2.4	1900x1900	3300	ST	
2 vidicons	4x4	3350x3350	3350	DT	
2 vidicons	2.8x2.8	1900x1900	3300	ST	
2 vidicons	4x4	3350x3350	3350	DT	
2 vidicons	4x4	3350x3350	3350	DT	
	... Nimbus scientific research series ...				
3 vidicons	0.8x0.8	750x750	2500	ST	A satellite with 3-axis orientation (the accuracy of orientation is ±1° in roll and pitch, ±2° in yaw), an improved system of 3 simultaneously operating TV cameras for scheduled surveying of a strip whose width is adequate for solid coverage of the earth without breaks between adjacent revolutions. The satellite is heliosynchronous. Equipment was tested for nighttime surveying of clouds in the near infrared "transparency window". The orbit is uncalculated.
1 vidicon	3.5x3.5	2500x2500	2500	DT	
1 radiometer	7x7		2400	DT-ST	
3 vidicons	0.8x0.8	750x750	2500	ST	
1 vidicon	3.5x3.5	2500x2500	2500	DT	
1 rad.	7x7	-	2400	DT-ST	
3 vidicons	0.8x0.8	750x750	2500	ST	
1 vidicon	3.5x3.5	2500x2500	2500	DT	
1 rad.	7x7	-	2400	DT-ST	
3 vidicons	0.8x0.8	750x750	2500	ST	
1 vidicon	3.5x3.5	2500x2500	2500	DT	
1 radiometer	7x7	-	2400	DT-ST	

Table 1 (continued)

Name of satellite	Launch date	Altitude, km		Orbital inclination, deg.	Orbiting period, min.	Spectral sensitivity, μm
		apogee	perigee			
	...ATS scientific research series...					
ATS-1	6 Dec. 1966	36,888	35,880	0.23	1446	0.5-0.75
ATS-2	6 April 1967	11,180	186	28.4	220	0.5-0.75
ATS-3	5 Nov. 1967	35,880	35,772	0.4	1440	Color pictures (blue, yellow, red) 0.5-0.75

Table 1 (continued)

Type of sensor	Television system parameters: terrain resolution in scheduled surveying, km²	terrain coverage in scheduled surveying, km²	total width of terrain coverage strip in scheduled surveying, km	operating mode (direct transmission--DT, with storage--ST)	Remarks
... ATS scientific research series ...					
1 radiometer	3x3	30% of the earth's surface	-	DT	The satellite is geosynchronous and stationary above the equator at 151° W longitude. Scanning is accomplished by rotation of the satellite (line scanning) and by rotation of a mirror in the radiation sensor (frame scanning), the image of the earth's entire visible disc is obtained within 22 min., and the frames continuously overlap each other, which makes it possible to observe the motion and evolution of clouds.
1 vidicon	0.9x0.9	900x900	-	DT	A satellite with 3-axis orientation in an intermediate altitude orbit. The actual orbit is uncalculated.
1 vidicon	18x18	the entire visible disc of the earth	-	DT	
1 radiom.	3.5x3.5	30% of the earth's surface	-	DT	The geosynchronous satellite is located at 57° W longitude and is equipped with a mechanically scanning TV with 3 light filters for spectrozonal surveying, which essentially makes it possible to estimate the altitude of clouds. One color photograph is made every 28 min. Surveying is carried out continuously all day. The TV camera (dissector) is used to transmit the cloud images to the simplified ground station.
1 dissector	6.2x6.2	3000x3000	-	DT	

Table 1 (continued)

Name of satellite	Launch date	Altitude, km		Orbital inclination, deg.	Orbiting period, min.	Spectral sensitivity, μm
		apogee	perigee			
ATS-4	24 July 1968	787	218	29.0	94.6	0.5-0.75
ATS-5	12 Aug. 1969	36,894	35,760	2.6	1463.8	0.5-0.75
Aitos-1	23 Jan. 1970	1476	1432	101.8	115.2	0.5-0.75 0.5-0.75 10.0-11.0
NOAA-1	11 Dec. 1970	1472	1422	101.9	114.8	0.5-0.75 0.5-0.75 10.0-11.0

Table 1 (continued)

Television system parameters					Remarks
Type of sensor	terrain resolution in scheduled surveying, km²	terrain coverage in scheduled surveying, km²	total width of terrain coverage strip in scheduled surveying, km	operating mode (direct transmission--DT, with storage--ST)	
1 dissector	6.2x6.2	3000x3000	-	DT	A satellite with 3-axis orientation. The launch was unsuccessful.
1 dissector	6.2x6.2	3000x3000	-	DT	Quasi-geosynchronous satellite with 3-axis orientation.
2 vidicons	3x3	3300x2200	3300	DT	New operational satellite with 3-axis orientation (with an accuracy of ±1°), designed for collection of data on cloud cover on a global scale and to serve local users at simplified ground stations. In the DT and ST modes 11 TV photographs with 30% overlapping are made during each revolution. Infrared surveying is carried out both day and night.
2 vidicons	3x3	3300x3300	3300	ST	
1 radiometer	3x3 (daytime) 6x6 (night)	-	4000	DT-ST	
2 vidicons	3x3	3300x2200	3300	DT	The same.
2 vidicons	3x3	3300x3300	3300	ST	
1 radiometer	3x3 (daytime) 6x6 (night)		4000	DT-ST	

Table 2. Soviet satellites launched for tracking cloud cover with the aid of television systems.

Name of satellite	Launch date	Altitude, km		Orbital inclination, deg.	Orbiting period, min.	Spectral sensitivity, μm
		apogee	perigee			
Molniya-1	18 May 1966	39,300	538	65	720	visible
The Cosmos scientific research series						
Cosmos-122	25 June 1966	625		65	97.1	visible 8-12
Cosmos-144	28 Feb. 1967	636	604	81.2	96.9	visible 8-12

Table 2 (continued)

Television system parameters					Remarks
Type of sensor	terrain resolution in scheduled surveying, km^2	terrain coverage in scheduled surveying, km^2	total width of terrain coverage strip in scheduled surveying, km	operation mode (direct transmission--DT, with storage--ST)	
1 vidicon	-	-	-	DT	A satellite in a strongly extended elliptical orbit with 3-axis orientation, not specially designed for meteorological observations. The TV camera is equipped with changeable light filters for photographing under various lighting conditions and with 2 changeable objectives which provide coverage of the entire visible disc of the earth over the entire range of orbital altitudes of the satellite. Surveying with the aid of a narrow-angle objective provides a more detailed cloud cover pattern. The resolution of the images is about 20x20 km^2. Surveying may be carried out continuously for several hours while the satellite is located in the zone of radiovisibility of the ground receiving station. The surveying mode may be changed by operational commands from the ground station. The experiment was carried out only on Molniya-1 launched on 18 May 1966.
The Cosmos scientific research series					
2 vidicons	1.25x1.25		840	ST	The Cosmos-122 satellite was the prototype for the Meteor satellite system with 3-axis orientation (±1°), two alternately operating TV cameras track daytime cloud cover, and the mechanically scanning radiometer is used for surveying clouds day and night.
1 radiom.	15x15		1000	ST	
2 vidicons	1.25x1.25	480x480	960	ST	
1 radiometer	15x15	-	1100	ST	

Table 2 (continued)

Name of satellite	Launch date	Altitude, km		Orbital inclination, deg.	Orbiting period, min.	Spectral sensitivity, μm
		apogee	perigee			
Cosmos-149	21 March 1967	297	248	48.8	89.9	visible
Cosmos-156	27 April 1967	635	593	81.2	97.1	visible 8-12
Cosmos-184	25 Oct. 1967	635		81.2	97.1	visible 8-12
Cosmos-206	14 March 1968	630	598	81.2	97.1	visible 8-12
Cosmos-226	12 June 1968	650	603	81.2	96.9	visible 8-12
		The Meteor operational system				
Meteor-1	26 March 1969	713	644	81.2	97.9	visible 8-12
Meteor-2	6 Oct. 1969	690	630	81.2	97.7	visible 8-12
Meteor-3	17 March 1970	643	555	81.2	96.4	visible 8-12

Table 2 (continued)

Television system parameters					
Type of sensor	terrain resolution in scheduled surveying, km²	terrain coverage in scheduled surveying, km²	total width of terrain coverage strip in scheduled surveying, km	operation mode (direct transmission--DT, with storage--ST)	Remarks
1 vidicon	0.3x0.3	140x140	140	DT	
2 vidicons	1.25x1.25	480x480	960	ST	The Cosmos-156 satellite, together with the Cosmos-144 comprised the experimental Meteor system, their orbital planes were mutually perpendicular, which makes it possible to track the evolution of cloud cover in separate regions of the earth twice during the day and twice at night at an interval of about 6 hours.
1 radiometer	15x15	-	1100	ST	
2 vidicons	1.25x1.25	480x480	960	ST	
1 radiom.	15x15	-	1100	ST	
2 vidicons	1.25x1.25	480x480	960	ST	
1 radiom.	15x15	-	1100	ST	
2 vidicons	1.25x1.25	480x480	960	ST	
1 radiometer	15x15	-	1100	ST	
The Meteor operational system					
2 vidicons	1.25x1.25	480x480	960	ST	All Meteor satellites are equipped with identical television systems for cloud surveying night and day in the visible and infrared regions similar to the systems of the Cosmos-122, 144, 156, 184, 206, and 226 satellites.
1 radiom.	15x15	-	1100	ST	
2 vidicons	1.25x1.25	480x480	960	ST	
1 radiom.	15x15	-	1100	ST	
2 vidicons	1.25x1.25	480x480	960	ST	
1 radiom.	15x15	-	1100	ST	

Table 2 (continued)

Name of satellite	Launch date	Altitude, km		Orbital inclination, deg.	Orbiting period, min.	Spectral sensitivity, μm
		apogee	perigee			
Meteor-4	28 April 1970	736	637	81.2	98.1	visible 8-12
Meteor-5	23 June 1970	906	863	81.2	102.0	visible 8-12
Meteor-6	15 Oct. 1970	674	633	81.2	97.5	visible 8-12
Meteor-7	20 Jan. 1971	679	630	81.2	97.6	visible 8-12
Meteor-8	17 April 1971	646	620	81.2	97.2	visible 8-12
Meteor-9	16 July 1971	650	618	81.2	97.3	visible 8-12

Table 2 (continued)

Type of sensor	Television system parameters: terrain resolution in scheduled surveying, km^2	terrain coverage in scheduled surveying, km^2	total width of terrain coverage strip in scheduled surveying, km	operational mode (direct transmission--DT, with storage--ST)	Remarks
2 vidicons	1.25x1.25	480x480	960	ST	
1 radiom.	15x15	–	1100	ST	
2 vidicons	1.25x1.25	480x480	960	ST	
1 radiom.	15x15	–	1100	ST	
2 vidicons	1.25x1.25	480x480	960	ST	
1 radiom.	15x15	–	1100	ST	
2 vidicons	1.25x1.25	480x480	960	ST	
1 radiom.	15x15	–	1100	ST	
2 vidicons	1.25x1.25	480x480	960	ST	
1 radiom.	15x15	–	1100	ST	
2 vidicons	1.25x1.25	480x480	960	ST	
1 radiometer	15x15	–	1100	ST	

/27

An electrical potential whose value at each point is related to the illumination intensity of this point by the luminous flux is generated upon exposure on the light-sensitive surface of the television tube. The light-sensitive surface is not ideal in the sense that, first, the potential value is randomly dependent on illumination intensity, secondly, the dependence of the potential on illumination intensity varies over the field of the light-sensitive surface and, third, the values of the potentials created in the vicinity of the point affect the potential value at each point. The signal formed in the transmitting television camera generally has no so-called measuring properties, i.e., the brightness of the corresponding section of the observed object cannot be assessed by the value of this signal. Moreover, there are transmitting television tubes (dissectors) which permit measurement of the brightness of the object in absolute units. They are distinguished by comparatively large dimensions and power consumption, sensitivity and vibrations, and by some other technical deficiencies, which the "vidicon", used on both the Meteor and on the American meteorological satellites, do not have. Therefore, dissectors have not yet /21
been used on operational meteorological satellites. We also note that the transmitting television tubes (orthicons and superorthicons) have such high light sensitivity in the visible region of the spectrum that they may be used for tracking cloud cover on the night side of the earth in moonlight and starlight. A disadvantage of these tubes is the halo surrounding the contrast details of the image. In single-element photoelectric converters, the absoluteness of brightness measurements is considerably easier to provide than in tubes, because there are no distortions in the image field.

The next step in formation of the electrical signal, characterizing the image, is readout of the electric potential from the receiving surface of the tube with the aid of a narrow electron beam. The potential drops on the receiving surface modulate the electron flow, which also leads to formation of a temporal signal characterizing the image. The television image is quantized into lines whose width is determined by the size of the "spot" aperture of the electron beam impinging on the receiving surface during readout. The number of lines per television frame determines the clarity of the received television image at right angles to the lines and with /26
consideration of the area encompassed by the frame on the terrain and its spatial resolution. The signal is usually intermittent within the limits of the line. Moreover, because of the finite dimensions of the aperture of the reading electron beam and "spreading" of the electrical potential on the light-sensitive surface of the tube, image clarity along the line is also limited. However, in some television systems the signal is quantized in the line as well, and sometimes it is also quantized by level. In particular the latter possibility is employed in mechanically scanning infrared

television systems of the Meteor, Nimbus, and Aitos meteorological satellites, where a digital system is used for transmitting the television signal to earth.

In mechanically scanning television systems, the second stage of signal formation, described above for the transmitting tube, is absent, and the electrical current generated in the radiation detector is amplified immediately due to the effects of the impinging radiation, and it is subsequently converted similar to the transformations which occur in the system with a transmitting television camera in the third stage. The purpose of these conversions is to transmit the signal characterizing the image to earth in the maximum undistorted form and to ensure reconstruction of the image from this signal in the ground portion of the system.

2. The Main Qualitative Indices of the Television Image

The possibilities of meteorological interpretation of television images of the earth, obtained with the aid of meteorological satellites, are determined by the degree of agreement of these images /27
to their original, which in turn depends on the parameters of the television equipment used. Essentially, the capabilities of each specific television system are assessed by its qualitative indices, which may be divided into two groups.

1. Optical indices: spectral sensitivity, the number of reproducible brightness gradations, and the homogeneity of their reproduction on the image field, as well as image clarity.

2. Geometric indices: the dimensions and format of the frame and its terrain coverage, nonlinear and geometric distortions, and terrain resolution and its variations in the frame field.

Spectral sensitivity is an important characteristic which determines the range of application of the television system. As already mentioned, the visible portion of the spectrum (sometimes only the yellow-red portion) and the "transparency window" of the atmosphere in the infrared portion of the spectrum—3.7-4.2 and 8-12 μm—are used for television tracking of clouds in meteorological satellites.

Selection of a given spectral range is determined by the values of the brightness contrasts between the cloud images and various types of ground surface. The greater the contrast the more favorable is the corresponding spectral range for surveying. However, investigations [83-85,99] have demonstrated that there is no such range in whose radiation intensity a cloud could be clearly distinguished from other types of ground surface. The use of spectrozonal or color surveying for this purpose is also of little use. /28

Therefore, the rather wide ranges of spectral sensitivity indicated above at least have the advantage that they contain much energy, at the same time providing a rather high image resolution.

The equipment is constructed so as to ensure receipt of sufficiently high-quality photographs over the entire range of possible values of radiation intensity from the earth to the satellite in these spectral ranges. Different means from variable signal amplification factor to changes of exposure time, and replaceable light filters and diaphragms are used for this. The former is usually employed for mechanically scanning systems (the IR of Meteor, the IR of Nimbus, and the TV of Aitos). The variation of the "amplification factor" is accomplished through the feedback circuit as a function of the average signal value. The latter methods are employed for systems with transmitting cameras (interchangeable diaphragms—the TV of Meteor, Tiros, ESSA, Aitos, and Nimbus, and interchangeable light filters—the TV of Molniya-1). The diaphragms are interchanged by signals from the solar elevation sensor, and the light filters are interchanged by commands from the ground receiving station and from image analysis.

According to the reflectivity of clouds and the earth's surface [33], the decrease in the brightness

$$\Pi = B_{max}/B_{min} \qquad (1.1)$$

of objects, simultaneously falling within the field of view of the television camera, has an order of 10, reaching an order of 10^2 in individual cases. At the same time the similar contrast on the phototelevision picture never exceeds an order of 10, so that for this reason identical visual perception of the clouds themselves and their television images may not be achieved.

Compared to the original, the television image is characterized not only by a smaller brightness range, but by a fewer number of distinguishable shadows of grey tone (brightness gradations). In visual perception of objects, the number of distinguishable gradations is determined only by the contrast sensitivity of the eye

$$k = \frac{B_1 - B_2}{B_1 \vee B_2}, \qquad (1.2)$$

B_1 and B_2 are the brightnesses corresponding to the different shades of grey. For the human eye the contrast sensitivity comprises an average of 0.02-0.03, which in the observed brightness range of clouds and the earth's surface makes it possible to distinguish up to 100 gradations. The contrast sensitivity of meteorological satellite television systems, which is determined mainly by the parameters

of the photoelectric converter, is much lower. A test pattern or test signal, which creates an image in the form of a number of strips of different brightness on the reproducing screen of the /29
television system, is usually employed to estimate contrast sensitivity. The test original is such that the brightness of the strips is perceived by the eye as uniformly varying. They are counted by the Weber-Fechner law. According to this law, visual perception of brightness variation is determined by brightness contrast (1.2), and in order that the brightness of the strips seems to be uniformly varying to the eye, the ratio of the brightness of adjacent strips should be constant. For a test pattern having ten strips, these brightnesses (or rather the brightness factors of the strip) are assumed to be equal to 1.00, 0.675, 0.455, 0.309, 0.214, 0.141 0.090, 0.064, 0.043, and 0.029. In examining the television image of this test pattern, it is usually impossible to distinguish all ten strips, but only five or six at a moderate, and 7 or 8 at a low level of television noise. Essentially, a greater portion of gradations is distinguished in some portion of half-tones. Thus, it is desirable that the dark half-tones be reproduced in more detail for reliable delineation of any clouds and images of open sections of the earth's surface on the photograph, because the brightness of some cloud forms, for example cirrus, is comparatively low. It is desirable to distinguish bright half-tones in order to investigate the structure of the upper cloud surface on a snow and ice background. The best conditions for reproduction of gradations are usually in the middle portion of the half-tone scale. However, by varying the exposure-time values in the appropriate manner and by changing light filters and the active diaphragm apertures, it is possible to achieve optimum distribution of the reproducible gradations on the half-tone scale of objects.

An essential property of television systems is the inhomogeneity of image field brightness reproduction. This inhomogeneity is manifested in a comparatively smooth darkening or lightening of the image toward the edges of the photograph, reaching 0.30-0.40 of its average brightness in current equipment. This inhomogeneity is often caused by nonuniform illumination of clouds and the earth's surface for different sections of the observed area. However, the greater part of illumination is related to inhomogeneity of the light-sensitive surface of the transmitting camera, the nonuniformity of motion and changes of the aperture of the reading and scanning electron beam. In this regard mechanically scanning television systems have an undoubted advantage, because the inhomogeneity of image field brightness distribution inherent to them is caused only by nonuniform illumination of the observed objects and sometimes by the instability of image scanning in the ground receiving facility. In principle it may be compensated for.

However, it must be said that in visual inspection of photographs, the inhomogeneity of brightness distribution by their field is not an appreciable barrier to meteorological interpretation, with the exception of cases of surveying of very low-contrast objects (clouds on a snow and ice background, etc.). The reason for /30 this is the fact that the most important qualitative parameter of the television image, which determines its interpretability, is clarity (resolution).

The inhomogeneity of brightness reproduction by the image field may arbitrarily include the presence of different types of defects of the light-sensitive surface of the transmitting camera. They are manifested on the image in the form of more or less large spots of black or light tone with clearly defined boundaries, cross-hatching, and ripples ("fingerprints"). These defects retain their shape, brightness, and position on the image regardless of the object; therefore, they essentially do not interfere with meteorological interpretation of the images of course in those cases when the defects occupy too small a portion of the photograph.

The resolving power of the television system is usually understood as its capability to reproduce small details of the image on the photograph. Resolving power is essentially evaluated by the maximum number of black and white lines which can still be separately distinguished from the image. Test patterns consisting of such lines are calculated for the maximum possible brightness range of observed objects, i.e., black lines correspond to objects with minimum and white line to those with maximum brightness. Depending on the width of the lines, their television image is distorted: abrupt variations of brightness on the edges of the lines are smoothed out and the brightness contrast of black and white is reduced almost to complete disappearance (Fig. 4). Maximum resolution is usually assumed to be the number of lines whose image contrast comprises 0.30 of the black and white contrast of the original focusing board.

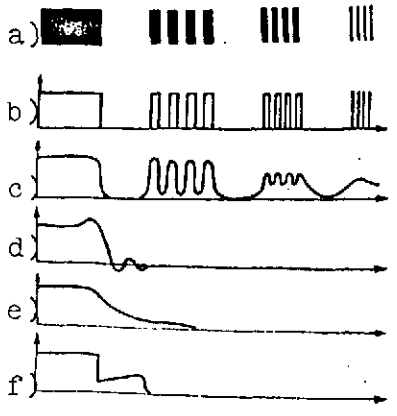

Fig. 4. Schematic representation of the television signal of black and white (two-gradation) strips of different width. a) Test pattern with image of black and white strips, b) law of brightness variation of strips of different widths in the original test pattern at right angles to the strips, c) shape of TV signal for strips of different width, d) shape of the black and white boundary of the TV signal in the presence of a tilt, e) shape of black and white boundary of TV signal in the presence of keystoning, f) shape of the black and white boundary of TV signal in the presence of ghosts.

Besides the number of reproducible black and white lines, the quality of transmitting the structure of the imaged objects is also characterized by a number of features, the most important of which are: the sharpness of the edges (contours) of the images, the discernibility of the boundary outlines, extended continuations of contrast objects, repeated images, and the level of random and periodic noise (Fig. 4).

The geometric indices of the television image are determined both by the parameters of the television system and by the type of meteorological satellite. In the given case the latter is characterized by the altitude and the ellipticity of the orbit, as well as by the mode of orienting the optical axis of the television system with respect to the satellite vertical. These parameters, in combination with the viewing angle of the television system, determine the dimensions and size of the frame and its terrain coverage.

As already mentioned, by using a television system with a transmitting camera, frame-by-frame surveying of the earth is usually accomplished, and the frame often has the shape of a square, while the orbital strip of the survey consists of a number of frames. Surveying is sometimes carried out with overlapping frames to increase the reliability of tracking cloud cover and to create a stereoscopic effect. Depending on the satellite altitude and viewing angle of the onboard television equipment, the terrain coverage by a single frame varies considerably: from approximately hundreds of kilometers in cross-section to tens of thousands of kilometers, comprising a more or less considerable portion of the earth's disc, visible from the satellite, or encompassing it completely. /31

When the terrain coverage by the television frame and the optical axis of the television equipment, directed toward the nadir, is relatively small, the visible portion of the earth's surface may be considered flat, because perspective distortions at the edges of the photograph occur only due to deviation of the sighting beam from the satellite vertical, and therefore are not too great. Thus, twofold perspective distortions on the edge of the orbital scanning strip for low-orbital satellites at an orbital altitude of the order of 1000 km occur when the width of this strip is approximately twice as great as the orbital altitude of the satellite. The angle of view of the onboard television equipment (it may consist of the angles of view of one or several television cameras or will be achieved by scanning of a single-element photoelectric converter) comprises ~90° in this case. When the fraction of the earth's visible disc encompassed by the television plane increases, perspective distortions increase rapidly since the earth's curvature begins to have an effect. Therefore, the orbital altitude of the satellite must be increased to increase the survey coverage of the television system.

Perspective distortions of the image essentially depend on the earth's curvature alone for very high orbits (of the order of 10,000 km). The deviation of the sighting beam from the satellite vertical may be disregarded due to the small angular dimensions of the earth's visible disc. In this regard installation of television equipment on the moon would be ideal. However, for other reasons a lunar meteorological observatory can hardly be constructed (because of the special conditions of its rotation around the earth, the moon is unsuitable for organization of regular local observations of the earth's cloud cover). /32

Returning to the television equipment of meteorological satellites, we note that an increase in the surveying area with fixed clarity leads to a decrease in the resolution of the television image on terrain. In order to avoid this, the angle of view of the single-element sensor on mechanically scanning systems must be decreased, at the same time increasing the scanning rate, and in television systems with transmitting cameras, in which the number of scanning lines is severly limited, several cameras must be employed simultaneously and their fields of view must be adjacent (two cameras are used on the Meteor satellites (Fig. 5) and three on the Nimbus satellites). Since adjustment of the orbital surveying strip is inevitably complicated when several cameras are used, mechanically scanning television systems should be recognized as more promising for obtaining a detailed pattern of cloud cover distribution on a planetary scale. /33

Besides the perspective distortions which cause irreversible deterioration of resolution on the edges of the scanning strip, there are other types of geometric distortions of the television image related primarily to the disruption of the synchronism and cophasality of shifting the tracking beam in the onboard television equipment and of the electron beam which develops the image on the screen of the television receiver. All the types of distortions of geometrically similar images impinging on the input of the television system and the images received at its output may be divided into nonlinear (large-scale) and essentially geometric. The former are manifested in the form of constriction or expansion of individual sections of the image, which leads to different scales of different parts of the photograph. The latter reduce to curvature of straight lines and variation of the values of the angles between lines. Distortions of both types are essentially evaluated by the images of the test patterns, which are some simple figures (circles, squares, etc.) where the relative distortion of their areas characterizes nonlinear distortions, and of their sides and angles—essentially geometric distortions (Fig. 6).

Geometric distortions are usually too small (of the order of 0.05) to affect the meteorological interpretability of the images,

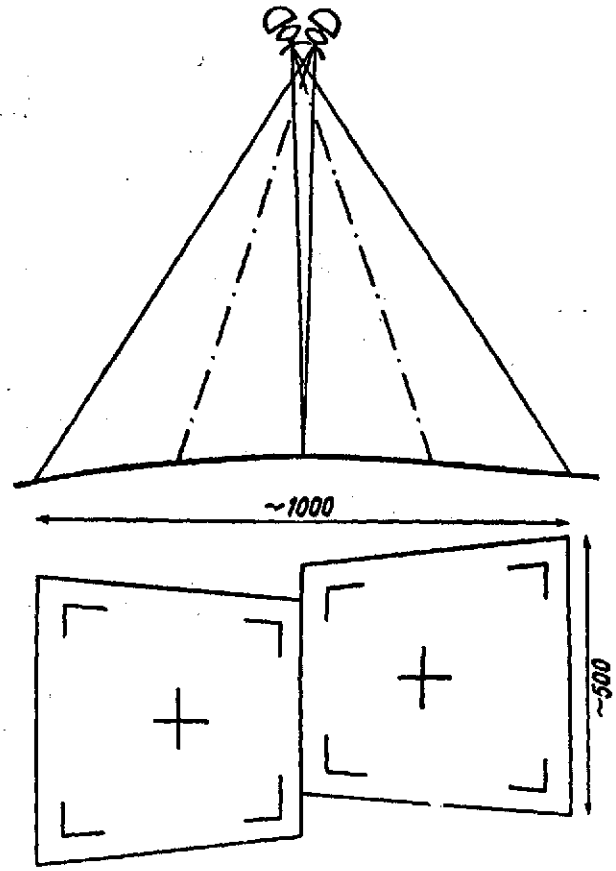

Fig. 5. Diagram of television surveying from Meteor satellites using alternately operating television cameras.

but they must be taken into account in geographic control matching of photographs. The first means of taking them into account for the latter purpose is to apply a regular geometric grid, for example a grid of squares, onto the light-sensitive surface of the transmitting television camera. With such a grid, not only a considerable portion of the geometric distortions may be corrected, /34 but the shifting of the television raster with respect to the optical axis of the camera may also be taken into account, which also may induce an additional error in the geographic control match. The correction procedure in the presence of a grid of squares on the image reduces, as is completely obvious, to use of it as the coordinate grid. In mechanically scanning systems, geometric distortions occur due to the ground facilities for reproducing the image, as well as due to the instability of scanning line length (this is

eliminated when a digital image transmission system is used) and due to rocking of the satellite. On the whole, the level of geometric distortions of the image in these systems is lower than in those with a camera, which is one more factor in favor of using mechanical television on meteorological satellites.

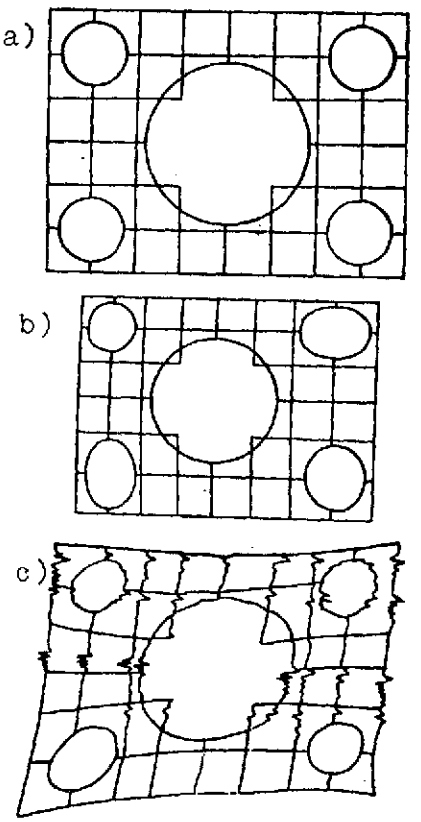

Fig. 6. Types of nonlinear and geometric distortions of television images. a) test pattern with image on circles and squares, b) image of test pattern in the presence of nonlinear distortions, and c) image of test pattern in the presence of geometric distortions and disruptions of line synchronism.

The most essential for meteorological interpretation of images by the type of geometric distortions is the factor resulting in synchronization failures and in some other cases the shift of the elements of adjacent lines of the image, due to which smooth vertical lines on the photograph seem to be broken or even torn (Fig. 6).

3. Primary Processing of Television Photographs

Processing of television and infrared photographs of the earth, obtained with the use of satellites, is usually understood to be a combination of operations, as a result of which certain meteorological information is obtained on the basis of the radio signals received from the satellite. The term "processing" can also be more narrowly interpreted as a combination of operations on conversion of the radio signals of the meteorological satellite into photographs and photodiagrams, related to a specific moment (or time interval), geographically localized and corrected of different types of distortions, owing to technical reasons and perhaps to natural causes, having no relationship to meteorology. For example, the brightness of photographs is normalized regardless of solar elevation (when surveying in the visible region of the spectrum) or the time of year (when surveying in the infrared region). All this may be called primary processing.

In the second stage of creating television systems for tracking cloud cover from satellites, when there was no problem of operative utilization of the incoming photographs, processing was accomplished essentially without use of any auxiliary technical facilities. Most processing operations (in the narrow sense) are presently automated.

The orbital elements are regularly measured for each meteorological satellite, which makes it possible to predict the time of its passage above one or another region of the earth, and hence to plan the time and area of television surveying by day and night /35 and the time of passage above the ground stations which control the operation of the satellite, monitor its functioning, and receive the television signals over radio channels. Each television picture received from the satellite, if it is received in a mode other than direct transmission, i.e., at the actual moment of its reception on earth, is accompanied by auxiliary information which makes it possible to establish the time of surveying, which, in combination with the orbital data, is adequate for geographic localization of the clouds and elements of the earth's surface imaged on it. Data on the actual orientation of the optical axis of the television system at the moment of surveying are sometimes used as well to refine such localization. These data are obtained on the satellite with the aid of a special system for monitoring the satellite's orientation and are transmitted to earth over radio channels.

The television signals are received at the ground station, are amplified, and with the aid of an electron beam tube or phototelegraph device are converted to an image which is recorded on photographic film or paper. The photographs obtained in this manner are placed at the disposal of the meteorologist-interpreter for geographic control matching and subsequent meteorological interpretation.

Geographic control mathcing is understood as determination of the geographic coordinates (latitude ϕ and longitude λ) of any image point. Geographic control matching may be accomplished either by drawing a grid of meridians and parallels on the photographs or by transfering the photographic image to a geographic map of some projection.

In the latter case the geographic latitude B and longitude L of the angles of the rectangular grid, drawn on the photograph so that the central junction of the grid is joined, for example, with the center of the photograph, must be taken into account. The coordinates of the grid points (x, y) are defined in the rectangular coordinate system of the photograph, whose center coincides with the main point of the photograph (the center of the photograph), the x-axis is in the direction of motion of the satellite and the y-axis is in a vertical direction (Fig. 7). Conversion

from the coordinate system of the photograph to the corresponding horizontal coordinate system is first accomplished:

$$x' = f\frac{xb_{11} + yb_{12} - fb_{13}}{-xb_{31} + yb_{32} - fb_{33}}; \tag{1.3}$$

$$y' = f\frac{xb_{21} + yb_{22} - fb_{23}}{-xb_{31} + yb_{32} - fb_{33}}, \tag{1.4}$$

where f is the focal distance of the TV camera; b_{ij} are the direction cosines of the coordinate system of the TV camera with respect to the corresponding horizontal coordinate system; x', y' are the coordinates of the corresponding horizontal system.

/36

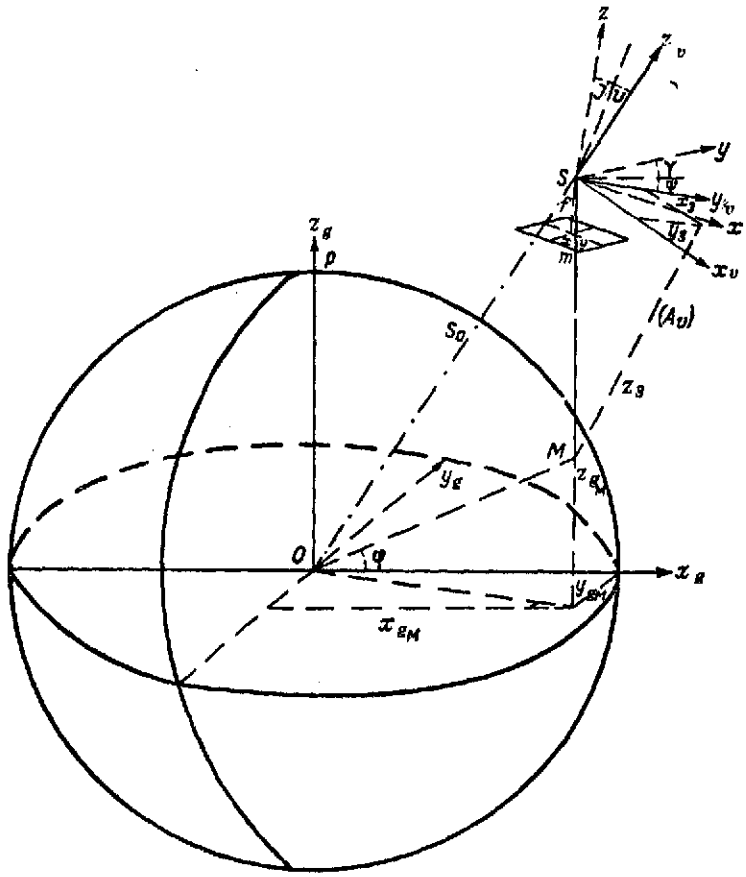

Fig. 7. The system of coordinates used in geographic control tie-in of television images from known data on the position of the optical axis of the television camera in space at the moment of surveying.

From the calculated coordinates, x' and y' may be converted to the intermediate coordinates x_B and y_B by the formulas

$$x_B = x' \frac{z_B}{f}; \quad y_B = y' \frac{z_B}{f};$$

$$z_B = H + R(1 - \cos\sigma);$$

$$\sigma = \arcsin\left(\frac{H+R}{R}\sin\theta\right) - \theta;$$

$$\theta = \operatorname{arctg}\frac{\sqrt{(x')^2 + (y')^2}}{f} \qquad (1.5)$$

(H is the satellite altitude; R is the earth's radius), and then /37 from the formulas of rotation and conversion of the coordinate system to geodetic rectangular coordinates of the grid points x_g, y_g, and z_g:

$$\begin{aligned} x_g &= x_{gs} + x_B a_{11} + y_B a_{21} + z_B a_{31}; \\ y_g &= y_{gs} + x_B a_{12} + y_B a_{22} + z_B a_{32}; \\ z_g &= z_{gs} + x_B a_{13} + y_B a_{23} + z_B a_{33}, \end{aligned} \qquad (1.6)$$

where

$$\begin{aligned} x_{gs} &= (R+H)\cos B_s \cos L_s; \\ y_{gs} &= (R+H)\cos B_s \sin L_s; \\ z_{gs} &= (R+H)\sin B_s \end{aligned} \qquad (1.7)$$

are the rectangular geographic coordinates of the satellite at the moment of photographing; B_s, L_s, and H are the lattitude, longitude, and altitude of the satellite:

$$\begin{aligned} a_{11} &= -\sin A_v \sin L_s - \cos L_s \sin B_s \cos A_v; \\ a_{12} &= \cos L_s \sin A_v - \sin L_s \sin B_s \cos A_v; \\ a_{13} &= \cos B_s \cos A_v; \\ a_{21} &= \cos A_v \sin L_s - \cos L_s \sin B_s \sin A_v; \\ a_{22} &= -\cos L_s \cos A_v - \sin L_s \sin B_s \sin A_v; \\ a_{23} &= \cos B_s \sin A_v; \\ a_{31} &= \cos L_s \cos B_s; \\ a_{32} &= \sin L_s \cos B_s; \\ a_{33} &= \sin B_s, \end{aligned} \qquad (1.8)$$

A_v is the azimuth of the satellite's velocity vector.

The geographic coordinates B and L are calculated by the coordinates x_g, y_g, and z_g for any point of the TV photograph:

$$B = \operatorname{arctg} \frac{z_g}{\sqrt{x_g^2 + y_g^2}};$$

$$L = \operatorname{arctg} (y_g / x_g). \qquad (1.9)$$

A grid which is the image of projecting the rectangular grid of the photograph onto the earth is constructed on the chart from the calculated coordinates B and L. These two corresponding grids make it possible to transfer the image from the photograph directly to the chart.

An example of such a grid (transformation table) for a stereographic projection chart is shown in Fig. 8. These types of transformation table are employed in the Hydrometeorological Center of the USSR in geographic control matching of TV photographs received from the satellites of the Meteor system.

The principle of transformation tables is also the basis for /39
geographic control matching of American photographs received in the direct transmission mode [93,122,164].

Geographic control matching of TV photographs received from satellites, whose geographic coordinates and altitude at the moment of surveying are known only approximately and the position of the optical axis of the TV camera with respect to the satellite coordinate system is unknown, is more complicated. We encounter such a case, for example, in geographic matching of photographs received from the Molniya-1 satellite or in control tie-in of the photographs taken by cosmonauts.

Control matching in these cases is possible if some geographic reference points can be recognized in the photographs. The image of the horizon line, available on some photographs, may also be used [62,63]. We note that the accuracy of geographic control matching using recognized reference points may be much higher in principle than that achieved in the method of transformation tables described above.

The coordinate systems used here are presented in Fig. 9. (x_g, y_g, and z_g) is a geocentric coordinate system; $S_{x,y,z}$ is the coordinate system of the TV camera, rotated in pitch (v), roll (j), and yaw (ψ) angles with respect to an auxiliary coordinate system, one axis of which is directed toward the north and the two others of which form a righthanded coordinate system.

The problem reduces to sequential calculation: first using common transformation formulas (1.3) and (1.4), the point coordinates

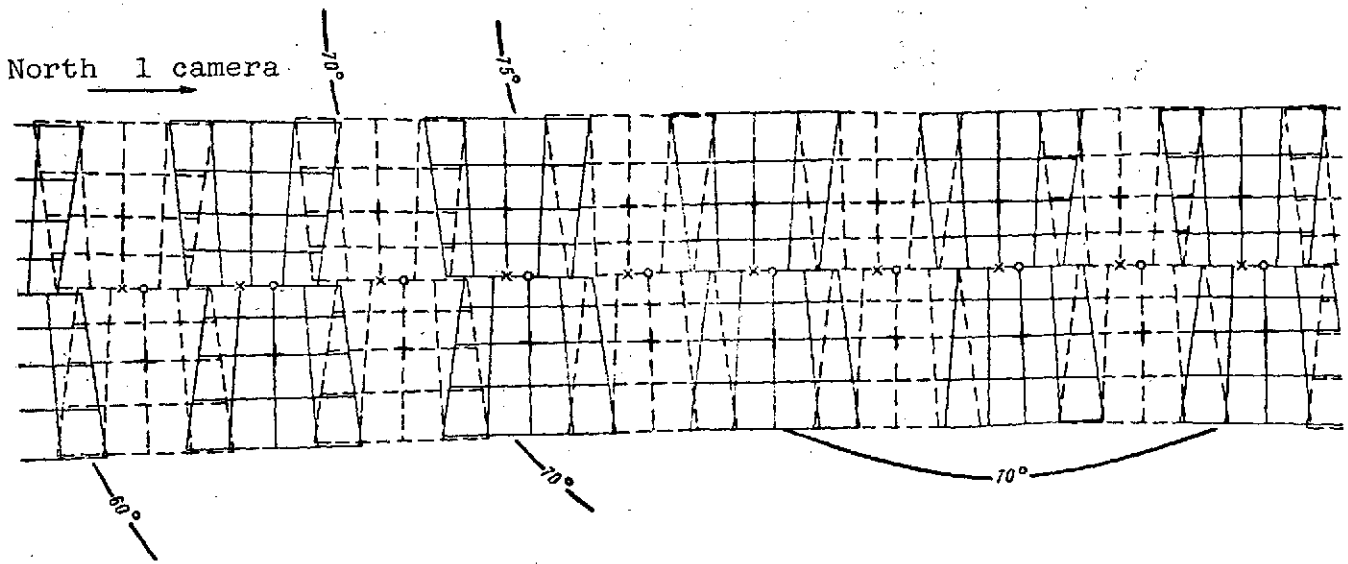

Fig. 8. Transformation table used for geographic control matching of television photographs received from the Meteor satellites. Stereographic polar projection. Scale 1:15,000,000. H = 645 km.

of the nadir x_n and y_n are found from the position of the line, which for an inclined photograph are related to the pitch and roll angles by the relations

$$x_n = f\frac{\operatorname{tg} v}{\cos j}; \tag{1.10}$$

$$y_n = -f \operatorname{tg} j. \tag{1.11}$$

The latter, consequently, may be found from formulas (1.10)-(1.11), after which from formulas (1.3)-(1.4) may be found the radius of the visible horizon line r and satellite altitude at the moment of surveying H

$$r = \sqrt{x_t^2 + y_t^2}; \tag{1.12}$$

$$H = \frac{R\cos\left(\operatorname{arctg}\frac{r}{f}\right)f}{r} - R\left[1 - \sin\left(\operatorname{arctg}\frac{r}{f}\right)\right]. \tag{1.13}$$

where (x_t, y_t) are the point coordinates of the horizon on the photograph.

The remaining orientation elements—the coordinates of the center of projection (ϕ_s, λ_s) and the yaw angle (ψ)—may be found in the presence of points with known geographic coordinates (reference points) on the photograph and with approximate knowledge of the satellite position at the moment of surveying (ϕ_s', λ_s'). For this, setting the yaw angle $\psi = 0$, we calculate the point coordi- /40
nates M with known geographic coordinates in the auxiliary coordinate system

$$x'_{s.M} = z_{s.M}\frac{xb_{11} + yb_{21} - fb_{31}}{xb_{13} + yb_{23} - fb_{33}} = z_{s.M}\frac{x'}{z'}; \tag{1.14}$$

$$y'_{s.M} = z_{s.M}\frac{xb_{12} + yb_{22} - fb_{32}}{xb_{13} + yb_{23} - fb_{33}} = z_{s.M}\frac{y'}{z'}; \tag{1.15}$$

$$z_{s.M} = -[H + R(1 - \cos\sigma)], \tag{1.16}$$

$$\sigma = \arcsin\left[\frac{H+R}{R}\sin\theta\right] - \theta; \tag{1.17}/41$$

$$\theta = \operatorname{arctg}\frac{\sqrt{(x')^2 + (y')^2}}{z'}, \tag{1.18}$$

b_{ij} are the direction cosines of the coordinate system of the TV camera with respect to the auxiliary coordinate system.

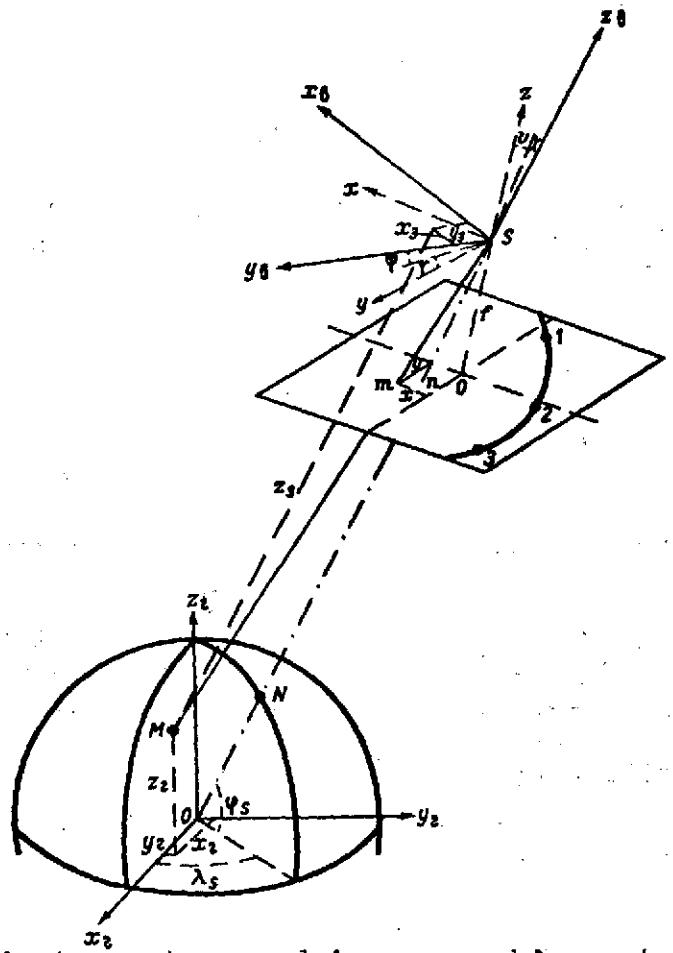

Fig. 9. Coordinate system used in grographic control matching of television images from the geographic reference points and horizon line recognized on the photograph.

The coordinate system can be rotated by the desired yaw angle (ψ)

$$x_{вМ} = x'_{вМ}\cos\psi - y'_{вМ}\sin\psi; \tag{1.19}$$

$$y_{вМ} = x'_{пМ}\sin\psi + y'_{вМ}\cos\psi. \tag{1.20}$$

The yaw angle may be found from (1.19)-(1.20), after which by using formula (1.6) and knowing the approximate coordinates (ϕ'_s, λ'_s) of the projection center, the approximate geocentric coordinates on any point on the photograph may be found. The point coordinates are then found after introduction of corrections $\Delta\phi_s$ and $\Delta\lambda_s$ into the coordinates of the projection center, which in turn are found by differating (1.6) with respect to ϕ'_s and λ'_s and by solution of the set of n (n is the number of reference points recognized on the photograph) linear equations

$$\begin{aligned}
&\{(z'_{gi})^2 a_{21}^2+(z'_{gi})^2 a_{22}^2+[(H+R+z_{n.u})a_{13}-x_{n.u}a_{33}]\}_1^n \Delta\varphi_s- \\
&-[z'_{g.u}x'_{g.u}a_{21}+z'_{gu}y'_{gu}a_{22}]_1^n \Delta\lambda_s-\{-z'_g a_{21}\Delta y_g+z'_g a_{22}\Delta x_g+ \\
&+[(H+R+z_{n.u})a_{13}-x_{n.u}a_{33}]\Delta z\}_1^n; \\
&[-z'_{gu}x'_{gu}a_{21}-z'_g y'_g a_{22}]_1^n \Delta\varphi_s+[(x'_g)^2+(y'_g)^2]_1^n \Delta\lambda_s= \\
&=[x'_{gu}\Delta y_g-y'_g\Delta x_g]_1^n.
\end{aligned} \tag{1.21}$$

After calculation of the reference elements on the photograph by formulas (1.9), a transformation table may be constructed by which the problem of geographic control matching will be solved.

The television signal is sometimes subjected to normalizing transformations prior to photographic recording, which improves the quality of the image, for which both analog and digital devices or even universal computers may be used. The next stage in improving the processing of the photographs is automation of their geographic control matching which is achieved in the simplest case by "mixing into" the television signal the signal describing the grid image of the geographic coordinates (TV photographs of the ESSA satellites, which are received in the direct transmission mode). In the more complete version, the television photograph itself is transformed into direct cartographic projection of the given scale [100,103,104] (TV photographs of ESSA received by intermediate storage of data onboard the satellite).

An analog machine for "electronic transformation and control matching" (ETCM) was used experimentally for automatic geographic control matching of television photographs of Meteor. With the aid of ETCM the television photographs are formed (without regard to the earth's curvature, but taking into account the actual orientation of the satellite) into the transformation projection already mentioned, and are reduced to a scale of 1:7,500,000, taking into account the actual orbital altitude of the satellite. The signal of the geographic grid is "mixed" into the television signal of /43

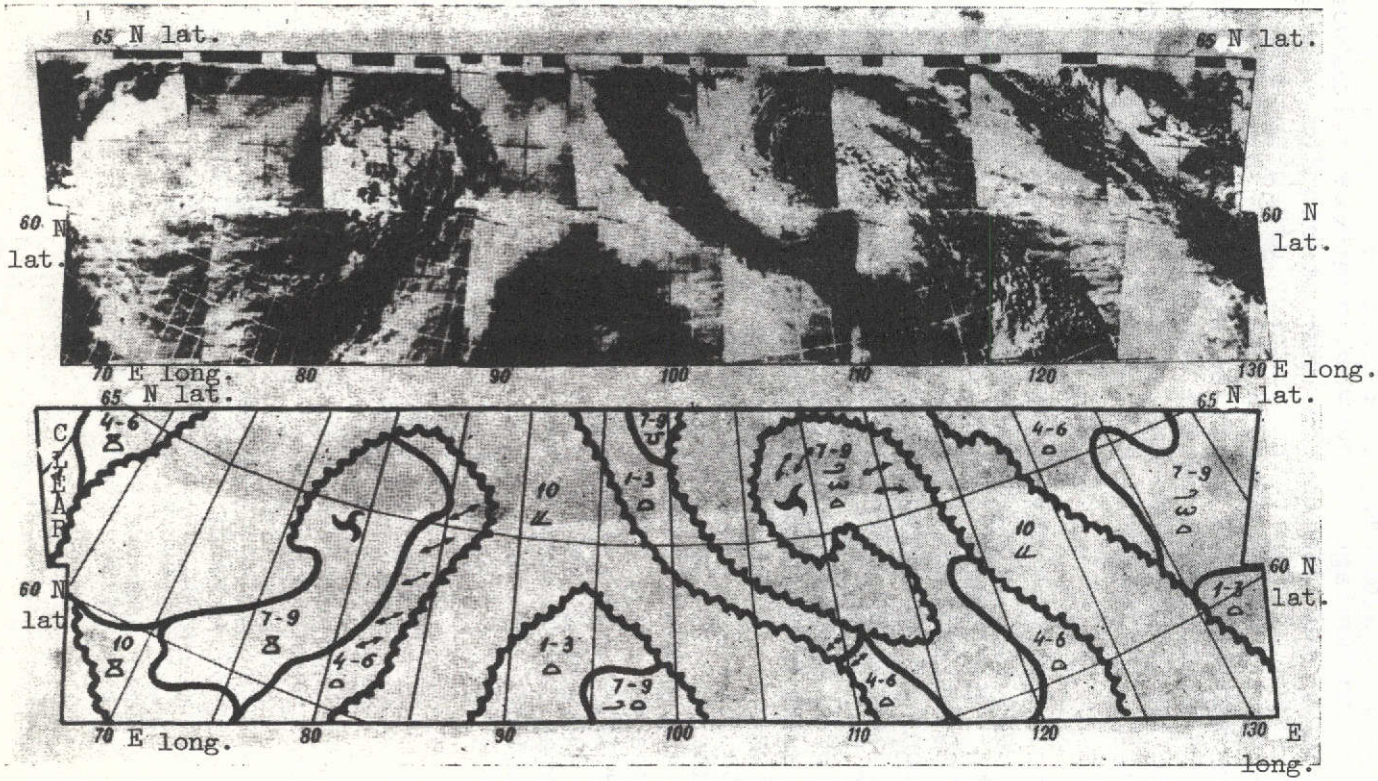

Fig. 10. Orbital montage of television photographs received from Meteor satellite and their nephanalysis. The photographs were transformed into a perspective cartographic projection with the aid of equipment for electronic transformation and control matching (ETCM).

the transformed photograph, and the resulting signal is transformed to an image for subsequent photographic recording (Fig. 10). Photographs with transformed images may be represented in the form of an orbital photographic montage. However, montages of adjacent orbits may not be connected due to the characteristics of the photographic projection used. This is the primary disadvantage of the ETCM system, due to which it is not used in operational work. The ETCM system is very suitable for those scientific investigations which are related to measurement of the distances and angles on the photograph, because the projection employed is conformal, i.e., there are essentially no geometric and nonlinear distortions of the imaged objects.

With regard to improving the quality of the television images during primary processing, up to the present time there have only been experiments in this field. Thus, American meteorologists [94, 118,139,163,170,172] attempted to take into account geometric and nonlinear distortions of the image in geographic control matching, reduction of the noise level, and correction of inhomogeneities in reproduction of brightness from the image field, as well as solar elevation during surveying in the visible region. It should be noted that all such investigations involve rather complicated transformation of the television signal with consideration of the additional data on the surveying mode, so that a large amount of time must be expended for such transformations and very large computers must be employed. These are usually universal digital computers with a speed on the order of 10^6 operations per second and a storage capacity on the order of 10^6 bits. Such high requirements on the equipment undoubtedly hinder introduction of automation into this branch of primary processing of television photographs on an operational basis.

Chapter 2
METEOROLOGICAL INTERPRETATION OF SPACE PHOTOGRAPHS OF THE EARTH

1. Interpretation of Cloud Cover

Television and infrared photographs of the earth may be used in analysis and forecasting of weather only after the photographs received from the satellite have been processed in the appropriate manner. Processing of the photographs includes a large number of operations: ground reception of the radio signals depicting the /44
image, recording of the signals in the form of photographs, photo chemical processing of the photographs, and temporal and geographic control matching of the images. Besides these purely technical operations, processing includes meteorological interpretation of the images as the most important link [53,64,66,73,109,121].

In interpretation the meteorologist interpreter examines and analyzes the photographs received, recreating on their basis the pattern of atmospheric processes in the region of the survey. The result of interpretation is so-called nephanalysis. In schematic and graphical form, nephanalysis contains the information on the meteorological characteristics of the state of the atmosphere which could be established from the photographs. Nephanalyses, compiled operationally at present, usually contain information on the average amount, prevalence and form, and mesostructure of clouds in some sufficiently large region of the earth. Excessive detail in space is detrimental due to the comparatively low accuracy of geographic control matching of photographs, comprising for example an average of about 50 km in the Meteor satellites. Surveying of cloud cover from satellites is now carried out once or twice per day, because only sufficiently long-lived cloud formations, which are usually large-scale cloud fields, may be depicted in nephanalysis. All this, as well as the necessity of presenting the data in a form suitable for transmission over communications lines and for comparison with charts of other meteorological elements, requires that nephanalysis be presented in the form of a chart (Figs. 10-12). The notations on a nephanalysis chart (with and without regard to scale) are:

- the location of various parts of cloud field boundaries, the boundaries being subdivided into clearly and weakly expressed;

- the total average amount and prevalent form of clouds for each cloud field boundary delineated. The cloud field in this case is understood as the section of cloud cover within the limits of which properties of cloudiness hardly vary or their variations are periodic; accordingly, the cloud field boundary is drawn where the properties of cloudiness vary sharply or the nature of their periodic variations changes; the type of mesostructure and sometimes

the dimensions and orientation of cloud elements are indicated as additional characteristics of cloudiness.

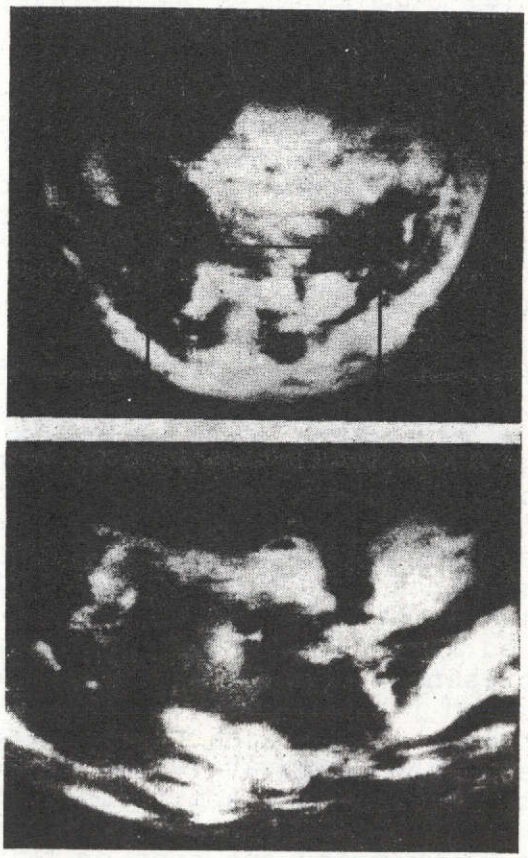

Fig. 11. Wide- and narrow-cut television photographs obtained from the Molniya-1 satellite. The field of the narrow-cut photograph is delineated by the frame on the wide-cut photograph.

Non-scale features are special points and lines in the cloud cover (vortex centers and the location of large-scale cloud strips) and other small but especially important cloud formations. Moreover, when photographs are used for synoptic analysis and forecasting of weather, interpretation is often accomplished directly by the synoptic forecaster. In this case the interpretation results are not depicted in the form of nephanalysis (charts), but remain in the "memory" of the synoptic meteorologist. The latter procedure is usually based on the fact that the original photoimage is clearer than the schematic chart of nephanalysis. However, while in complete agreement with this, the experience of using aerial photographs in geography must be pointed out. /45

After the appearance of aerial photographs of the earth's surface, many geographers predicted the disappearance of geographic maps, since they are incomparably more schematic and contain much less information on terrain than the original aerial photographs. We know that this has not happened. The overwhelming majority of users now use maps rather than aerial photographs. The reason for this is the simplicity of their use: there is good conformity between the notations of the map and the geographic object, whereas /46 the image of the same objects on the aerial photograph require interpretation, which is accessible only to a sufficiently experienced interpreter, but not to any user of such information. Further, besides the loss of the external similarity to the original, the map is easier to "read" because the more essential features of the imaged region are retained on it or are especially delineated. They are "drowned" in minor and secondary details on the aerial photograph. Therefore, we may think that in meteorology the period

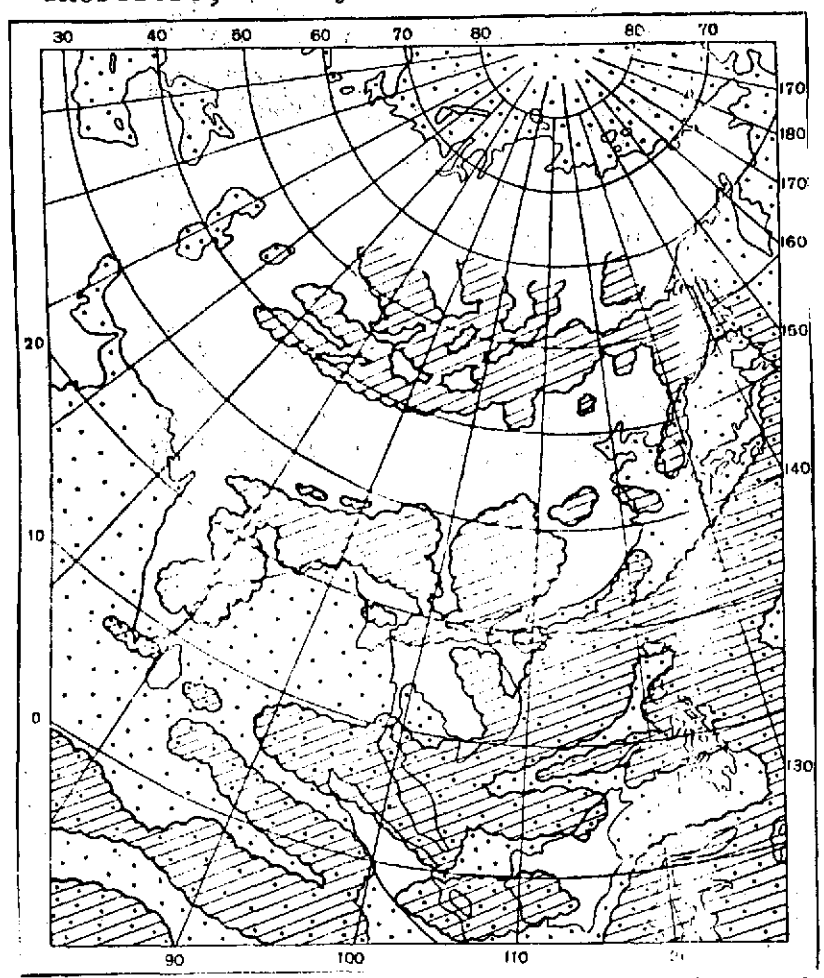

Fig. 12. Nephanalysis of the television photographs shown in Fig. 11.

of interest in the original images ends during analysis and forecasting of weather. But it is now clear that only schematic neph- /47
analysis may be used in numerical procedures of weather forecasting as well as for climatological generalization.

The list of meteorological parameters which are expressed in nephanalysis, and in the detail and accuracy of their imaging, naturally depends on the purposes for which this analysis is carried out. The consumer also determines the external form of nephanalysis. Thus, nephanalysis, intended for use in global analysis and forecasting in weather, will differ considerably both externally and in content from analysis for aviation services, etc. On the other hand, the content and even the form of nephanalysis is dictated to a considerable extent by the physical principles and specific technical layout of the television equipment and the satellite used. Therefore, when developing methods of image interpretation, the principles, principal characteristics, and qualitative indicators of operation of the entire complex of the onboard and ground television equipment, described in the preceding sections, must be taken into account.

The tone (brightness) and pattern (structure) of the image are employed as the interpretation features, i.e., the properties which make it possible to distinguish cloud images of different types and the earth's surface from each other. When surveying in the visible region, the image brightness is determined by the reflective properties of the underlying surfaces (cloudiness, snow and ice cover, vegetation, soil, water surface, etc.) in the scanning direction of the satellite.

The image brightness of the same underlying surface may vary considerably as a function of the time of surveying, mutual disposition of the television camera, the sun and the observed surface, exposure and other technical characteristics of surveying, and reproduction of the image. The result of this subdivision of images according to brightness is rather subjective, and the relationships of brightness rather than absolute brightnesses are employed in interpretation, because despite all distortions only the amplitude but not the sign of variations of image brightness changes.

It is convenient to use the albedo of the surfaces, not forgetting the possible anisotropy of their reflectivity, to judge the relative brightness which will usually occur on photographs of clouds and other underlying surfaces. Analysis of data from the literature on albedo [33,121] indicates that the brightest objects on photographs will usually be the cloudiness and ice fields and snow cover, and the darkest objects will be water surfaces. The albedo of clouds depends on their quantity, thickness, microstructure and phase state. The latter two factors are related to the

form of the clouds [77]; therefore, we may speak of the dependence of albedo on the form of cloudiness, although this dependence is rather weakly expressed. Other things being equal, the brightest on photographs will be nimbostratus and cumulonimbus clouds, followed by stratocumulus, stratus, altostratus, and altocumulus clouds.

The darkest will be high clouds. The albedo of thin transparent clouds depends on the albedo of the underlying surface of the earth or lower clouds. Patches of sunlight may be observed due to the anisotropy of solar radiation reflection under specific conditions on the images of the water surface, clouds, and certain types of land areas. /48

Unlike the television photographs obtained in the visible region, the tone of an infrared image is determined by the temperature of the clouds and the earth's surface, where the temperature of the tops of clouds depends considerably on their altitude, so that the tone of an infrared photograph is almost equally dependent on the quantity of clouds in the area corresponding to the scanning element and on the altitude of these clouds. The emissivity of the scanned surface, the thickness of the cloud layer, etc. have an additional effect on tone.

Let us also note that the thermal background on which infrared surveying is carried out is much more variable than the brightness background in surveying in the visible region. If automatic regulation of amplification of an infrared signal is taken into account, the role of tone as an interpretation feature should be recognized as rather modest. This feature indicates that, first, the tone of an infrared image under similar equal conditions is lighter the greater is the quantity and the higher the upper boundary of the clouds on the corresponding section of the observed surface. Second, variation of tone for adjacent scanning elements is again related, other things being equal, either to an increase in quantity or an increase in the altitude of clouds, or to both these factors simultaneously. Third, comparison of the tone of elements which are considerably separated from each other on the photograph provides no optical information on the differences of cloudiness in the corresponding regions.

Thus, when delineating regions of different tone on television photographs, made in the visible or infrared regions, some idea may be obtained about the quantity, altitude, shape, and density of clouds, but considerable errors in this case are possible, which arise due to the differences in the geometrical conditions of sighting (the anisotropy of reflection and emission of radiation by clouds and by the earth's surface, and transport of it through the atmosphere), as well as mainly due to the inhomogeneity of brightness

reproduction on the photographic field. The more informative are sharp variations of image tone, which form the image pattern.

The image pattern (structure) depends on the brightness (thermal) contrast of the observed objects, exceeding the threshold of the contrast sensitivity of the television equipment. The latter depends on the quality of reproduction of half-tones on the photographic field and differs for light and dark half-tones. Thus, five or six gradations of brightness can usually be distinguished in the daytime television equipment of the Meteor satellites upon reproduction of an image of a 10-step half-tone wedge with the characteristics indicated in Section 2 of the preceding chapter. This means that in the range of dark half-tones, which more often /49
reflect the brightness structure of the earth's surface, differences in reflectivity of 0.05-0.10 are discernible, and in the range of light half-tones only the more appreciable differences (0.30-0.50) are distinguishable. Of course the given figures are approximate. The infrared equipment of the Meteor satellites has more stable characteristics in this regard. Its sensitivity is about 2-3° at positive temperatures and 7-8° at temperatures of -40 and -50°. The thermal relief of the earth's surface is, consequently, reflected with greater detail than that near the upper boundary of the clouds. Accordingly, the possibilities of surveying at high altitudes, as well as at medium altitudes in winter, are more limited compared to subtropical and tropical regions, where the thermal background is much higher.

Variations of surveying conditions (illumination or total thermal background, exposures, stopping down, and automatic regulation of amplification), as noted in Chapter 1, affect the reproducibility of gradations on the half-tone scale and at the same time affect the image structure. Some details disappear and others appear. But on the whole the image structure is much more stable to the external factors of surveying than image tone.

When using image structure as an interpretation feature, the limited resolution and presence of geometric distortions of the image should be taken into account. The former (Fig. 13) places limitations on the possibilities of recognition with respect to small-scale objects. Thus, perturbations in the reflected or emitted radiation field, which do not exceed the scanning element in size, are barely reflected on the photograph. An exception is perturbations whose contrast with the background exceeds by many times the threshold sensitivity of the television system. Such perturbation is reflected on the photograph. In this case its amplitude will be reduced considerably and the area will be decreased. The greater the area of perturbation in the radiation field the greater are the possibilities of recognizing the form of this perturbation, and the more complicated its form the greater the

number of scanning elements of the photograph it should require for recognition.

Three types of structure may arbitrarily be distinguished on the photographs. The first type—texture—corresponds to the case when the image perturbation is made up of a few scanning elements of the photograph (from units to approximately hundreds). Only the main features of a perturbation which ondicates whether it is rounded or elongated, lighter (colder) than the surrounding background or vice versa, are then reproduced on the photograph The second type of image structure—mesostructure—occurs when a perturbation is sufficiently large in area (hundreds of scanning elements) for which it is reflected on the photograph in details, but not too few, in order to take into account the geometric distortions of the photograph during analysis of its form. The third type is the macrostructure of the images of objects, comparable in area to the region encompassed on the locale by the TV frame. Geometric /50 distortions of the image must be taken into account here.

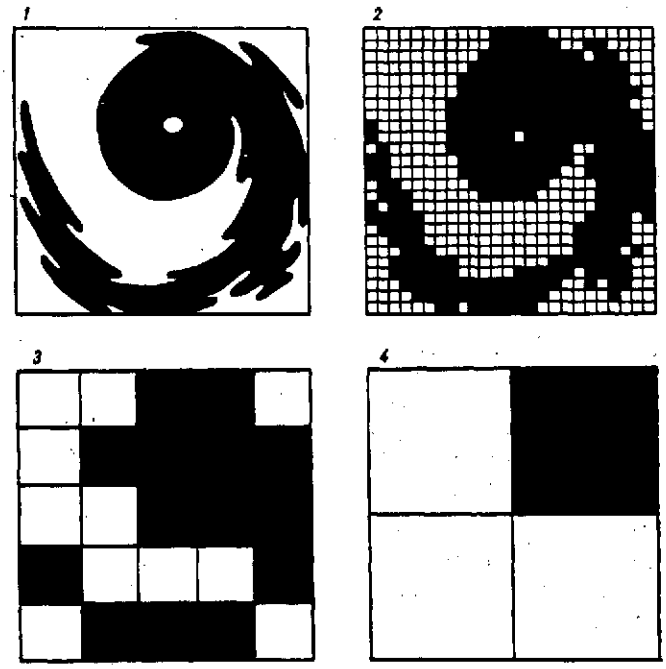

Fig. 13. Generalization of the shape of an object due to the limited resolution of the image.

1- the original of the object, 2- certain recognizable image on a photograph with high resolution, 3- image on the edge of recognition of an object at lower resolution, 4- image on the edge of detection of an object at very low resolution.

All these types of TV image structures are analyzed in meteorological interpretation of photographs of the earth obtained with the aid of satellites, since a high degree of organization both on the synoptic scale and on the mesoscale and small scale is inherent to cloud cover. On the basis of the characteristics of a three-dimensional spectrum of cloud formations and their emission fields [29,30,41,42,44,76,97,121], it should be said, however, that small scale is the more informative for recognition of cloud forms and their distinction from the images of open sections of the earth's surface.

This circumstance was taken into account in creation of the daytime TV equipment for the Meteor satellite, whose resolution (about 1×1 km^2) closely coincides with the prevailing dimensions of individual clouds. Because of this, the largest amount of information on the form and quantity of clouds is carried by the texture of the image in the given case. Two other types of image patterns are essential mainly for identification of meso- and large-scale /51
(synoptic) cloud formations, although they are also useful for recognition of cloud forms, since the synoptic systems of the clouds of atmospheric fronts and other large-scale cloud formations, consisting primarily of clouds of specific forms, are well-known.

It should be noted here that, besides the direct interpretation features (tone and image pattern), various indirect features which are available in the geographic descriptions and on the maps of the photographed region of the earth, and in the climatic handbooks for it, should be taken into account in interpretation of the photographs. Finally, it is useful to take into account the data of ordinary ground meteorological observations in the photographed region for the time of surveying (or the most recent "history"), because a knowledge of the synoptic situation sometimes makes it possible to clearly determine the form of the observed clouds or the fact of their absence, although this cannot be done from the photograph itself.

Returning to daytime TV photographs, received from the Meteor satellites, we note that a large number of photographs has been accumulated as a result of successful functioning of the satellites. These photographs have abundant information on the morphology of the cloud cover in different geographical regions at different times of the year. Systematic inspection of these photographs made it possible to determine the typical characteristics of the TV images of clouds of different forms and mesoscale cloud formations, as well as of geographical landmarks at different times of the year. In this case both the properties of the cloud cover and of the earth's surface (brightness and morphological features) as well as the technical characteristics of the TV equipment used in satellites of the Meteor system were taken into account in this case.

A catalogue of typical images, classified according to brightness (tone), form, dimensions, and mutual orientation of the image elements, is presented in Figs. 14-16.

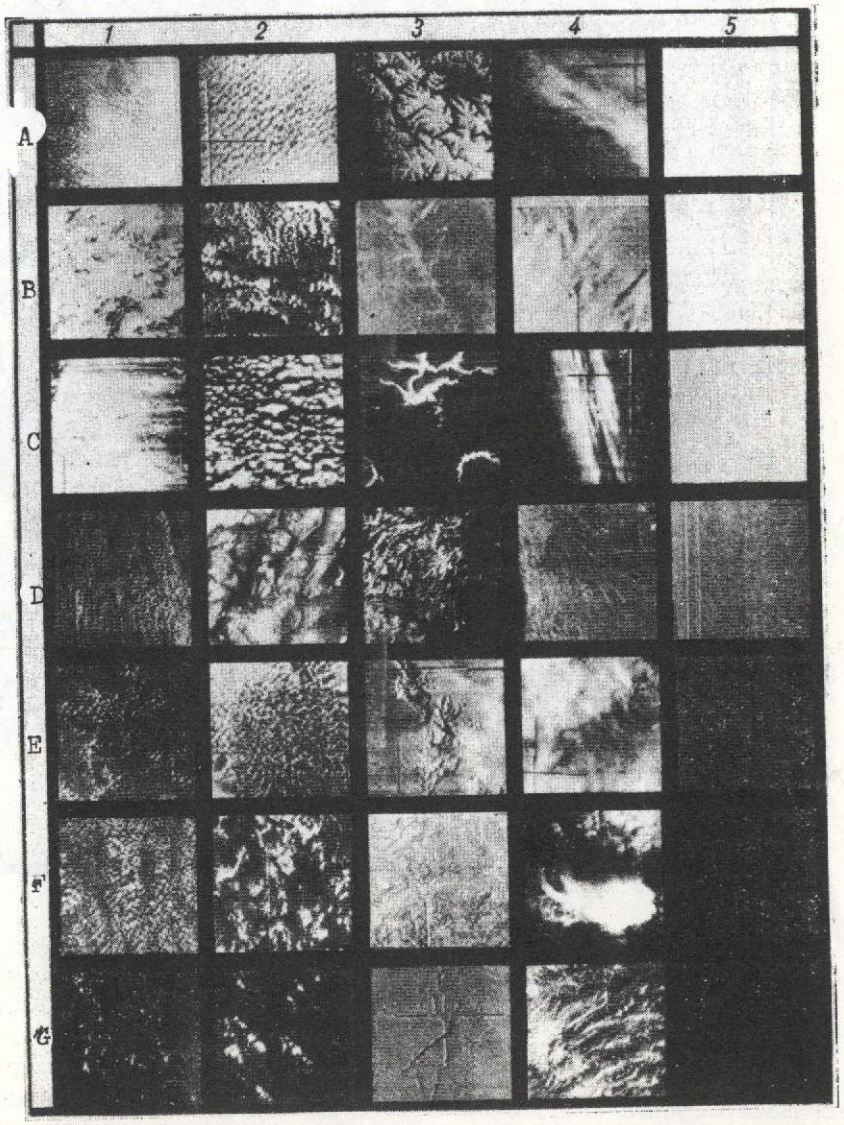

Fig. 14. Typical textures of television images of cloudiness and open sections of the earth's surface obtained with the aid of Meteor satellites.

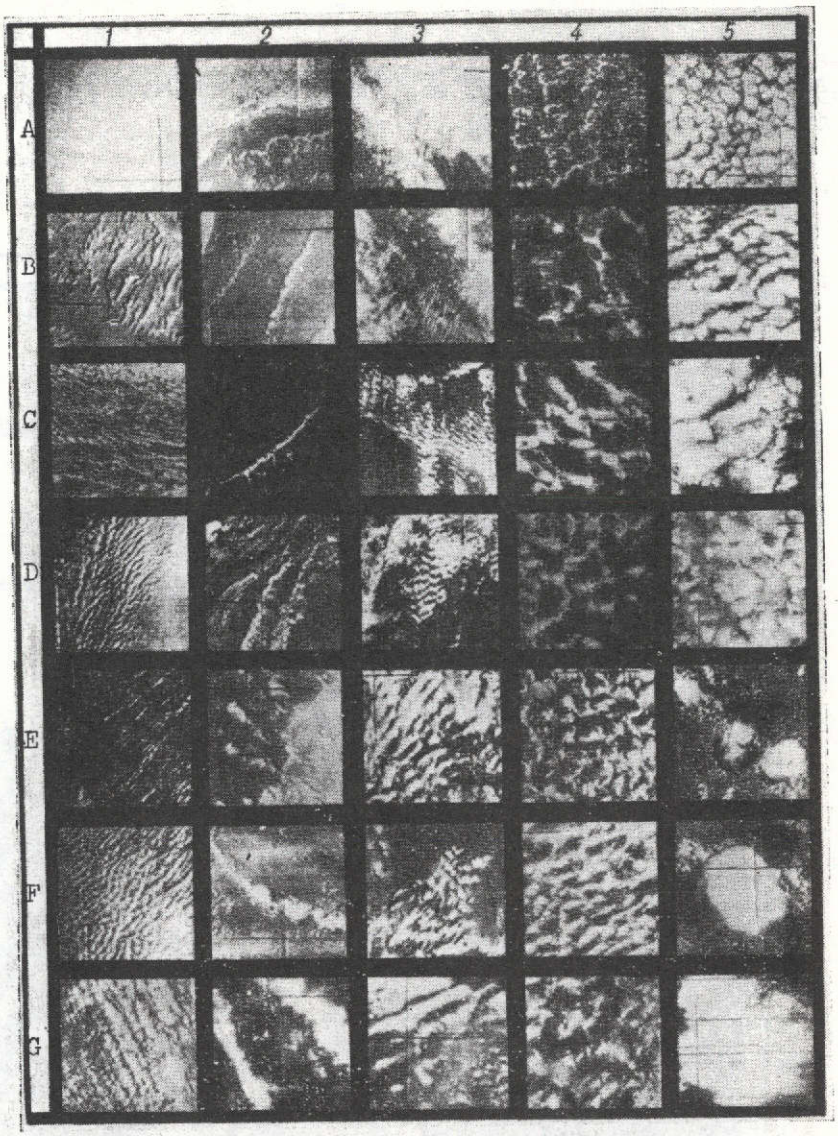

Fig. 15. Typical mesostructures of the television images of clouds obtained with the aid of the Meteor satellites.

Three main types of TV images—dull, granular, and fibrous—are distinguished in the classification.

The first type (dull texture) corresponds to cases where there are essentially no inhomogeneities of image tone. Television photographs with a dull texture are distinguished only by brightness (the fifth column in Fig. 14). Although only seven different tones

(gradations) of brightness are shown in the figure, this does not mean that other tones are not found on the photographs. A dull texture is inherent to images of open (cloudless) sections of water surface (fragments 5-E, 5-F, and 5-G in Fig. 14), dry land in regions of sufficient moisture (5-E, 5-F, and 5-G), arid sections of land areas (5-D and 5-E), solid ice and snow cover (5-A, 5-B, 5-C, and 5-D), and solid stratus-type cloudiness (5-A, 5-B, and 5-C).

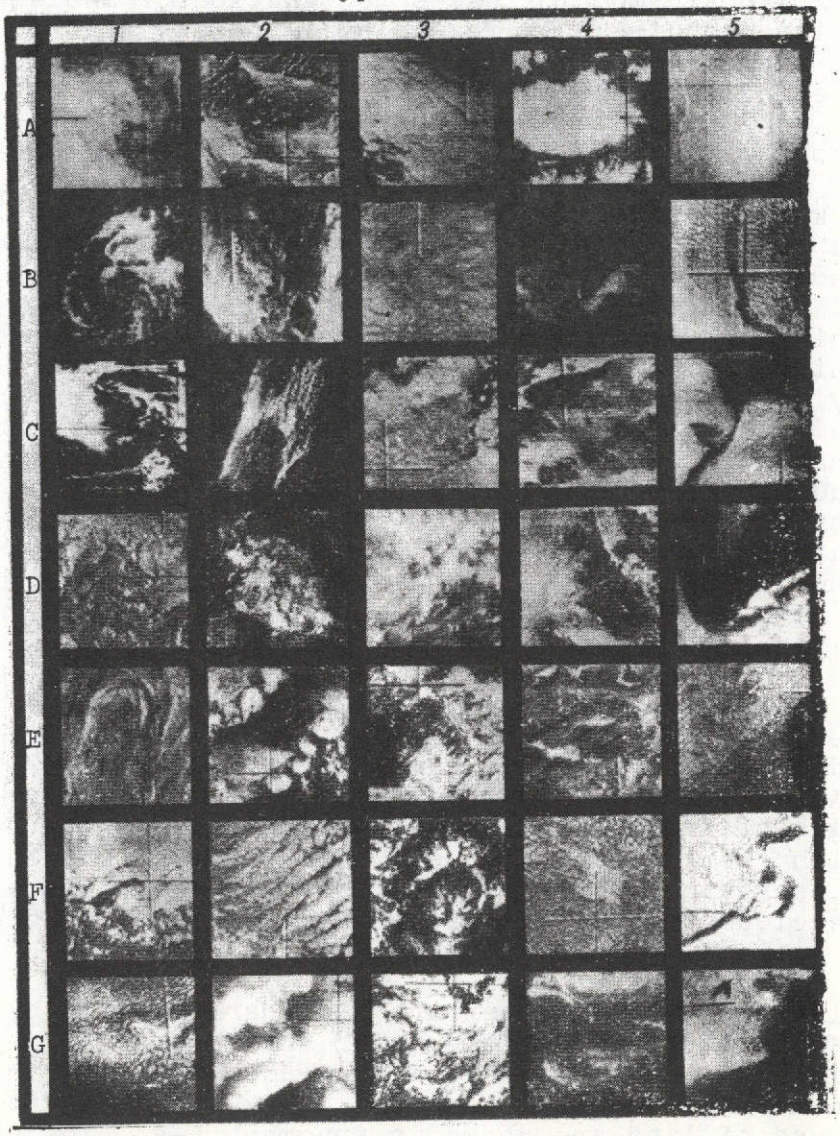

Fig. 16. Typical mesostructures of clouds and open sections of the earth's surface obtained with the aid of the Meteor satellites.

It should be noted that the brightness of the TV image is not in itself a sufficient interpretation feature by which the clouds on the photograph may be distinguished from the underlying surface of the land and sea. Without mentioning snow and ice, which are as bright as clouds, there are images of deserts and water surfaces /55 in the zone of sunlight patches. Stratus clouds cannot be distinguished by image brightness from altostratus or stratocumulus clouds, etc. However, in a number of cases recognition of individual forms of stratus-like cloudiness or fog is still possible if the structure of the large details of the photograph is taken into account. Such cases will be indicated below.

The second type of TV image (granular texture) looks like an accumulation of spots (grains) of light or dark color on a corresponding background (first and second columns in Fig. 14). The small grains usually correspond to images of cumulus clouds (1-D, 1-E, 1-F, and 1-G), where the dimensions of the grains in this case are so small that details of the form of individual clouds are completely hidden. Stratocumulus clouds look similar, except the grains in this case are dark on a light background (1-A). This is explained by the fact that openings in the clouds appear as grains. However, the presence of dark grains on a light background is no guarantee that stratocumulus clouds are imaged. These may also be cumulus clouds in a zone of sunlight patches over a water surface (1-C). In this case the clouds themselves are not visible, but the dark grains represent the shadows of them. Another possible case is shown in fragment 1-B. These are tracks and separations of sea ice. The typical feature is a certain angularity and sharpness of outlines.

Larger grains of light tone usually represent large cumulus clouds, especially in the tropical zone (2-B); individual cumulonimbus clouds, especially at medium latitudes (2-F and 2-G), stratocumulus (2-A, 2-C, and 2-E), altocumulus (2-D), and their combinations. Images of cumulonimbus clouds of this group are difficult to distinguish from similar clouds. Sometimes the presence of erosion and serration on the edges of the grains indicates the ability of a cloud to produce showers. With regard to the brightness of the grains, this is an unreliable feature.

The third type (fibrous texture) is characterized by the presence of fibers, threads, and bands with eneven edges (the fourth column in Fig. 14). This texture represents primarily the cloudiness of high and medium cloud layers. Thus, dense cirrus clouds on a background of land are shown in fragment 4-A. The edge of cirrostratus clouds on a background of solid ice is seen in fragment 4-B. In this case the brightness of the clouds and of the ice is practically the same and recognition is possible only due to the presence of the typical shadows of the clouds (dark fibers

on a light background). The pattern of shadows is usually the main feature in interpretation of cloudiness on a background of snow, ice, and sand. Altostratus clouds, which are distinguished by more even outlines, are represented in fragment 4-C. Fragment 4-E shows multilayer cloudiness with cirrus clouds, and 4-F illustrates the typical form of cirrus clouds, which have developed from the anvils of cumulonimbus clouds. A fibrous texture is sometimes found in images of chains of small cumulus cloud (4-G), and even of the earth's surface (4-D, river valleys).

A special type of texture is inherent to images of land relief /56
(dendritic). Examples of a dendritic texture are shown in the third column of Fig. 14. Its more typical form (3-A) is an image of snow-covered mountains. In the given case these are the Alps. River valleys create a dendritic pattern in fragments 3-B and 3-C. But whereas in the first case the light background of the valley is explained by the predominance of sand and dark soil in the watersheds of it, in the second case the cause is fog in the photographed river valleys. The image of a medium mountainous relief is shown in fragment 3-D. Because of the low position of the sun, some mountain cliffs seem to be shaded during surveying, while others were brightly illuminated, which led to the appearance of a dendritic texture. A dull texture, for example in fragment 5-E, could be obtained under different conditions of surveying this region. Yet another variety of dendritic texture is shown in fragment 3-E. The relief is also determined here due to the low position of the sun. However, unlike the preceding case, the mountainous relief of a snow-covered island, surrounded by continuous sea ice, is represented. It is easy to see that the pattern of the shadows of the mountains in this case is sharply distinguished from that of the clouds in fragment 4-B. Finally, in 3-F, the dendritic texture is created by a hydrographic network, and in 3-G by cracks in ice.

Classification of larger cloud formations (meso-scales) and of the elements of the earth's surface is illustrated in Fig. 15 and 16. The mesostructures, represented in the figures, may be divided into elementary (textural) components. Thus, the grains connected in chains form a striated mesostructure, and the sharply outlined sections of the image with a dull texture—closed cells, etc. The following main types of mesostructure are accepted: banded, cellular, spiral-like, and geometrically irregular.

Typical images of meso-scale bands of cloudiness are presented in the first, second, and third columns of Fig. 15. Whereas the bands are formed of individual or fused grains, these are cumulus or stratocumulus clouds (the first column). There are cases when the clouds themselves are more poorly visible than their shadows (1-B and 1-D) or the shadows only are visible (1-A). If the cloud band has a considerable width, it is often composed of several

series of cumuloform clouds, as is shown in the second column, the presence of serrations of the edges of individual grains in the band being possible (2-E and 2-G), which indicates the ability of the clouds to produce precipitation.

In most cases the bands of cumuloform clouds are extended in the direction of the wind, although not strictly so. But there are exceptions. Thus, in fragment 2-A, breeze clouds, extended along the coast, are represented, and in fragment 2-F the position of the bank of cumulonimbus clouds is caused not so much by the wind as by the humidity of the area (this is a region of one of the oases in the Sahara Desert).

Bands of cumuloform clouds are found very often in practically /57 any synoptic situations and geographical regions.

Examples of bands of fibrous cloudiness are shown in the third column of Fig. 15. The edges of the bands are more eroded (fibrous). This feature, as well as the uniform "trimming" of the ends of the bands often encountered (3-A, 3-B, 3-C, 3-D), assists in distinguishing such clouds, the chains of cumuloform clouds considered above.

The bands of clouds shown in the third column of Fig. 15 are extended at right angles to the air flow and are found especially often in mountainous regions (3-D, 3-E, 3-F, and 3-G) and above islands (Sicily in fragment 3-C).

Open cells, i.e., cloud formations with clearings in the center, are shown in the fourth column of Fig. 15. They are observed in development of convection above a water surface. Such convection develops in a comparatively weak wind in two cases: in the tropics, especially after the arrival of cold air from middle latitudes, and in the rear portions of non-tropical cyclones where the wind has already been attenuated.

Fragment 4-A shows open cells formed of individual cumulus clouds. The cells in fragment 4-B and 4-C are already completely formed, but have been deformed into ellipses due to the presence of the comparatively high force of the wind in the convection layer. The clouds shown in these fragments are capable of producing showers. Fragment 4-D is the classical form of open cells. Forms changing to closed cells are shown in 4-E and especially in 4-G. With respect to fragment 4-F, multilayer cloudiness is represented: bands of altocumulus clouds are oriented at an angle to the underlying chains of cumulus clouds, which creates the visibility of the presence of open cells.

The closed convection cells, shown in the fifth column of Fig. 15, are clearly separated into two types. The first type (5-A, 5-B, 5-C, and 5-D) are altocumulus and stratocumulus clouds forming

lenses, rounded or multiangular spots, separated by narrow small-cloud zones. Such clouds are usually found in the tropics above water surfaces, but are sometimes observed (5-B) above land masses of middle latitudes in a cold air mass.

The second type (5-E, 5-F, and 5-G) is related to the different stages of development of thunderstorm focal areas above land masses at low latitudes. All three fragments are related to equatorial Africa, but similar clouds also form in Southern and Central America and Southeast Asia. The fused focal areas usually comprise a zone of intratropical convergence.

Various types of cloud spirals or, as they are usually called, cloud eddies are shown in the first column of Fig. 16. Large-scale eddies of occluded non-tropical and also of tropical cyclones are more often encountered. Their central portions may consist of both strati- and cirriform and cumuloform clouds (1-A, 1-B, 1-C, and 1-D). Meso-scale eddies are more rarely observed. These eddies develop /58 on the lee side of islands (1-F and 1-G) and more rarely above an open water surface or near the high shores of continents (1-E).

The four remaining columns in Fig. 16 illustrate the different types of cloudiness images, which have no geometrically regular mesostructure, and the various types of images of the earth's surface. These are the types of television images encountered most often, which in themselves attract less attention than, for example, cloud eddies or cells. Moreover, they are much more widely distributed and are more difficult to identify. The fragments in Fig. 16 are selected so that all the varieties of these images encountered are reflected if possible, and, on the other hand, so that the more difficult to recognize are pointed out.

The upper three fragments of the second column are examples of images of combinations of cirrus and cumulus overcast. The lower four fragments of this column, on the other hand, are related to cases where there are cumuloform clouds of medium and lower cloud layers and where there are no cirrus clouds. The upper five fragments of the third column represent multilayer cirri- and stratiform overcast. Stratocumulus clouds with a small amount of cumulus and altocumulus clouds are shown in fragments 3-F and 3-G.

The fourth and fifth columns are devoted mainly to images of the earth's surface. Outlines of the Fergana Valley are easily recognized in fragment 4-A because of a thick fog covering the valley solidly up to the foothills. A similar case is shown in fragment 4-B. Only here the fog is observed in the coastal zone above the Yellow Sea. We note that coastal fog is easy to confuse with images of calm seawater and shallow waters. All the remaining fragments of the fourth column represent only the earth's surface.

Thus, dark cliffs among light sand of the Sahara Desert are visible in 4-C. Coniferous forests (the dark spots) among snow-covered fields in the north European USSR are shown in fragment 4-D, which is quite similar to 4-C. The image of a section of desert in Mexico (4-E) differs somewhat from both the fragments described above. The outlines of the Rybinskoye Vodokhranilishche, covered with ice, can be recognized in 4-F and Crete in 4-G.

The two upper fragments in the fifth column show how large river valleys (the Niger in 5-A and the Nile in 5-B) look in TV photographs. It is obvious in 5-A that a sandy desert may produce patches of sunlight. The five lower fragments of this column were selected especially to show how the brightness of different objects of the earth's surface may vary. The region of the Nile Delta is shown in 5-C. The Delta itself and the irrigated land in the valley have the dark tone of the image, and the deserts the light tone. The desert in 5-D (the Persian Gulf) is also light, while the tone of the water surface is the same as in the irrigated land in the preceding fragment. On the other hand, the land mass in 5-E (the mouth of the St. Lawrence River) is dark, while the water surface is light. This is explained by the fact that surveying was carried out in winter, when the ice and the coastal surface of the Atlantic Ocean are covered with ice. Coniferous forests, as we ascertained /59 earlier, look just as dark in winter as in summer. The coast of Antarctica is shown in 5-F. The snows of the mainland and the sea ice here are almost equally as light, while the clear water zone near the coast is dark.

The last fragment (5-G) shows overcast on a background of a water surface. The sharp edge and the dull texture of the image render this overcast very similar to the sections of land area presented above. A guarantee of correct interpretation may be only a good knowledge of the geographical map in such cases.

The principles of meteorological interpretation of IR photographs of the earth, obtained with the aid of satellites, are the same as those of the photographs in the visible region described above, although there are known differences related to the greater variability of the thermal background of surveying, the dependence of the image tone on cloud height, the considerably lower resolution of IR images, as well as an essentially different mechanism of generation of radiation, serving as the primary data source.

Thus, the IR equipment of the Meteor satellites provides a terrain resolution of only 15×15 km^2 with a coverage of about 1000 km. Therefore it is clear that photographs contain information only about meso- and large-scale formations. In particular, the texture indicates the meso-scale perturbations in the radiation field. Meso-scale perturbations are not typical for the atmosphere;

therefore, the texture of IR photographs is rather poor compared to that of daytime TV photographs with much higher resolution obtained with the aid of satellites of the Meteor system. The following classes of texture—granular, fibrous, mat, and complex—may be distinguished for purposes of interpretation.

A granular texture is a combination of rounded spots of light or dark tone on a corresponding background and is subdivided into fine-grain and coarse-grain (platy). In the first case the grains consist of no more than one or two tens of scanning elements of the IR photograph, from which it is practically impossible to recognize to what extent the form of the perturbations, represented in the "grains" differ from oval shape. The grains of a coarse-grained texture are so large that they may be subdivided into circles, polygons, etc.

Examples of IR images of granular texture are shown in Fig. 17, where 30 typical fragments of IR images of clouds and of the earth's surface obtained with the aid of the Cosmos-122, 144, and 156 satellites are mounted. Each fragment corresponds to a terrain section of approximately 400×400 km^2. The second column in Fig. 17 gives five examples of fine-grained texture. Thus, fragment 2-A is an IR image of stratocumulus clouds. The dark grains are the image of openings in these clouds. On the other hand, fragment 2-E is an example of light grains (cumulonimbus clouds on a background of a water surface). Fragments 2-B and 2-D show that a granular texture does not always correspond to cumuloform overcast. The Island of /60
Sokotra, taken from the Cosmos-144 satellite during the day when the surface of the island was warmer than the surrounding water surface, is shown in fragment 2-B. This fragment is quite similar to fragment 2-A with the "cloud" grains already mentioned. The importance of the meteorologist interpreter having a knowledge of the geography of the photographed region of the earth may be judged from this example. However, if the dimensions of the grains are larger so that some details of their shape may be recognized, differentiation of the clouds and of the earth's surface is facilitated. An example is fragment 2-C, where the structure of so-called open cloud cells was rather clearly manifested. Finally, the very fine grains of fragment 2-D are the result of the effects of interference and some disruptions in operation of the IR equipment.

Variants of large-grained texture are shown in the third column of Fig. 17. Typical examples of it are shown in fragments 3-B and 3-C. These are cumulonimbus clouds: the first—in tropical latitudes above Africa—and the second—above land areas of middle latitudes. Plates of stratocumulus clouds with a lower elevation of the upper boundary and therefore darker are shown in fragment 3-E. As already mentioned, the tone of the image is not, however, a reliable interpretation feature, since cases are quite possible when /61

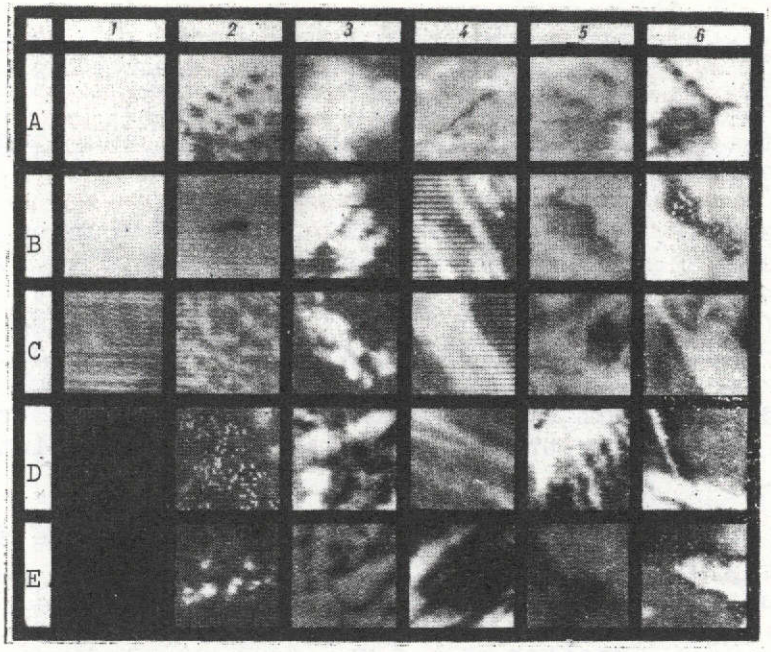

Fig. 17. Typical textures of infrared images of clouds and of open sections of the earth's surface, obtained with the aid of Meteor satellites.

stratocumulus clouds will not look the same as in 3-E, but will be quite similar to the cumulonimbus clouds in fragment 3-C. But then the case illustrated in fragment 3-D is quite reliable. Here the bright white grains of cumulonimbus clouds are closely adjacent to the darker grains of lower clouds, between which, in turn, black cloudless sections are visible. The presence of two clear jumps of image tone is reliable proof of vertical stratification of the clouds. Fragment 3-A is the jump from coarse-grained to fibrous texture. The bright white spots of thunderclouds, photographed in the tropics, do not have sharply defined edges in this fragment. This is related to development of cirrus clouds from anvils.

Examples of fibrous texture are presented in the fourth column of Fig. 17. The images here consist of individual threads and bands which usually have no sharp boundaries. Images of cirrus and altostratus clouds (fragments 4-D and 4-C, respectively) usually have such texture, but these may also be chains of cumulonimbus (4-B) and bands of stratocumulus and altocumulus clouds (4-E). Large river valleys are also represented on IR photographs as fibers: light, if they are photographed on a background of hot dry soil, or dark, as in fragment 4-A, where the Volga River was photographed in summer at night.

Those cases where there are no meso-scale inhomogeneities in the temperature field of the emitting surface form a special class, so that the IR image has a uniform light or dark background (a mat texture). Five examples of a mat texture, which illustrate the scale of half-tones of IR images, are given in the first column of Fig. 17. The lightest tone (1-A) usually corresponds to an image of solid overcast from a high upper boundary. But these may also be snow-covered sections of land areas or ice, as in fragment 1-B. Grey tones are more frequently encountered and they are less stable. For example, a cloudless section of water surface of the Pacific Ocean west of California is shown in fragment 1-C. Fields of stratoform cloud cover in middle and high latitudes often have exactly the same tone. On the other hand, an open water surface is often represented by a much darker tone (fragment 1-E). Land areas during warm seasons more often have the tone of fragments 1-C and 1-D, and in cold seasons of fragments 1-B and 1-C.

The fifth and sixth columns of Fig. 17 are given as examples of images having a complex texture. Grains, fibers, and sections of uniform tone may be found here simultaneously. For example, fragments 5-A and 5-C are apparently the most typical images of cloud cover with breaks in the background of the land area. Fragment 5-B is an example of an IR image of washouts and cracks in the ice near the shores of Antarctica. Multilayer overcast, represented by intersecting fibers of cirrus and cumulus clouds, is shown in fragment 5-D. Fragment 5-E is proof of the fact that the dendritic /62 texture of a mountain image, which is so typical for daytime TV photographs in the visible region, may be absent on an infrared image. The light upper angle of this fragment corresponds to an image of the Malyy Kavkaz Mountains, and the dark lower angle represents Mesopotamia.

The sixth column of Fig. 17 mainly illustrates the typical configurations of sections of a mat texture. The first three fragments are the result of daytime surveying of the Baku region, California, and the Sinai Peninsula, respectively. In all cases, a cloudless water surface has a mat texture of light grey or grey tones (as in 1-B or 1-C). Land areas, where they are not covered by clouds, have a uniform dark grey tone (as 1-D); where clouds appear, some inhomogeneities of tone are discernible. The white section of fragment 6-A, as in the corresponding sections of 6-D and 6-E, is an image of the Caucasus Mountains, partially covered by clouds. The overcast band in fragment 6-D is especially discernible. This is a bank of altocumulus clouds. It extends from the northwest to the southeast (from the region of Rostov-na-Donu to the Elbrus region) and is lost on a background of cold snow-covered peaks. Moreover, a narrow dark border along the southern extremity of the Caucasus Mountains—a warmed coastal zone—is discernible in fragment 6-E.

Using the tone and pattern of the image as interpretation features, any photograph may be divided into zones, within the limits of which the tone and pattern of the image are more or less invariable. In most cases this means that the nature of the overcast in each of these zones is also relatively constant. The fraction of scanning elements which may be related to cloud elements within the limits of each distinguished zone indicates the total amount of clouds in a corresponding section of the atmosphere. A gradation of ten units may be indicated in nephanalysis in the seeming total absence of openings in clouds. If there are openings, but they are clearly less than 50% of the area of the zone, this is considerable overcast (9-7 units). When the area of cloudy and inter-cloudy elements is approximately identical, variable overcast (6-4 units) may be indicated. If there are clouds, but they are clearly less than half of the total area of the zone under consideration, we use the gradation of light overcast (3-1 units). The total absence of any traces of clouds is the basis to use the gradation "clear" in nephanalysis.

It should be noted that the indicated gradations differ from those which are presently used in operative practice. However, as we will show further, our proposed gradations correspond better to the interpretation capabilities of the TV equipment of Meteor satellites.

The considered characteristics of the image of meso-scale perturbations in the temperature field of an emitting surface does not exhaust all the meteorological information which may be used as a result of interpretation of IR photographs. The structure of large sections of IR images, consisting of many thousands of scanning /63 elements, has valuable interpretation possibilities. This structure represents the characteristics of the overcast field of synoptic scale: clouds and atmospheric fronts, cyclones, and intratropic zones, etc. Therefore, we note in conclusion of the description of methods for interpretation of overcast from space photographs of the earth, obtained with the aid of satellites, that, although overcast is the only meteorological phenomenon directly observable in TV surveying of the earth from space, many other important meteorological characteristics may be determined from the type of clouds, including pressure, wind, and atmospheric humidity, which are directly usable in forecasting procedures. Among the qualitative and quantitative procedures used for this, we may name indirect interpretation of TV images.

Indirect methods usually yield poorer results than those which are used in direct measurement of the characteristics of interest to us. Therefore, we may think that indirect interpretation has not been widely developed and will be pushed out in the future by "direct" analysis of the meteorological fields, for example, by spectrometric data.

However, a large number of publications are presently devoted to indirect interpretation of TV images. A survey of a considerable number of them, devoted mainly to qualitative methods of indirect interpretation, is given in L. S. Minina's book [45]. Of the number of investigations devoted to quantitative methods, the cycle of articles of Sh. A. Musayelyan et al [46-50], as well as detailed statistical investigation of the relationships of the overcast field to the fields of other meteorological elements, carried out in the work of Ya. R. Klauss [108], should be mentioned first. Various special approaches to solution of the problem of indirect interpretation are presented in [9,27,39,40,101,108,148,153,154,161, 167], where the amount and form of clouds, evaluated from photographs, are used as the feature. Mesostructure is used as the feature in [15-17,19,20,61,92,102,110,111,119,120,123,124,133,135,138, 143,146,147,158,160,173] and the macrostructure of overcast is used in [3,4,13,14,18,24,26,45,52,57,58,91,92,96,105,134,136,137,142,144, 149,154,155,156,157,165,166,171,172,174].

2. Evaluation of the Quality of Interpretation

The quality of nephanalyses is evaluated by comparison of them with data of ground observations of overcast during the nearest synoptic period in the corresponding region. Besides interpretation errors, such factors as errors in geographic control matching of photographs, the asynchronism of satellite and ground observations of overcast, the sparseness of the ground meteorological station network [65], and errors in ground observation of overcast have a considerable effect on the results of such comparison. Therefore, the first task which must be resolved when evaluating the /64 quality of interpretation is to take into account all the enumerated factors.

Taking into account errors in ground data on overcast presents no great difficulties, insofar as it is known that these errors are within the limits of one or two units. Taking into account the asynchronism of observations and errors in geographic control matching of images is a more complicated matter.

The given problem was solved by developing a special method for evaluating the information content of satellite data.[1] In this case an error in geographic control matching and the asynchronism of receiving satellite data with the synoptic period is manifested

[1]Associates of the Hydrometeorological Center of the USSR M. G. Nayshuller and T. A. Yakovleva, as well as graduate of the Department of Meteorology of Moscow State University A. Zhigalkin, participated in the calculations carried out in realization of the method.

in a phase shift of the overcast field. Then, for the individual harmonics of the overcast field, the relative mean square error of nephanalysis may be calculated by the formula

$$\varepsilon^2 = \frac{1}{\sqrt{2\pi}\,\sigma} \int_{-\infty}^{\infty} \exp\left\{-\frac{1}{2}\left(\frac{\varphi}{\sigma}\right)^2\right\}(1-\cos\varphi)\,d\varphi, \qquad (2.1)$$

where σ is the mean square error of geographic control matching; ϕ is the error in geographic control matching of individual nephanalysis, where the law of error distribution of geographic control matching is assumed to be normal.

Figure 18 illustrates the results obtained in this case: the mean square error of nephanalysis reaches the value of the natural variability of overcast in a phase shift equal to the length of the half wave of the harmonics being considered. Therefore, in practical nephanalysis the area of averaging of data on overcast should be no less than twice as great as the value of the mean square error in geographic control matching and, taking into account the ordinary asynchronism of satellite TV (IR) surveying during one or two hours, this value should be again increased by two- or three-fold.

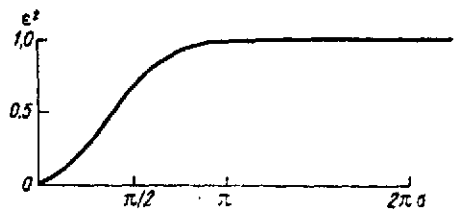

Fig. 18. Dependence of mean square error of estimating the total amount of clouds for the individual harmonics of the overcast field on the value of the mean square error of geographic control matching of photographs.

These recommendations were checked after the launching of the Cosmos-122 satellite. It turned out that, due to the high earth resolution and greater accuracy of geographic control matching, the information content of the nephanalyses, constructed from data of TV surveying from satellites of the Meteor system, is higher than that of the nephanalyses obtained from data of the ESSA satellites. The main cloud patterns (according to generally accepted classification) may be confidently recognized with visual interpretation of the TV photographs of Meteor satellites. Difficulties /65 arise only in recognition of clouds on a background of snow and ice. But even in this case a knowledge of the synoptic and climatic characteristics of overcast for the corresponding geographic region makes it possible to recognize clouds with a reliability no less than that of ESSA nephanalyses in the absence of snow and ice.

However, despite the high interpretation possibilities of TV images of Meteor satellites, the information content of nephanalyses

obtained upon interpretation of them with respect to the state of overcast during the synoptic period was still rather low due to the asynchronism of the TV surveying with this period, errors in geographic control matching, and the different scale of averaging in satellite and ground observations. Taking into account the value of the mean square error in geographic control matching of data from Meteor satellites (about 50 km) and proceeding on the requirements to minimize the mean square error in estimation of the total amount of clouds, an optimum form for presentation of nephanalysis may be recommended. In particular, it was indicated above that the optimum dimensions of averaging in interpretation should be approximately equal to the quadruple value of the error in geographic control matching. In the case of Meteor satellites, this value comprises about 200 km.

The results of practical checking of the given recommendation are presented in Table 3, compiled on the basis of comparing ground data (in the central regions of the European USSR) on the total amount of clouds with data of interpretation of TV photographs of the Cosmos-144 satellite. Essentially synchronous satellite and ground data (the difference is no greater than 0.5 hours) were selected, which made it possible to study the effect of the error /66 in geographic control matching of TV photographs.

Table 3. Average a posteriori uncertainty (entropy) of diagnosis of total amount of cloud (in parentheses) and the amount of information contained in nephanalysis from satellite data of the experimental Meteor system as a function of the scale of averaging in interpretation of TV photographs.

True total amount of clouds, points	Scale of averaging, km					
	50	100	150	200	300	400
10	(0.880) 1.440	(0.997) 1.323	(0.986) 1.334	(0.902) 1.418	(0.755) 1.565)	(0.844) 1.476
9—7	(1.637) 0.683	(1.671) 0.649	(1.557) 0.764	(1.592) 0.728	(1.497) 0.823	(1.501) 0.819
6—4	(2.130) 0.190	(2.148) 0.172	(2.136) 0.184	(2.112) 0.208	(2.141) 0.179	(2.192) 0.128
3—1	(2.053) 0.627	(2.018) 0.308	(1.993) 0.327	(2.072) 0.248	(1.954) 0.366	(1.972) 0.348
0	(2.000) 0.300	(2.136) 0.184	(1.996) 0.324	(2.018) 0.302	(2.057) 0.263	(1.627) 0.693

The values of the a posteriori entropy of diagnosis of the total amount of clouds with a different degree of averaging of satellite nephanalyses are presented in Table 3. It is obvious that the entropy is minimal in the averaging diameter equal to an average of

200-300 km. Thus, rational smoothing actually improves the quality of satellite data on overcast.

The maximum accuracy of restoring the overcast field from data of TV surveying from the Meteor satellites is such that five gradations of the total amount of clouds (solid, significant, variable, slight, and clear) and the main cloud patterns may be indicated in the nephanalysis.

The results of comparison of the main characteristics indicated in nephanalysis (total amount of clouds) are presented in Tables 4-7. The method of comparison of the tables was the following. Each ground observation of overcast was compared to the amount of clouds according to satellite data, indicated in the nephanalysis for the cloud contour covered by the corresponding meteorological station. In this case each comparison of satellite and ground estimates of the total amount of clouds was "weighted" in proportion to the correlation coefficient of cloudiness with a shift in time equal to the value of the time divergence of the satellite and ground data being considered. Thus, if the time differences between the synoptic period and the moment of surveying did not exceed one-half hour, a "weight" was selected equal to ten. The "weight" was equal to nine if the value of asynchronism varied from one-half hour to one hour.

Table 4. Recurrence (number of "weighted" cases and percentage in parentheses) of the various total amount of clouds (in points) from ground observations at a separate station provided that the total amount of clouds according to data of TV survey from the Cosmos-122 satellite is known.

Satellite data	Ground data					Total, unconditional recurrence (in parens.)
	10	9–7	6–4	3–1	0	
10	1502 (62.6)	607 (29.0)	129 (5.4)	38 (1.6)	34 (1.4)	2400 (12.0)
9–7	2169 (27.0)	4215 (52.2)	915 (11.3)	611 (7.6)	155 (1.9)	8065 (40.1)
6–4	277 (9.5)	1129 (38.7)	685 (23.5)	531 (18.2)	296 (10.1)	2918 (14.6)
3–1	196 (4.9)	847 (21.2)	655 (16.4)	1472 (36.8)	830 (20.7)	4000 (19.8)
0	124 (4.5)	255 (9.4)	217 (7.4)	441 (16.2)	1670 (61.5)	2707 (13.5)
Total	4268	7143	2601	3093	2985	20090
Unconditional recurrence	(21.3)	(35.3)	(13.0)	(15.4)	(15.0)	(100.0)

Table 5. Recurrence (number of "weighted" cases and percent in parentheses) of various total amount of clouds (in points) from ground data for different gradations of nephanalysis according to data of IR surveying from Cosmos-144, 156, and 184 satellites. Middle latitudes, one season. /67

Gradations of nephanalysis	Ground data					Total, unconditional recurrence (in parens.)
	10	9–7	6–4	3–1	0	
10	488 (42)	484 (42)	122 (10)	32 (3)	27 (3)	1153 (9)
9–7	812 (31)	1364 (52)	299 (11)	53 (2)	113 (4)	2641 (20)
6–4	360 (12)	1204 (41)	628 (21)	555 (19)	208 (7)	2955 (23)
3–1	177 (4)	996 (22)	737 (17)	1200 (27)	1350 (30)	4460 (34)
0	63 (3)	138 (7)	240 (13)	496 (25)	1008 (52)	1945 (14)
Total	1900	4186	2026	2336	2706	13154
Unconditional recurrence	(14)	(32)	(15)	(19)	(20)	(100)

Table 6. Recurrence (number of "weighted" cases and percent in parentheses) of various total amount of clouds (in points) from ground data for different gradations of nephanalysis according to data of IR surveying from Cosmos-144, 156, and 184 satellites. Middle latitudes, cold season (with snow and ice cover).

Gradations of nephanalysis	Ground data					Total, unconditional recurrence (in parens.)
	10	9–7	6–4	3–1	0	
10	342 (48)	280 (39)	43 (7)	21 (3)	20 (3)	709 (14)
9–7	398 (54)	244 (33)	23 (4)	35 (5)	30 (4)	730 (14)
6–4	534 (45)	483 (40)	68 (5)	56 (5)	56 (5)	1197 (23)
3–1	228 (18)	190 (15)	136 (10)	472 (36)	270 (21)	1296 (25)
0	228 (18)	190 (15)	136 (10)	270 (21)	472 (36)	1296 (24)
Total	1730	1387	406	857	848	5228
Unconditional recurrence	(34)	(26)	(8)	(16)	(16)	(100)

The values of the correlation coefficients are borrowed from [69]. Since it is recommended that the total amount of the clouds is assumed to be an average between the amount indicated for both

cloud fields forming the boundary when using nephanalysis for regions through which the boundary of the cloud field (contours) passes, the derived "weight" is multiplied by two in those cases where the meteorological station is located at a distance of 100 km or more from the point at which the boundary was located. Otherwise the "weight" was multiplied by one. At the same time the possible error in geographic control matching of the image was taken into account during comparison.

Table 7. Recurrence (number of "weighted" cases and percent in parentheses) of various total amount of clouds (in points) from ground data for different gradations of nephanalysis according to data of IR surveying from Cosmos-144, 156, and 184 satellites. Tropical zone. /68

Gradations of nephanalysis	Ground data					Total, unconditional recurrence (in parens.)
	10	9–7	6–4	3–1	0	
10	63 (43)	58 (40)	12 (8)	4 (3)	9 (6)	146 (8)
9–7	49 (18)	139 (51)	63 (23)	4 (2)	16 (6)	271 (16)
6–4	35 (7)	115 (24)	85 (17)	139 (29)	111 (23)	485 (29)
3–1	0 (0)	57 (11)	68 (14)	129 (26)	246 (49)	500 (30)
0	4 (2)	2 (1)	28 (10)	4 (12)	248 (85)	286 (17)
Total	151	371	256	280	630	1688
Unconditional recurrence	(9)	(22)	(15)	(17)	(37)	(100)

The totals of the "weights" for all pairs of nephanalyses—the ground meteorological station and the "weighted" frequencies with which the different gradations of overcast according to ground data were observed with different gradations of nephanalysis—are presented in Tables 4-7. As can be seen from the data of the tables an overcast from solid to "clear" is possible with any nephanalysis according to ground data. However, this does not mean that nephanalysis is all bad.

As already mentioned, the results of comparison are affected by a number of factors besides the errors in interpretation. Although asynchronism and errors in geographic control matching were often taken into account by "weighting" the observations, their effect was not completely excluded. The effect of the infrequency of the network of errors in ground observations is also not completely excluded. In order to take all this completely into account, the data of Tables 4-7 should be compared to reference

tables compiled according to the following principle. Some kind of errorless data on overcast, for example data of such a dense network of ground meteorological stations in which the scanning sectors of adjacent stations overlap, should be used in the reference tables instead of satellite data. These "ideal" data should be compared to those of the same ground network which was used for comparison with satellite nephanalyses. Moreover, the value of the asynchronism of the compared observations of the "ideal" and /69 of the infrequent network should be the same as the satellite data. The time shift in our case should essentially comprise one hour for the data of Tables 4-6 and six hours for Table 7. Tables which can be used as references are presented in the Appendix (Tables I and II). The observations of meteorological stations in the environs of Moscow are used as the "ideal" network in them. The average amount of clouds according to the ring of stations within a radius of 100 km of Moscow was compared to observations in Moscow itself. This average radius was selected on the basis of the fact that the mean square error in geographic control matching of the images comprises approximately 50 km.

The reference tables obtained may be compared with Tables 5 and 6. Good agreement was obtained for Table 5. Thus, for example, the recurrence of solid overcast comprises 42% in Table 5 provided that it is also indicated in the nephanalysis as solid, and, according to data of comparing the "ideal" and infrequent network of ground stations (Appendix I), this value should be equal to 49%, for which the nephanalysis may be assumed to be errorless. The recurrences of other gradations of overcast also agree rather closely. The average information content of nephanalysis, calculated according to the method indicated in [7], comprises 16% according to the data of Table 5, which almost coincides with the value of the information content, which under similar conditions provides an "ideal" network of observations of overcast. This makes it possible to state that five gradations of the total amount of overcast may be confidently distinguished in interpretation of IR photographs obtained from satellites of the Meteor system, in the case of surveying at middle latitudes during the warm season. The spread of values in Table 5 is entirely explained by the reasons indicated above and primarily by the non-coincidence of the surveying and synoptic periods.

With regard to IR surveying of clouds on a background of subzero temperatures of the earth's surface (Table 6), the matter here is much worse. For example, the recurrence of solid overcast in nephanalysis of ten points is equal to 48%, but it should be 93% in the case of errorless interpretation; the recurrence of clear weather in nephanalysis of zero points was equal to 36%, but should be 93%. The average information content of nephanalysis was equal to 17%, but should be 54%. Thus, in the case of IR surveying of

clouds during the cold season, when the temperature of the underlying surface is close to that of the tops of the clouds, reliable recognition of the nature of overcast is impossible, because the interpretation errors are very large. We note, however, that due to the much lower time variability of overcast during the cold as compared to the warm season, the average information content of nephanalysis with respect to the state of the cloud cover during the synoptic period under the considered conditions is not inferior to that for the warm season.

The data presented in Tables 4 and 7 may not be evaluated quantitatively, because the data of a dense network of meteorological stations in the tropics are required for this. However, qualitative comparison of them with the data of Tables 5 and 6, taking into /70
account the average value of the time shift of the moment of surveying with respect to the synoptic period, permits the assumption that nephanalysis by TV photographs for the entire earth during the warm season and by IR photographs in tropical latitudes may be no worse than in the case of IR surveying at middle latitudes during the warm season.

All the foregoing is related to analysis of the quality of interpretation. Meteorologists are not primarily interested in the information content of satellite nephanalysis with consideration of its actual asynchronism with the synoptic period, etc. In connection with this, the fact that an overcast from 10 to 0 points (see Tables 4-7) is possible in any nephanalysis is an important disadvantage, although, as we have already explained, it follows from the asynchronism of surveying with the synoptic period rather than from the poor quality of interpretation. Mechanical reference of nephanalysis to the synoptic period essentially provides satellite data as the information source on the state of overcast at an individual station. In order to raise the information content of nephanalysis under these conditions, it is suggested that satellite data be assumed to characterize the average state of the cloud cover over rather large areas. Thus, the amount of overcast indicated in some contour of nephanalysis may be interpreted as the average amount of clouds over the entire area encompassed by this contour.

Tables similar to Tables 4-7 were compiled for quantitative analysis of the information content of nephanalysis in such interpretation, except the nephanalysis in them was compared to ground data averaged within the limits of each contour. The recurrences /71
in percent for all groups of nephanalysis are shown in Tables 8 and 9. When these data are compared to the corresponding data of Tables 4-7, it is obvious that the spread of values decreased. This should have been expected, because like the average overcast within the limits of the periphery, we almost completely exclude

the spread due to errors in geographic control matching, and we considerably reduce the effect of asynchronism, because the large-scale perturbations in the overcast field have a lesser temporal variability.

Table 8. Recurrence (number of "weighted" cases and percent in parentheses) of various total amount of clouds (in points) according to ground observations for an average cloud field provided that the total amount of clouds in the field is known from data of TV surveying from the Cosmos-122 satellite.

Satellite data	Ground data					Total, unconditional recurrence (in parens.)
	10	9—7	6—4	3—1	0	
10	266 (48,2)	261 (47,2)	22 (3,9)	0 (0,0)	4 (0,7)	553 (15,0)
9—7	179 (14,8)	801 (65,5)	220 (18,1)	15 (1,3)	7 (0,3)	1222 (33,3)
6—4	31 (4,1)	295 (38,8)	354 (46,6)	79 (10,5)	0 (0,0)	759 (21,3)
3—1	7 (0,8)	118 (14,0)	378 (44,8)	325 (38,6)	16 (1,8)	844 (22,8)
0	0 (0,0)	0 (0,0)	87 (30,9)	170 (61,1)	22 (8,0)	279 (7,6)
Total Unconditional recurrence	483 (13,2)	1475 (40,2)	1061 (29,0)	599 (16,3)	49 (1,3)	3657 (100,0)

The remaining spread of points is still rather large. In order to assess the importance of the differences between the gradations of nephanalysis, let us use the Kolmogorov criterion to check the hypothesis that two random samples are taken from the same general set [90]. As we know, according to this criterion, the difference between two empirical distribution functions F_1 and F_2 is significant with a probability α, if for the value of the maximum difference between these (integral) functions $\max |F_1 - F_2|$ the following condition is fulfilled

$$1 - K\left\{\max|F_1 - F_2| \sqrt{\frac{n_1 n_2}{n_1 + n_2}}\right\} \leqslant \alpha, \qquad (2.2)$$

where n_1 and n_2 are the volumes of the first and second samplings, respectively, and $K\{\cdot\}$ is the Kolmogorov function tabulated in [90].

The following conclusions were reached according to the Kolmogorov criterion for the data presented in Tables 8 and 9. For TV

Table 9. Recurrence (in percent) of various total amount of clouds (in points), averaged according to the coverage of nephanalysis, according to ground observations for different gradations of nephanalysis from data of IR surveying from the Cosmos-144, 156, and 184 satellites at middle latitudes during the warm season, at middle and high latitudes during the cold season, and at tropical latitudes.

Gradation of nephanalysis	Gradation of ground data				
	10	9—7	6—4	3—1	0
10	19	65	12	4	0
	31	59	10	0	0
	41	39	20	0	0
9—7	3	63	30	2	2
	45	48	7	0	0
	6	50	40	4	0
6—4	3	48	38	8	3
	0	56	29	7	8
	4	16	35	29	16
3—1	5	20	39	34	3
	14	32	36	17	1
	0	5	36	44	15
0	7	8	16	60	9
	11	12	17	30	30
	0	6	7	27	60

surveying during the warm season at middle and tropical latitudes, the probability of the fact that the nephanalysis, in which is given 10 and 9-7 points, 9-7 and 6-4 points, and 6-4 and 3-1 points, is actually related to the different overcast, exceeds 99%. Only gradations of 3-1 and 0 points have a greater chance of being related to the same overcast (3%). Thus, when the period of TV surveying differs from the synoptic period by approximately one hour, five gradations of nephanalysis (solid, significant, variable, slight, and clear) may be used reliably. For IR surveying during the warm season at middle latitudes, the probability of the fact that nephanalysis in which is given 10 and 9-7 points refers to the same overcast, was equal to 80%. These gradations of nephanalysis may be assumed to refer to the actually different overcast only with a probability of 20%. For other adjacent gradations the levels of importance of differences in samplings were 50, 86, and 61%, respectively. A gradation of 10 points then differs from that of 6-4 points with a probability of 85%, that of 9-7 points differs from that of 3-1 points with a probability of 99.7%, and that of 6-4 points differs from "clear" with a probability of 99.4%.

Thus, when the period of IR surveying differs from the synoptic period by approximately an hour, a minimum of three gradations of nephanalysis (significant, variable, and slight) may be used, but it is quite probable that four gradations are best.

The corresponding levels of significance are the following for middle latitudes during the cold season and for high latitudes during IR surveying: practically zero for the difference between nephanalysis in which is given 10 and 9-7 points; the same is true for other adjacent gradations. For gradations through one, beginning from 10 and 6-4 points, it is 65, 99, and 65%. Consequently, overcast may be confidently divided into two gradations (many clouds or few clouds) according to nephanalysis under the given conditions. It is possible (probability of 65%) that three gradations are recognizable.

The differences between adjacent gradations for tropical regions have a level of significance of 72% for comparison of cases for 10 to 9-7 points; 99.6% for 9-7 to 6-4 points; 27% for 6-4 to 3-1 points; and 60% for 3-1 points to "clear". In other words, a comparatively small number of analyzed cases does not permit assumption of a reliable divergence between the laws of distribution of recurrences of different gradations of overcast in the case of 6-4 and 3-1 points. Thus, despite the greater difference of the moment of surveying from the synoptic period, in the given case nephanalysis carries significant information as a minimum of four gradations of overcast.

Chapter 3
AUTOMATION OF INTERPRETATION

1. Statement of the Problem of Automating Interpretation of Overcast from Data of Television Surveying of the Earth from Satellites /73

The procedure for meteorological analysis of TV photographs of the earth obtained with the aid of satellites, as we have seen, is an extremely labor-consuming one. Its results are subjective because they depend on the experience and the personal prejudices of the meteorologist interpreter. The enormous amount of photographs incoming from the satellites daily and the mechanical nature of many operations of processing them all lead to the fact that crude errors are sometimes encountered in practical interpretation, and the average level of operatively compiled nephanalyses is comparatively low. Thus, the meteorologist interpreter, capable of high-quality analysis of the TV image of as many complex situations as desired, for example recognition of clouds on a background of snow and ice, is hardly suitable to carry out daily processing of satellite data. Mass processing should be turned over to the automatons. However, in the given case the absence of processing (interpretation) does not reduce to simple calculation, but consists in making complex logical decisions (differentiation of images of clouds and open sections of land and sea, recognition of the type and pattern of clouds, and estimation of their amount).

A recently developed branch of cybernetics—the theory of pattern recognition—is involved in problems of this type. This theory is still only being formed; therefore, it is difficult to calculate that in the future algorithms will be developed for automatic processing of photographs which, in the completeness of the meteorological data derived from the images, will exceed or even be comparable to the meteorologist interpreter. However, the problem of extracting the major portion of this information, for example estimation of the main patterns and total amount of clouds, is apparently achievable. In this case the advantages of such automatic processing should include its objectivity and guaranteed absence of crude omissions. Automation of interpretation of overcast is the essentially real possibility of utilizing satellite nephanalysis within the procedures of numerical analysis and weather forecasting.

In accordance with the theory of pattern recognition, formulation of the problem of automatic interpretation reduces to the following. The object of recognition is the TV (IR) image, which we will further denote by the vector x. The set of all possible images (of vectors x) forms the image space X, sometimes called the space of features on the basis that vector x contains all the information used for recognition. For example, the TV signal of the photograph, written line by line in a digital form, may be figured as x. /74

Various TV images generally correspond to various types of clouds, but this may not be true in individual cases. The reason is the comparative "crudeness" of the TV images of clouds, as well as the naturally existing gradual transition from clouds of one type to another, for example, from cumulus to stratocumulus, stratonimbus to altostratus, etc. Thus, the problem of recognition of clouds by the type of their TV image is essentially probabilistic. It is natural to take the probability of relating the overcast of the TV photograph to the type of clouds which it actually represents as the criterion of the quality of solution of the problem. To minimize recognition errors, it is sufficient to indicate the type of overcast, whose probability for a given TV image is maximum, as the result in each act of recognition. Let us denote the probability of m-th type of overcast upon receipt of a photograph x by p(m/x), and let us calculate some relationship between the probabilities corresponding to the different types of clouds to determine the maximum probabilities m ($\underline{m}$ = 1, 2, ..., M). This will most frequently be the quotient.

$$D(\mathbf{x})_{ij}=\frac{p(m_i/\mathbf{x})}{p(m_j/\mathbf{x})} \qquad \begin{matrix} i=1, 2, \ldots, M-1; \\ j=i+1, i+2, \ldots, M, \end{matrix} \tag{3.1}$$

called the ratio of probability, the classifying, resolving, or discriminant function.

Direct calculation of the probabilities for all possible TV images is impossible beforehand, even if the set of different TV photographs were limited. This follows from consideration of the following formula (the Bayes formula):

$$p(\mathbf{m}/\mathbf{x})=\frac{p(\mathbf{m})\,p(\mathbf{x}/\mathbf{m})}{\sum\limits_{\mathbf{m}} p(\mathbf{m})\,p(\mathbf{x}/\mathbf{m})}. \tag{3.2}$$

The a priori (climatic) probabilities of the various types of clouds p(m), figuring in it, depend on the geographic coordinates of the observed region of the earth, the time of the year, and time of day. For this reason we would have to estimate the a posteriori probabilities p(m/x) for all regions of the earth by the season of the year and for different times of day, which would make the problem of such estimation unbelievably cumbersome because, as is known [37,107,127,175], the distribution of overcast on the earth is extremely irregular.

More rational is estimation of the values of the probabilities that a specific TV image (vector x) will appear during observation of some specific type of clouds p(x/m), which in combination with the a priori probabilities of types of overcast p(m), found independently, provides calculation of the desired values of the

a posteriori probabilities p(m/x) by the Bayes formula (3.2). The conditional probabilities p(x/m) depend on the technical characteristics of the TV equipment being used and in the first approximation may be regarded as identical for all regions of the earth, time of year, and time of day. /75

If there is no additional information, the problem of estimating the conditional probabilities p(x/m) may be solved by constructing empirical distribution histograms p(x*/m), where x* are the quantified values of x. Selection of the quantification scales in this case is extremely important. A rough scale does not permit determination of the actual nature of the conditional distribution p(x/m), and an excess of detail leads to a decrease in the effectiveness of estimation by the histogram method.

A possible solution is accumulation of the vectors x themselves with an indication of their affiliation to one or another type of overcast, rather than the empirical frequencies of different gradations of vector x in the memory of the pattern recognition device. Let us call a set of such vectors instruction sampling.

Non-parametric statistics—the ratio of the number of images of the instruction sampling, related to one class, to that for another class—may be used [54] in this case to solve the affiliation of some new image to one or another type of clouds. This ratio should be calculated for some "neighborhood" of the recognized image in the criterion space. A variant of this rule is possible, consisting of calculation of the ratio of a fixed number of "nearest" images to the recognized image. The "distance" in the criterion space must be introduced both to select the neighborhood and to find the nearest images. It is usually introduced on the basis of heuristic concepts.

The quality of recognition in the given approach is determined by selection of the neighborhood or the corresponding number of nearest images. If the neighborhood (or the number of nearest images) is small, estimation will depend strongly on the random distribution of images from the instruction sample in the criterion space. If the neighborhood is large, estimation of it will not correspond to the true probability distribution. Thus, the defect indicated above for the histogram method is also inherent to the given method. However, it is not so serious here, because the possibilities of varying the parameters of the algorithm, and consequently optimization of them, are retained in the recognition process.

Let us call the procedure for optimization of the parameters of the recognition algorithms instruction. For example, it is shown in [115,159] that, with an unlimited increase in the volume of the instruction sample, estimation on the basis of the indicated

non-parametric statistics coincides with the true ratio of probabilities provided that the number of images, considered as nearest, increases without limit, and its ratio to the total number of images in the instruction sample approaches zero.

Interpreting this result for the first variant of the algorithm, we can say that the convergence condition for estimation is the tendency of the neighborhood toward zero with infinite increase of the instruction sample. In practice the sample is finite. Under /76
these conditions it is shown [115] that with a sufficiently large sample the probability of error in recognition is bounded above by the doubled value of the error probability obtained in using the Bayes formula (3.2) with complete information on climatic and conditional probabilities. For this it is sufficient to relate the recognized image to the type to which the nearest image of the instruction sample is related.

The upper bounds of the error in recognition of 2, 3, ... nearest neighbors are shown in [130]. For example, during recognition according to the three nearest images, the error does not exceed 1.32 errors of the optimum Bayes solution when the volume of the instruction sample is sufficiently large.

A variant of the recognition rule described above is essentially an algorithm [8,43] in which the entire criterion space is regarded as the neighborhood, but in estimation of the probabilities the distance of each image of the instruction sample from the recognized image is taken into account. The "weights" are selected in order to minimize the error in recognition of the images of the instruction sample themselves, for which repeated total sampling of the images of the instruction sample is carried out with recognition of each of them. If recognition is successful, the "weight" of this image does not vary. If an error is committed the "weight" is increased either by some constant value or by a value necessary to eliminate the error in recognition of the given image.

All the algorithms of the non-parametric recognition described above worked well in an instruction sample of such large dimensions that storage of it in the memory of the recognition device and operation with it is difficult. It would be desirable to reduce the volume of the instruction sample without increasing the recognition error. Many heuristic algorithms, resolving this problem, have been described in the literature on recognition [1,51,60,80]. The procedure usually employed consists in memorization of only those images of the instruction sample, in control recognition of which an error is committed, and in elimination from subsequent consideration those images which were correctly recognized. The disadvantages of this approach are obvious:

- the results of recognition depend on the order of display of the images of the instruction sample;

- the volume of the new reduced sample is not limited in any way and may also be extremely large.

The problem of finiteness of the volume of the stored instruction sample is principally solved when there are sufficient finite-dimensional statistics for those probability distributions employed in recognition. Formal determination of sufficient statistics consists in the given case in the following [5]. Let {x} be the instruction sample of images, each of which is randomly sampled independently of the other samples, with a probability density of $p(\{x\}, \theta)$, which depends on the vector of parameters $\theta \in \Theta$. The statistic T is sufficient with respect to θ if and only if the joint probability density may be represented in the form /77

$$p(\{x\}, \theta) = g(\{x\})\, h(T, \theta), \tag{3.3}$$

where $g(\{x\})$ does not depend on θ. Thus, if there exists a sufficient statistic, the instruction device must store only T and the problem of the increment in the capacity of the stored instruction images is eliminated. In order to prove this, let us use definition (3.3) and write the conditional probability required for making the decision in the form

$$p(x/m) = p(x/\{x\}, m) = \int_{\theta} p(x/\theta, m)\, p(\theta/\{x\}, m)\, d\theta. \tag{3.4}$$

For solution of it let us find $p(\theta/\{x\}, m)$.

According to the Bayes formula,

$$p(\theta/\{x\}, m) = \frac{p(\theta)\, p(\{x\}/\theta, m)}{\int_{\theta} p(\theta)\, p(\{x\}/\theta, m)\, d\theta} =$$

$$= \frac{p(\{x\}/\theta)}{\int_{\theta} p(\{x\}/\theta)\, d\theta} \cdot \frac{p(\theta)}{\int_{\theta} p(\theta) \left[\frac{p(\{x\}/\theta)}{\int_{\theta} p(\{x\}/\theta)\, d\theta} \right] d\theta}. \tag{3.5}$$

Let the parameter T be the sufficient statistic. We may then write

$$p(\{x\}/\theta) = g(\{x\})\, h(T, \theta)\, [p(\theta)]^{-1}. \tag{3.6}$$

Substituting this expression in (3.4), we obtain

$$p(\theta/|\mathbf{x}|, \mathbf{m}) = \frac{h(T, \theta)}{\int_{\Theta} h(T, \theta)\,[p(\theta)]^{-1}\,d\theta \int_{\Theta} \frac{h(T, \theta)}{\int_{\Theta} h(T, \theta)\,[p(\theta)]^{-1}\,d\theta}\,d\theta} =$$

$$= \frac{h(T, \theta)}{\int_{\Theta} h(T, \theta)\,d\theta}, \qquad (3.7)$$

proof of which was required.

Since the volume of the instruction sample used to instruct recognition is sometimes very small, it is desirable to supplement it by introduction of new information. It is convenient from this point of view that the probability distribution, figuring in (3.2), be of the so-called self-reproducing type, i.e., the laws of a posteriori probability distribution remain the same as those of a priori probability distribution. In other words, both of them should be characterized by the same vector of parameters θ. As shown in [168], this condition is fulfilled if the sufficient sta- /78
tistics described above exist. Consequently, when additional data is presented to the recognition device, it is unnecessary to include it in the instruction sample, but it is sufficient to correct the values of available sufficient statistics, taking into account this new information.

The simplicity of solving the problem of data storage by the recognition device in cases when distributions of the self-reproducing type are employed in recognition and are characterized by a small number of parameters has attracted many investigators [2,51,54,74,80,126]. The case of recognition of normal distributions has been investigated in special detail

$$p(\mathbf{x}/m_i) = (2\pi)^{-\frac{n}{2}} |\Sigma_i|^{-\frac{1}{2}} \exp\left\{-\frac{1}{2}(\mathbf{x}-\mu_i)' \Sigma_i^{-1} (\mathbf{x}-\mu_i)\right\}, \qquad (3.8)$$

where the parameters are the mathematical expectation and the covariational matrix (dispersion in the case when x is scalar). The presence of an exponential multiplier in expression (3.8) suggests taking the logarithm of the probability ratio as the resolving (discriminant) function (which is quite permissible in view of the monotonicity of the logarithmic function with respect to its argument):

$$D(\mathbf{x}) = \ln \frac{p(m_1/\mathbf{x})}{p(m_2/\mathbf{x})} =$$

$$\frac{1}{2}\left[(\mathbf{x}-\mu_2)' \Sigma_2^{-1} (\mathbf{x}-\mu_2) - (\mathbf{x}-\mu_1)' \Sigma_1^{-1} (\mathbf{x}-\mu_1)\right] - \varkappa. \qquad (3.9)$$

The value κ depends on the a priori probabilities $p(\underline{m}_1)$ and $p(\underline{m}_2)$ and the covariational matrices Σ_1 and Σ_2 and does not depend on the specific value of vector x, i.e., it is a constant for all recognized images and may be calculated beforehand. The decision-making rule in this case consists in determination of the sign of expression (3.9). If it is positive, vector x is related to the first type of clouds, and if negative, vector x is related to the second type.

Additional simplifications of the expression for the discriminant function are possible where either $\Sigma_1 = \Sigma_2 = \Sigma$, or $\mu_1 = \mu_2 = \mu$. In the first case the discriminant function is linear with respect to vector x

$$D(\mathbf{x}) = \mathbf{x}' \Sigma^{-1} (\mu_1 - \mu_2) - \frac{1}{2} (\mu_1 + \mu_2)' \Sigma^{-1} (\mu_1 - \mu_2) - \varkappa, \tag{3.10}$$

which considerably facilitates investigation and utilization. In particular, a simple expression may be obtained for the recognition error. For this it is sufficient to take into account that the discriminant function is itself distributed according to normal law as a linear function of the normally distributed value of x: for the first type with mathematical expectation $1/2(\mu_1-\mu_2)'\Sigma^{-1}(\mu_1-\mu_2)$ and dispersion $(\mu_1-\mu_2)'\Sigma^{-1}(\mu_1-\mu_2)$, and for the second type with the same mathematical expectation, taken with a minus sign and /79 the same dispersion. The probability of erroneous recognition in this case is equal to

$$r = \frac{1}{\sqrt{2\pi}} \int_{-\infty}^{-\frac{\sqrt{\alpha}}{2}} \exp\left\{-\frac{1}{2} y^2\right\} dy, \tag{3.11}$$

where $\alpha = (\mu_1-\mu_2)'\Sigma^{-1}(\mu_1-\mu_2)$ is the "distance" in the criterion space between distributions $p(x/\underline{m}_1)$ and $p(x/\underline{m}_2)$, often called the Makhalanobis distance.

In the second case with equal mathematical expectation $\mu_1 = \mu_2 = \mu$, the discriminant function remains quadratic with respect to x:

$$D(\mathbf{x}) = \left[(\mathbf{x}-\mu)'\left(\Sigma_1^{-1} - \Sigma_2^{-1}\right)(\mathbf{x}-\mu)\right] - \varkappa \tag{3.12}$$

and a simple expression for the error in recognition cannot be obtained.

In practice the dimensionality of vector x, used for identification, is very high. In combination with the limited volume of the instruction sample, this leads to large errors in estimation of parameters μ_i and Σ_i. In particular, the covariational matrices Σ_i are often similar to special matrices and the operation of inverting them, necessary to calculate the discriminant function, is practically impossible. In order to avoid this disadvantage, the dimensionality of vector x must be reduced, for which it is necessary to convert to the main statistical components of distributions $p(x/\underline{m}_i)$ which correspond to the directions of the eigenvectors (natural components) of covariational matrices Σ_1 and Σ_2 in the criterion space.

Geometrically finding these main statistical components consists of a sequence of subsequent linear transformations of the coordinates of the criterion space X. The origin of the coordinates is shifted to a point corresponding to mathematical expectation of one of the types, let us assume the first type:

$$\mathbf{y}=\mathbf{x}-\mu_1; \quad \mu=\mu_2-\mu_1. \tag{3.13}$$

The coordinate system obtained is then rotated around its origin in order to reduce the covaritional matrix of the first type to diagonal form. The criterion space is further compressed so that the diagonal matrix becomes a unit matrix, which is possible if this matrix is defined strictly positively. Finally, a new rotation is carried out to reduce the covariational matrix of the second type to diagonal form while retaining the singularity of the matrix of the first part. The set of these three operations may be written as

$$\mathbf{z}=\mathbf{A}\mathbf{y}; \quad \nu=\mathbf{A}\mu, \tag{3.14}$$

where the transformation matrix satisfies the conditions

$$\begin{aligned}\mathbf{A}'\Sigma_1\mathbf{A}&=\mathbf{I};\\ \mathbf{A}'\Sigma_2\mathbf{A}&=\Lambda,\end{aligned} \tag{3.15}$$

and Λ is the diagonal matrix whose diagonal elements $\lambda_1, \lambda_2, \ldots,$ /80
λ_n are the roots of the characteristic equation

$$|\Sigma_1-\lambda\Sigma_2|=0. \tag{3.16}$$

After making the transformations indicated above, the distribution functions assume the form

$$p(\mathbf{z}/m_1)=(2\pi)^{-\frac{n}{2}}\exp\left\{-\frac{1}{2}\sum_{j=1}^{n}z_j^2\right\} \tag{3.17}$$

for the first type and

$$p(\mathbf{z}/m_2)=(2\pi)^{-\frac{n}{2}}|\Lambda|^{-\frac{1}{2}}\exp\left\{-\frac{1}{2}\sum_{j=1}^{n}\lambda_j^{-1}(z_j-\nu_j)^2\right\} \tag{3.18}$$

for the second type.

Hence, it is easy to find the discriminant function

$$D(\mathbf{z})=\sum_{j=1}^{n}\left[\left(1-\frac{1}{\lambda_j}\right)\left(z_j+\frac{\nu_j}{\lambda_j-1}\right)^2-\left(\frac{\nu_j^2}{\lambda_j-1}+\ln\lambda_j\right)\right]-\varkappa. \tag{3.19}$$

If we further assume that the mathematical expectations of both types are identical, so that in the new coordinate system $\nu \equiv 0$, the expression for the discriminant function is simplified even more:

$$D(\mathbf{z})=\sum_{j=1}^{n}\left[\left(1-\frac{1}{\lambda_j}\right)z_j^2-\ln\lambda_j\right]-\varkappa \tag{3.20}$$

and the problem of reducing the dimensionality of vector x is easily solved, because we can see from (3.20) that only those directions in the criterion space for which the value λ_j is distinct from unity are essential for recognition. Therefore, we can regulate new variables of z_j according to their "information content" for recognition according to the value $(\lambda_j + \lambda_j^{-1})$. It is important to note in this case that in practice we must operate not with eigenvalues themselves, but with estimates of the limited instruction sample, which are more reliable the greater their value [74,75].

Returning to the common case of (3.19), we can see that there is no easy way to select the more informative variables. It is obvious that such selection is related to some method of estimating the recognition error when using different subsets of variables. Since the recognition error for discriminant function (3.19), like most other discriminant functions, is calculated with great difficulty, quasi-optimal methods of selecting the informative features

by the value of the "distance" between the distributions of both types are described in the literature [6,35,125,126,131,140,141, 150].

The convenience of representing the discriminant function in the form of (3.19) is manifested in this case in the fact that the "distance" for the variables, expressed by the main statistical components, is calculated additively. For example, this is the way matters stand with the often-used Bhattacharyya distance: /81

$$B=-\ln\int_X\sqrt{p(\mathbf{x}/m_1)\,p(\mathbf{x}/m_2)}\,d\mathbf{x}=$$

$$=\sum_{j=1}^{n}B_j-\frac{1}{2}\ln\left[p(m_1)\,p(m_2)\right], \tag{3.21}$$

where

$$B_j=\frac{1}{4}\left[\frac{v_j^2}{\lambda_j+1}+2\ln(1+\lambda_j)-\ln\lambda_j\right]. \tag{3.22}$$

Ordering of the variables by their corresponding values B_j usually permits selection of the more informative of them.

The discriminant functions (3.9), (3.10), (3.12), (3.19), and (3.20), considered above, are optimum for pattern recognition, which are normally characterized by the distribution vector x. On the basis of the physical mechanism of radiation transport through the atmosphere and of the nature of its reflection or emission by the underlying surface of the earth and by clouds, and taking into account the effect of the TV equipment used for surveying the earth from space, it is difficult to expect that the distribution function of the TV signal will be normal. For arbitrary distributions, the mentioned discriminant functions may generally not be optimum. However, as shown in [113], the discriminant functions mentioned above are optimum for a class of unimodal, symmetric distributions of the form

$$p(\mathbf{x}/\mathbf{m})=A\,|W|^{\frac{1}{2}}f\left[(\mathbf{x}-\mu)'\,\mathbf{W}(\mathbf{x}-\mu)\right], \tag{3.23}$$

where A is the normalizing factor, W is the positively calculated matrix characterizing the variability of vector x, and f[·] is a monotone function integrable everywhere. In particular, this class includes multidimensional normal distribution where

$$\mathbf{W}=\Sigma^{-1},\quad A=(2\pi)^{-\frac{n}{2}}\quad\text{and}$$

$$f[\cdot]=\exp\left\{-\frac{1}{2}(\mathbf{x}-\mu)'\,\Sigma^{-1}(\mathbf{x}-\mu)\right\},$$

and also multidimensional analogs of Pearson distributions of the II and VII type.

Although the indicated class of distribution functions is very broad, when identifying clouds on TV photographs we must cope with the possible lack of necessity for its further expansion. In particular, the differences in the brightness of structure of the backgrounds which are observed from a satellite (water surface, snow, vegetation of various types, etc.) force us to assume the multimodality of distribution functions. /82

A large number of heuristic algorithms for finding the modes of multidimensional distribution fuctions has been described in the literature (see, for example, [23,54,78,151]). The procedure used most often consists in the following.

The first objects of the instruction sample, related to one each of the types of images identified, are used as initial approximations for the modes. The next image is recognized from the instruction sample. If it is correctly recognized, which will occur if its distance in the criterion space to the initial mode of its own type is less than the distances to modes of all other types, then the mode of this type is recalculated, for example by the formula

$$\bar{\mathbf{x}}_m[1] = \bar{\mathbf{x}}_m[0] + 0{,}5\mathbf{x}_m[1], \tag{3.24}$$

i.e., the new value of the mode of the m-th type is shifted to the center of the segment, connecting the initial mode and the newly selected recognized pattern in the criterion space. If an error is committed in identification, the recognized image is stored as the second mode of the given type, etc. The process of alternate pattern recognition from the instruction sample is continued, correction of the modes being carried out by the formula generalizing (3.24), namely, by relating the t-th image to the τ-th mode of m-th type:

$$\bar{\mathbf{x}}_{m,\tau}[t] = \bar{\mathbf{x}}_{m,\tau}[t-1] + t^{-1}(\mathbf{x}_{m,\tau}[t] - \bar{\mathbf{x}}_{m,\tau}[t-1]). \tag{3.25}$$

In this algorithm the discriminant function is piecewise linear

$$D(\mathbf{x}) = \min_{\tau_1} R(\mathbf{x}, \bar{\mathbf{x}}_{m_1,\tau_1}) - \min_{\tau_2} R(\mathbf{x}, \bar{\mathbf{x}}_{m_2,\tau_2}), \tag{3.26}$$

where

$$R(\mathbf{x}, \bar{\mathbf{x}}_{m_l,\tau_l}) = \|\mathbf{x} - \bar{\mathbf{x}}_{m_l,\tau_l}\| \tag{3.27}$$

is the distance in the criterion space.

Superfluous modes may develop during selection of the instruction sample. To eliminate them, the distances between the modes of one and other types of images may be compared. If the τ-th mode of $\underline{m}$-th type is more similar in the sense of (3.27) to some other mode of its own type than to any mode of the other types, it may be eliminated. Other modes of the same type in this case should be somehow recalculated, which requires repeated sampling of the images of the instruction sample.

An essential disadvantage of the algorithm is the fact that a set of false modes is created during instruction in the zones of intersection of the distribution functions of different types, and the result of recognition of the patterns falling into such zones during operational recognition is random. Transition from recognition by the nearest mode to recognition by the majority of a fixed number of nearest modes may be pointed out as a possible means of controlling this disadvantage, which returns us to the /83
non-parametric algorithm described at the beginning of the given section. Elimination of all modes to which was related a small number of images during instruction is also possible.

Another possible procedure for finding the modes consists in the following [23]. The averages of the images of the instruction sample for the corresponding type are taken as the initial estimates of the mode (one for each type of image). The criterion space is then divided into two domains of linear discriminant function of type (3.10), where it is assumed that $\Sigma \equiv I$, so that we may assume upon recognition

$$\begin{aligned} &\mathbf{x} \in m_1, \quad \text{if} \quad D(\mathbf{x}) < 0; \\ &\mathbf{x} \in m_2, \quad \text{if} \quad D(\mathbf{x}) \geqslant 0. \end{aligned} \tag{3.28}$$

The instruction sample is then divided into two sub-samples according to condition (3.28) and the number of incorrectly recognized patterns of the number falling into each sub-sample is estimated. If the number of committed errors is large, the first step is repeated for that sub-sample in which it is greatest. And the average values for each of the types of images are, in turn, found in it, and the sub-sample is divided into two second-order sub-samples of the linear discriminant function of type (3.10), etc. The process is continued until an acceptable level of recognition errors is achieved, which of course is better controlled by an independent sample.

Finally, we recall the possibility of realizing piecewise linear discriminant functions with the aid of so-called multilayer

machines [23,54,59]. This method of realization was already known during the early stages of development of pattern recognition methods, when investigators were attempting direct simulation of the working of the brain. It is not very popular at present because of the complexity of its strict investigation. However, there are no strict proofs of the compatibility of teaching algorithms with mode search. There are no rules for calculating the optimum number of modes. Therefore, more promising in recent years is the trend in pattern recognition which is related to finding the best approximations of the discriminant function by functions of given form [1,51,78,79,81,82]:

$$D(\mathbf{x}) = \sum_{j=1}^{\infty} a_j \varphi_j(\mathbf{x}). \tag{3.29}$$

Assuming the "smoothness" of the discriminant function in the criterion space, we can limit ourselves to a finite number of terms of the series (3.29). Two problems arise in this case: first, how to select the set of functions $\phi(x)$ so that this assumption is justified and may be limited by a minimum number of terms of the series, and second, how to find the expansion coefficients a_j for /84 the selected function.

The first problem is more difficult and its complete solution is related to supporting consideration of the problem. In particular, these functions should be constructed with consideration of the more obvious non-invariance of description of the image by vector x. In identification of space TV photographs of the earth, these will be: variation of the average brightness and contrast of the image, and its shift and rotations with respect to the direction of line scanning. For consideration of them it is sufficient to turn to description of the image by expansion in a Fourier series with respect to a complete system of functions $\psi(x, y)$, orthogonal in the set of recognized patterns. The coordinates of the photographs are denoted here by (x, y). Because of the limited resolution of the TV photographs, truncation of the series is always possible.

$$B(x, y) = \sum_{m=0}^{M} \sum_{n=0}^{N} c_{m,n} \psi_{m,n}(x, y). \tag{3.30}$$

The problem of selecting a suitable system of orthogonal functions is not really essential here, although it is practically important. Thus, an optimum system from the point of view of economy of description is one of empirical orthogonal functions (natural components), which are eigenfunctions for solution of the homogeneous Fredholm integral equation with respect to the covariational function of a recognized set of images:

$$\int\int K(x_1, x_2, y_1, y_2)\,\phi(x_1, y_1)\,dx_1\,dy_1 = \lambda\,\phi(x_2, y_2). \qquad (3.31)$$

This expansion is optimum in the sense of a minimum mean square error and a minimum a posteriori entropy of expansion (3.30) with a fixed number of calculated terms of the series. The more popular of the number of analytically orthogonal functions in the expansion [32] are trigonometric functions, especially convenient for calculating the non-invariance of the type of shift and rotation of the image. Walsh functions [25,56] are optimum from the viewpoint of computation. Polynomial functions make it possible to disregard a specific type of distribution function of TV image brightness.

Let us consider the procedure for eliminating the more obvious non-invariances for description of images using an expansion of trigonometric functions [51,89]. For this let us write the image spectrum in the polar coordinate system:

$$c_{m,n} = \frac{1}{S}\int_S\int B(x, y)\exp\{-jmZ(\theta_n)\}\,dx\,dy. \qquad (3.32)$$

Here m = 0, ±1, ±2, ... determines the frequency of variation of the image brightness in the direction of straight line Z = x + ny, and angle θ_n (n = 0, 1, 2, ...) is the direction of the straight line in the image plane with respect to the direction of the scanning lines. For normalization of the spectrum with respect to the average image brightness, it is sufficient to divide all expansion coefficients by the zero coefficient /85

$$c^*_{m,n} = \frac{c_{m,n}}{c_{0,0}}. \qquad (3.33)$$

The invariance to image contrast is provided by performing the operation

$$c^{**}_{m,n} = \frac{c^*_{m,n}}{\sum_{m=1}^{M}\sum_{n=1}^{N} c^*_{m,n}}, \qquad (3.34)$$

and invariance to shift is

$$c^{***}_{m,n} = c^{**}_{m,n}\left(c^{**}_{1,n}\right)^{-m}\left|c^{**}_{1,n}\right|^{m}. \qquad (3.35)$$

The spectrum of (3.35) may be expressed by modulus and phase

where

$$c^{***}_{m,n} = |c^{***}_{m,n}| \exp\{j\xi_{m,n}\}, \tag{3.36}$$

$$|c^{***}_{m,n}| = \sqrt{(a^{***}_{m,n})^2 + (b^{***}_{m,n})^2}; \tag{3.37}$$

$$\operatorname{tg}\xi_{m,n} = \frac{b^{***}_{m,n} T_m(\omega_{1,n}) - a^{***}_{m,n} U_m(\omega_{1,n})}{a^{***}_{m,n} T_m(\omega_{1,n}) + b^{***}_{m,n} U_m(\omega_{1,n})}; \tag{3.38}$$

$$\omega_{1,n} = \frac{a^{***}_{1,n}}{\sqrt{(a^{***}_{1,n})^2 + (b^{***}_{1,n})^2}}, \tag{3.39}$$

and $T_m(\cdot)$ and $U_m(\cdot)$ are first and second order Chebyshev functions.

In order to achieve invariance to rotation of the image, the amplitude and phase spectra must be presented in the form of an expansion

$$r_{m,n} = \frac{d_{00}}{2} + \sum_{p=1}^{P} \sum_{q=0}^{Q-1} (d_{p,q} \cos p\theta_n + e_{p,q} \sin p\theta_n) V_q\left(\frac{m}{M}\right), \tag{3.40}$$

where $V_q(\frac{m}{M})$ is a Chebyshev polynomial of degree q, defined by the system of points $\{\frac{m}{M}\}$, and $r_{m,n} \equiv |c^{***}_{m,n}|^2 \operatorname{tg} \xi_{m,n}$. From the formulas similar to (3.35)-(3.39), four spectra are then obtained: the amplitude spectrum of the amplitudes, the amplitude spectrum of the phases, the phase spectrum of the amplitudes, and the phase spectrum of the phases, which in combination provide the required invariance. These four spectra together with data on the average brightness $c_{0,0}$ and contrast $\sum_{m=1}^{M}\sum_{n=1}^{N} c^{*}_{m,n}$ completely describe the ini- /86
tial image, and in the criterion space which they form, the position of the surfaces dividing the domains of various types of images hardly varies when the non-essential properties of the image vary, which also denotes the required "smoothness" of discriminant function (3.29).

Returning to this discriminant function, let us first assume that it may be precisely described by a finite series of J terms

$$D(\mathbf{x}) = \sum_{j=1}^{J} a_j \varphi_j(\mathbf{x}), \tag{3.41}$$

i.e., it belongs to a J-dimensional subspace of an infinite-dimensional space of function $\phi(x)$. Many algorithms have been described in the literature to find it from the images of the instruction sample. The better known of them are the method of potential

functions [1], stochastic approximation [81,82], generalized portrait [12], and sequential methods [79]. All of them, after a number of non-essential transformations which take into account the form of functions $\phi(x)$ and the criterion of the quality of recognition used, reduced to an iteration procedure

$$D(x)[t]=D(x)[t-1]+\gamma[t]F(x, x[t])\{m[t]-D(x)[t-1]\}, \qquad (3.42)$$

where x[t] is the next recognized image from the instruction sample belonging to m-th type, this type (m[t]) may be in general incorrectly indicated in the instruction sample, F(x, x[t]) is a function and $\gamma[t]$ is a number, which are different in different algorithms. On the condition that $\phi(x)$ is a system of orthogonal or at least linearly independent functions, instead of the procedure of (3.42) we can use a similar procedure for estimating the expansion coefficients

$$\mathbf{a}[t]=\mathbf{a}[t-1]+\gamma[t]\rho^{-\frac{1}{2}}\mathbf{A}\rho^{-\frac{1}{2}}\varphi(x[t])\{m[t]-\mathbf{a}'[t-1]\varphi(x[t])\}, \qquad (3.43)$$

where $\phi'(x)\rho^{-1/2}A\rho^{-1/2}\phi(x[t]) = F(x, x[t])$, and A is a matrix. It is shown in [70,71] that the optimum algorithm is one having $\gamma[t] = t^{-1}$; $A = 1$; $F(x, x[t]) = \delta(x, x[t]) = \phi'(x)\rho^{-1}\phi(x[t])$, the mean square error of recovery of discriminant function (3.41) by a finite instruction sample equal to

$$\varepsilon_j^2=\frac{\overline{[\varepsilon(m)]^2 J}}{t}-\frac{\overline{[[\varepsilon(m)]^2 j]^2}}{t^2(a'\rho a)}+\frac{\overline{[\varepsilon(m)]^2[\delta(x, x[t])^2-m[t]}}{t^2}, \qquad (3.44)$$

i.e., the error is mainly directly proportional to the number of terms of series (3.41) to the spread of the error of indication of the type of image in the instruction sample and is inversely proportional to the volume of the instruction sample. Consequently, all a priori data on the form of discriminant functions are useful because they permit selection of those functions of set $\phi(x)$, which are not contained in expansion (3.41), at the same time reducing the error. If it is required that algorithm (3.42) and (3.43) restore any discriminant function, it would be necessary to take the complete set of functions of $\phi(x)$, i.e., to operate with infinite series (3.29). In this case the restoration error would become infinite. We note that the a priori given value $\delta(x, x[t])$ affects the extent of the error. However, its effect is of the second order of smallness

/87

with respect to t and, consequently, is immaterial in any large instruction sample.

Let us now consider a general case when the discriminant function does not belong to the J-dimensional subspace of functions $\phi(x)$. Then only its projection onto this subspace is restored by algorithm (3.42), (3.43). The part of it orthogonal to the given subspace is generally not restored. If it is necessary to completely restore a discriminant function about which it is not known beforehand that it belongs to some finite-dimensional functional subspace, the considered subspace must be expanded during restoration as the volume of the instruction sample increases.

If the a priori information about the discriminant function in the form of its mathematical expectation $D_0(x) = D(x)$ (without loss of generality it may be assumed equal to zero) and of its correlation function $R(x, x^*) = \overline{[D(x) - D_0(x)][D(x^*) - D_0(x^*)]}$, is accounted for the total error in restoration of the arbitrary discriminant function by finite series (3.41) will be equal to [72]

$$\varepsilon^2 \cong \sum_{j=J+1}^{\infty} \lambda_j + \varepsilon_J^2, \tag{3.45}$$

where λ_j are the eigenvalues of correlation function $R(x, x^*)$, corresponding to the unconsidered functions of the complete set of $\phi(x)$, regarded as a set of eigenfunctions for $R(x, x^*)$. In order to minimize the restoration error, it is necessary to take into account in series (3.41) only those functions whose eigenvalues are greater than ε_J^2/J. As a result, the optimum restoration algorithm yields an error of

$$\varepsilon^2 \cong \sum_{j=1}^{\infty} \min(\lambda_j, \varepsilon_J^2/J). \tag{3.46}$$

2. First Experiments in Automation of Processing and Analysis of Satellite Television Photographs of the Earth /88

Taking into account the current state of the theory of pattern recognition, we may conclude that various recognition procedures, both parametric and non-parametric, may be used in solving the problem of automating processing and analysis of the TV and IR photographs transmitted from meteorological satellites. The main task is to find an effective system of interpretation features which describe the image.

Several attempts to solve this latter problem are presently known. Thus, the author of this investigation, relying on the principal characteristics of TV photographs of clouds consisting in their "randomness", has proposed [36,67] that the statistical characteristics of the TV signal may be used as features for automatic recognition, since they are somehow related to those near the radiation field of the observed clouds. The latter, as stated in [29-31,36,41,42,76], depend on the type of clouds. The fact was taken into account primarily that clouds are on the average lighter (colder) than the open sections of land and sea. It was suggested that practical interpretation in this case be carried out by quantizing the TV signal according to levels of uniform brightness.

Figure 19 illustrates the results obtained in this case. Five different TV photographs received from the Meteor satellites are shown in it. They depict the more typical cloud structures observed from space. Row A is non-quantized TV photographs with a superimposed grid of geographic coordinates. The photographs themselves have been transformed into a perspective cartographic projection with the aid of ETCM. Rows B, C, and D are the same photographs quantized in four, two, and one levels of brightness, respectively, located at 0.20, 0.40, 0.60, and 0.80 of the TV signal amplitude. As can be seen, no level of brightness can be found which would satisfactorily delineate the images of the clouds and underlying surface in the photographs.

Some cloud boundaries clearly distinguishable in the non-quantized originals disappear upon quantization and, moreover, false boundaries appear. Thus, automation of interpretation by quantization does not yield the desired results. The reason for this is the different illumination of the observed sections of cloud cover and distortion of brightness imparted by the TV equipment. The latter is especially discernible in the fifth column of Fig. 19, where false outlines appeared upon quantization due to the inhomogeneity of reproduction of brightness over the field of the TV photograph.

Attempts have been made [98,152,162] to improve the results by measurement of the absolute intensities of the radiation from the clouds and the earth's surface, with subsequent correction of the measured values for the value of illumination (for the visible region of the spectrum) or for the climatic temperature of the /90
earth's surface and of the atmosphere at different levels of the troposphere (for the IR range). The failures here were the result not only of difficulties in absolute calibration of the TV equipment, but due to the complexity of taking into accont all the factors affecting radiation transport in the atmosphere. Current data on the thermal and optical properties of clouds and of the earth's surface are also too sparse.

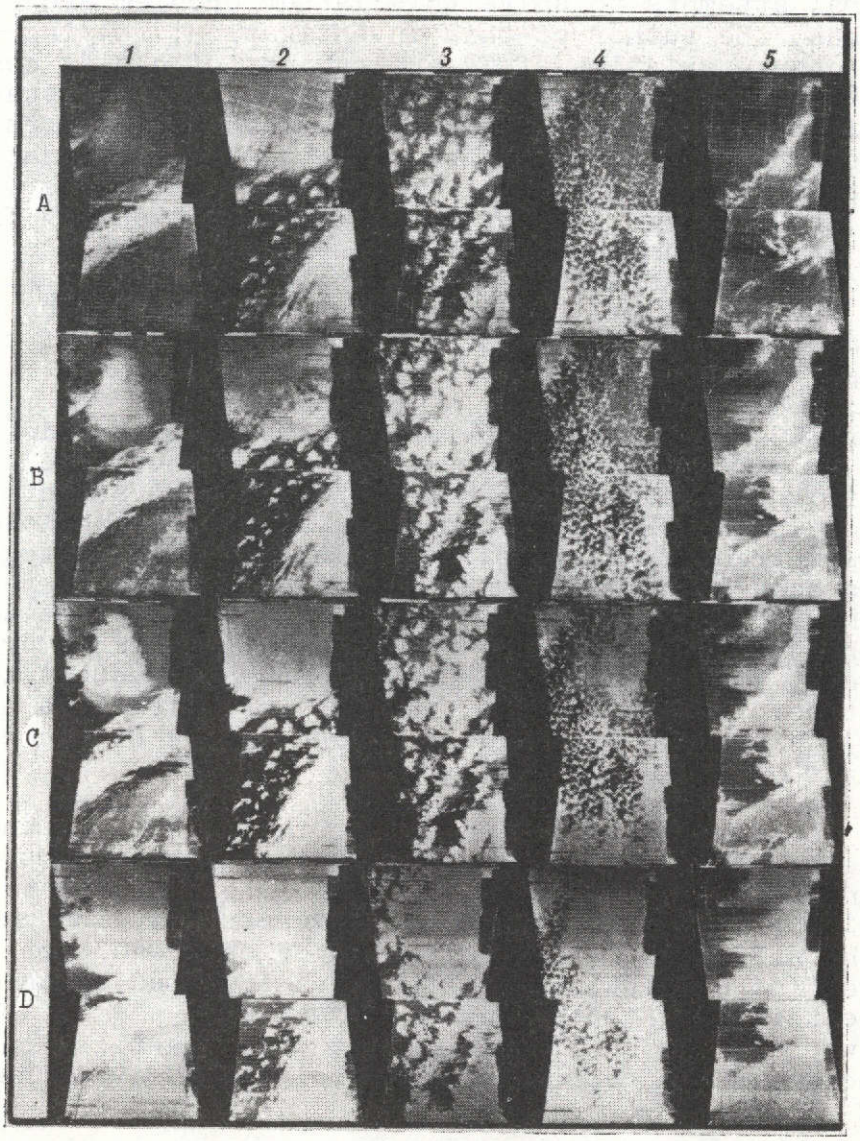

Fig. 19. Originals and quantized versions of television photographs obtained from satellites of the Meteor system.

1- frontal overcast; 2- clouds inside a developed cyclone; 3- "closed" convection cells; 4- "open" convection cells; 5- chains of cumulus clouds. A- non-quantized originals with a superimposed grid of geographic coordinates; B- photographs quantized for five gradations of brightness according to levels 0.20, 0.40, 0.60, and 0.80 of the total television signal amplitude; C- photographs quantized for three gradations according to levels 0.20 and 0.40; D- photographs quantized for two gradations according to level 0.20.

The failure in using average brightness alone in interpretation made it necessary to turn to the search for more complex features. Since the brightness distribution function for uniform sections of cloud cover was similar to the logarithmically normal function [67], it seemed feasible to use the difference from unimodality of estimating the distribution function of the value of the TV signal to detect the boundaries of various types of cloud fields in the photographs. The incompetence of this interpretation procedure is explained by the fact that the three-dimensional inhomogeneity of the radiation field of clouds is too great for correct estimation of the required function. The failure of the attempt to objectively describe the cloud structures observed in the photographs by the spectrum of their brightness field is explained by the same reason [145].

Let us mention yet another interesting attempt [88] to obtain the deterministic features of cloud patterns by preliminary quantization of the TV signal for two levels ("dark" - no clouds, and "light"—clouds) for which a model of the brightness field is constructed which corresponds to the true brightness field of the photograph by the first three single-point moments. After the cloud images have been separated from the images of the cloudless sections, such elements of the pattern as straight and curved lines, closed and open lines, etc. are distinguished on the photograph for identification of the cloud patterns.

Such a specific set of features is selected which is recommended in the manual on visual interpretation of TV photographs obtained from the Tiros satellites [109]. No more significant experiments with the features obtained were carried out, which is partially explained by the obvious laboriousness of calculating them even on rather large electronic computers. But the main thing is that these features are apparently suitable only for automatic identification of clouds photographed on a homogeneous background.

Using simultaneous measurements of the intensity of reflected (0.5-0.7 μm) and emitted (8-12 μm) radiation with the aid of the medium resolution radiometer of the Nimbus-2 satellite as the features, American meteorologists [127] carried out climatic regionalization of overcast on a planetary scale with differentiation of the main cloud patterns, cuch as cirrus, altocumulus, stratocumulus, etc. However, the reliability of identifying these patterns is apparently too low for application of the data [127] to analysis of individual cloud situations. As a whole, spectrozonal surveying under the condition of high spatial resolution seems promising for use in a system for automatic processing and analysis of space photographs of the earth [129]. Since such surveying will /91 not be used on operational meteorological satellites in the near future, we shall limit ourselves to a statement of its prospects and we will subsequently consider only single-color images.

C 2

The most extensive of the experiments on automatic recognition of TV photographs of clouds with consideration of the pattern (structure) of the image as the feature is described in [117]. These experiments included all stages necessary for automation of processing and analysis of photographs, although they were not performed on original photographs, but on photocopies in non-operational order.

The raw data was fed into an electronic computer with the aid of a special scanning phototelevision device. The stages of processing were:

- primary processing including input of the raw data into the computer and normalization of it which facilitates subsequent calculation of the interpretation features. For example, the outlines of the image were emphasized by calculating the Laplacian of the brightness and subtracting from the original image, the constancy of the image scale was provided and invariants to shift and rotation were introduced;

- delineation of a small number of interpretation signals from a larger number of them by instruction by the trial and error method;

- essential identification, i.e., relation of each of the images fed into the computer to a specific type.

All experiments were carried out with visually selected photographs of homogeneous sections of cloud cover of one of three types: non-cumuliform (117 photographs), cumuliform consisting of open convection cells (108 photographs), and cumuliform of closed cells (113 photographs). Images of open sections of land were not considered. Each photograph was represented in the computer memory by a file of 75×75 numbers (expansion elements), each number being encoded by an 8-bit binary code.

Two systems of features were tested: purely random, obtained by summation of the image brightness values in its randomly selected elements, and non-random—different statistical characteristics of the brightness field. The number of random features in all the experiments was equal to 400. The number of non-random features was initially selected at 28, but the number was reduced to 3-4. Six different non-parametric algorithms were used for identification, the images first being divided into non-cumuliform and cumuliform and then those of them which were related to cumuliform were subdivided into open and closed cells.

Control identification of the independent sample was carried out after instruction. It turned out that all six methods are approximately equivalent and provide the probability of correct

identification at a level of 0.83-0.89, where 3-4 non-random features are just as effective as 400 random features.

Evaluating the results obtained, it should be noted that the /92
rather high percentage of correct identification was obtained on a limited set of specially selected photographs on a background of water surface. The problem of identification of nonhomogeneous overcast, the boundaries of different types of cloud fields, and the case of surveying clouds on a background of a "mottled" underlying surface was not considered at all. Without consideration of the enumerated situations the results obtained may not serve as a basis for positive solution of the problem on the possibilities and feasible ways of automating cloud identification.

The necessary investigations were carried out at the Hydrometeorological Center of the USSR under the supervision of the author. The investigation was carried out on the Minsk-22 computer; a preliminary condition was development of a special device for analog-digital conversion and input of the TV signal in digital form into the computer memory. Taking into account the experimental nature of the investigation, the device was developed with respect to the comparatively low-frequency signal, received in the direct transmission mode from ESSA satellites.

Processing of the photographs included the following steps:

- reception of the TV signal from the satellite,
- input of the signal into the computer,
- organization of the data for interpretation,
- (interpretation) calculation of the interpretation features,
- geographic control matching,
- essential identification,
- release of the results for printing in the form of charts.

The TV signal is received by the Department of Reception and Recording of Satellite Data of the Hydrometeorological Center of the USSR. The received signal was converted to digital form and recorded on magnetic tape of the satellite data receiving station in a 9-bit binary code. Input of the recorded data into the computer was then carried out. Since the tape of the receiving stations differs from magnetic computer tape, a special code-conversion device was used for input. The data was then organized in the computer memory. This is understood as the search for the beginning of the photograph and formation of the frame lines. The organization algorithm is based on the specific structure of the incoming signal.

After a starting signal continuing for three seconds, the automatic phase stabilization signal follows for five seconds. Each line in it begins with a synchronous pulse, transmitted on

the black level, and the signal itself moves continuously at the white level.

When the information signal is replaced by the phase signal, a synchronous pulse is transmitted at the white level, and the signal itself represents in digital form the brightness of each scanning element of the TV photograph. In searching for the beginning of the photograph, the phase signal is first sought—the specific number of measurements having the white level, and the synchronous pulse of this signal, and secondly, the point where the "black" synchronous pulse is replaced by the "white" synchronous pulse. In this case it is kept in mind that the length of the synchronous pulse comprises 5% and that of the signal, 95% of the length of /93
the entire line. The entire line is represented by 400 measurements when recording on a single channel. The synchronous pulse of each alternate line is then sought and a line signal is formed with conversion of 9-bit measurements into 6-bit.

The next stage of processing is analysis of the incoming photograph. The characteristics of this problem consist in the fact that:

- half-tone images, consisting of many thousands of scanning elements, are analyzed;

- the images are severely distorted by interference and noise of different nature;

- the images are not centered in the field of view of the camera;

- complex objects are identified which have no typical geometric outlines (clouds) on a background of other objects (elements of the underlying land and sea surface), whose image structure is at least as complicated and varied as the cloud structure;

- the nature of the image of both clouds and the earth's surface depends on the geographic coordinates of the photographed region of the earth, the time of year, and time of day;

- the comparatively low technical parameters of the TV equipment used leads to the fact that images of different types of clouds and of the earth's surface may be completely identical; therefore, the problem of identification is probabilistic;

- the problem of identification is not one of relating the entire photograph to some specific type (class), but is one of isolating on it the overcast fields related to different classes (Fig. 20). Therefore, the entire photograph is divided into

elementary sections, which are then subjected to identification. As shown by practice, the dimensions of the elementary sections are of great importance. The section should primarily be such that the structure of individual cloud patterns is completely included. Selection of the optimum dimensions of the section requires additional investigations. The size of the section in our investigation comprised 6×6 scanning elements. This is apparently not the optimum variant.

The correlation of the television signals for ESSA satellites, for example, constructed for such an elementary section (Fig. 21), does not reach zero within the limits of the section; this indicates that the structure of only part of the object rather than the whole objective is reflected in each individual section. However, the limitation of the Minsk-22 memory did not permit an increase in the dimensions of the section, since the required storage capacity is proportional to the number of scanning elements of the photograph within the limits of the section.

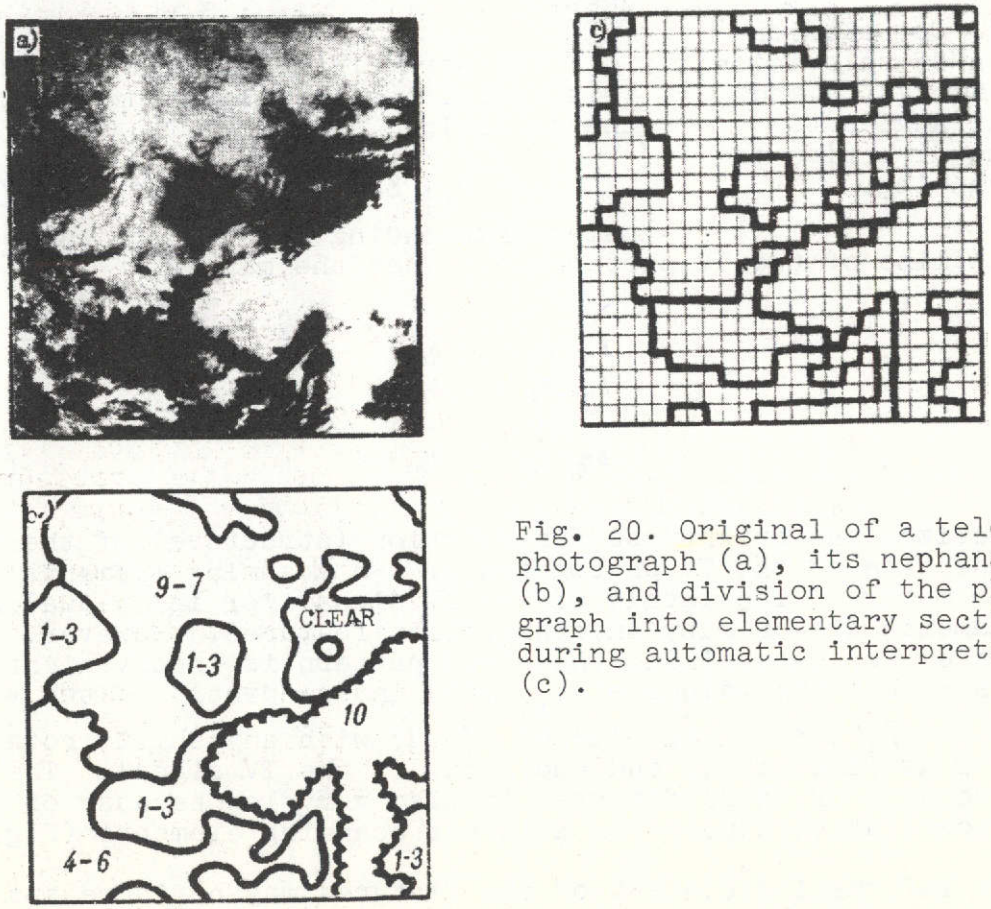

Fig. 20. Original of a television photograph (a), its nephanalysis (b), and division of the photograph into elementary sections during automatic interpretation (c).

The image pattern is determined for each of the isolated sections by its inherent brightness. If two adjacent sections of the photograph are related to the same type of pattern, the boundary between them is eliminated. This procedure may be called definition of the types of TV image. To carry out this procedure, it is not at all compulsory to know which objects are represented on the photograph, because a much simpler problem is resolved here: to determine those sections of the photograph on which similar objects are represented. /94

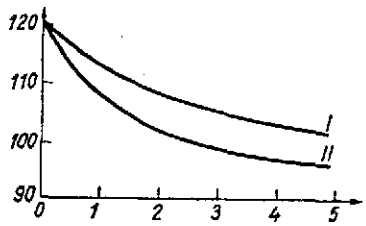

Fig. 21. Correlation function of television signal along (I) and at right angles to (II) the direction of line scanning.

The isolated types of image are subsequently used as complex interpretation features to establish which objects (clouds, etc.) are represented on the corresponding section of the photograph. In this case the same interpretation feature (type of image) will possibly correspond to different cloud patterns in different cases.

The work of the program realizing this interpretation algorithm consists in the following.

Let b_{ij} be the level of the TV signal corresponding to the i-th elements of the j-th line of the TV photograph. Then the matrix

$$\begin{matrix} b_{11}, b_{21}, \ldots, b_{n1}; \\ b_{12}, b_{22}, \ldots, b_{n2}; \\ \cdots\cdots\cdots \\ b_{1n}, b_{2n}, \ldots, b_{nn} \end{matrix} \qquad (3.47)$$

characterizes the brightness distribution (structure) of the image on the section of the TV photograph of n×n scanning elements in the computer memory. The levels of the TV signal for individual scanning elements are primary interpretation features. However, direct use of them for determining the cloud pattern is inconvenient for the reason that the values of b_{ij} vary independently of the variation in the pattern of the imaged clouds with any shift, rotation, change of average level, and amplitude of the TV signal. The information content of these features is also very low because of their strong correlative aspect for adjacent scanning elements (Fig. 21). /95

The information content of the features may be increased by several methods. For interpretation of overcast images, which have

no typical geometric outlines, we feel it is more expedient to use the scanning coefficients of the brightness field of the photograph for any set of functions as the features. The requirements in selection of such a system reduce to the fact that the system be complete, which ensures display of any possible images with its aid. Then, due to the concepts of the simplicity of determining the similarity of different images, we would hope that the scanning coefficients of these functions were non-correlated, and the accuracy of approximating the brightness field to increase the information content of the scanning coefficients should be sufficiently high even with a small number of scanning elements. All these requirements are satisfied to the greatest extent by scanning according to natural orthogonal functions

$$b_{ij} = \sum_k x_k \varphi_{ijk}, \qquad (3.48)$$

where x_k is the expansion coefficient of the k-th function, and ϕ_{ijk} is the eigenvector corresponding to the k-th eigenvalue, which satisfies the matrix equation

$$R\varphi_k = \lambda_k \varphi_k \qquad (3.49)$$

(R is the covariational matrix of the television signal within the limits of a section of n×n scanning elements).

All the experiments carried out on automatic identification of photographs were conducted with the use of numerical solution of equation (3.49) with the aid of an empirically determined covariational matrix, which is essential, and placed limitations on the dimensions of the analyzed section of photographs. However, taking into account that the television signal is homogeneous on the average, analytical methods may be used for this purpose [68]. The limitation of the computer storage capacity will then be less important, and the eigenvectors themselves will be more stable.

Returning to the problem of selecting the features, we note that the coefficients of expansion with respect to natural components are not features invariant to shifts and rotation of the image. Invariance may be achieved by combining the expansion coefficients with the aid of logical "AND", "OR", etc. This is a rather complicated pro- /96
cedure, and we preferred to avoid it, complicating the process of making a decision about the recognized objects. We again recall that from concepts of the economy of storage, occupied under the image features, a maximum of the first coefficients of the expansion with respect to natural components was selected for subsequent use, which provided an initial image approximation error of the order of 0.01-0.02.

In a six-dimensional criterion space it is difficult to expect that the points corresponding to each class of identifiable objects (clouds and the earth's surface) will be located in a single compact area due to the non-invariance of the space to shifts and rotations of the image. Rather, each class will yield several clusters—subclasses. In order to take this characteristic into account, and also the fact that practically identical sets of expansion coefficients may correspond to different types of objects, the identification process was also divided into two parts. A search is first made for all clusters of points in the criterion space (types of image), and then the conditional probabilities of the appearance of different classes of objects for the clusters found are determined.

A search for the clusters is made by the self-instruction method. The scanning coefficients are calculated by the selected natural functions $\underline{x}_1[t]$, $\underline{x}_2[t]$, ..., $\underline{x}_6[t]$ ($t = 1, 2, \ldots,$), where T is the total number of sections on the photographs, for each of the sections of the TV photograph. It is further assumed that each type of image is characterized by similar sets of numbers $\underline{x}_1$, $\underline{x}_2$, ..., $\underline{x}_6$ and different sets essentially correspond to different types. The domains of the values of $\overline{x}$, corresponding to the different types of images, must be calculated in the criterion space on whose axes are plotted the values of the selected expansion coefficients. Using the appropriate metrics and assuming a minimum distance between the points of this space as the criterion, we obtain the following recursion algorithm for calculation of the domain centers of all types of images:

$$\begin{aligned}
\overline{x_k^1[t]} &= \overline{x_k^1[t-1]} + \gamma^1[t]\,(x_n[t] - \overline{x_k^1[t-1]});\\
\overline{x_k^2[t]} &= \overline{x_k^2[t-1]};\\
&\cdots\cdots\cdots\\
\overline{x_k^m[t]} &= \overline{x_k^m[t-1]},
\end{aligned} \tag{3.50}$$

if x[t] belongs to the first type, and

$$\begin{aligned}
\overline{x_k^1[t]} &= \overline{x_k^1[t-1]};\\
\overline{x_k^2[t]} &= \overline{x_k^2[t-1]} + \gamma^2[t]\,(x_k[t] - \overline{x_k^2[t-1]});\\
\overline{x_k^3[t]} &= \overline{x_k^3[t-1]};\\
&\cdots\cdots\cdots\cdots\cdots\cdots\\
\overline{x_k^m[t]} &= \overline{x_k^m[t-1]},
\end{aligned}$$

if x[t] belongs to the second type, etc.

Any random sets of numbers may be used as the initial approxi- /97
mation for the domain centers. With certain limitations on the values of $\gamma^m[t]$, the described algorithm makes it possible to approximately calculate the desired domains of the types of images after a finite number of samples of all sections of the photograph. Self-instruction in this case is completed and a working display of each of the sections of TV photographs is carried out, in which are determined the types of images corresponding to each of the sections.

It was assumed until now that TV photographs have no specific distortions whatever. There are in fact distortions which may considerably affect the results of self-instruction. This is primarily pulse interference, which occurs during transmission of the digital data at the video signal level. The advantage of the method of approximating the image brightness field, used to obtain the criterion system, is also manifested in the fact that it makes it possible to automatically eliminate from consideration interference of this type, because the first six natural orthogonal functions, which are used for approximation, are "smooth".

The second more considerable distortion of the image is related to the inhomogeneity of reproducing the field brightness of the TV photograph. The inhomogeneity leads to the fact that the same object being reproduced in different sections of the photograph has a different brightness and contrast, as a result of which the self-instruction algorithm described above will yield different results as a function of to which part of the photographs the sections in the instruction sample were related. In order to avoid this, it is necessary to take into account the dependence of the domain centers of the types of images in the criterion space on the coordinates of the photograph, i.e.,

$$\overline{\mathbf{x}_k^m} = \overline{\mathbf{x}_{k,\varphi,\lambda}^m}, \tag{3.51}$$

where ϕ and λ are the rectangular coordinates of the photograph.

The self-instruction algorithm is then modified in the following manner. The form of the dependence of criteria on the coordinates of the photograph is defined, for example, in the form of a parabola

$$\mathbf{x}_{k,\varphi,\lambda} = \sum_{p=0}^{2}\sum_{q=0}^{2} a_{pq}\varphi^p\lambda^q;$$

$$p+q \leqslant 2, \tag{3.52}$$

where the coefficients a_{pq} are different for different types of images. The sets of coefficients of each type, which minimize the distance of the individual sets of criteria in the criterion space from the parabola of the corresponding class, are then found by alternate display of the elements of the instruction sample. Minimization is achieved with the aid of the recursion algorithm /98

$$\overline{a^1_{pq}[t]} = \overline{a^1_{pq}[t-1]} + \gamma^1[t]\frac{\varphi^p\lambda^q}{\sum_p\sum_q \varphi^{2p}\lambda^{2q}}\left(x[t] - \sum_p\sum_q a^1_{pq}[t-1]\varphi^p\lambda^q\right);$$
$$\overline{a^2_{pq}[t]} = \overline{a^2_{pq}[t-1]};$$
$$\overline{a^m_{pq}[t]} = \overline{a^m_{pq}[t-1]}, \qquad (3.53)$$

if x[t] belongs to the first type, and

$$\overline{a^1_{pq}[t]} = \overline{a^1_{pq}[t-1]};$$
$$\overline{a^2_{pq}[t]} = \overline{a^2_{pq}[t-1]} + \gamma^2[t]\frac{\varphi^p\lambda^q}{\sum_p\sum_q \varphi^{2p}\lambda^{2q}}\left(x[t] - \sum_p\sum_q \overline{a^2_{pq}[t-1]}\varphi^p\lambda^q\right);$$
$$\overline{a^3_{pq}[t]} = \overline{a^3_{pq}[t-1]};$$
$$\cdots\cdots\cdots$$
$$\overline{a^m_{pq}[t]} = \overline{a^m_{pq}[t-1]},$$

if x[t] belongs to the second type, etc.

Unlike the case considered earlier, we have here a multiextremum problem. To find the global extremem, we may use the method of isolating the extremum, applying to the values of the coefficients of the parabola the limitations which follow from the specifics of the considered problem, namely, all coefficients, with the exception of the free term, are hardly distinct from zero, and the free term is close to the corresponding value $\overline{x^m_n}$ of the self-instruction algorithm considered earlier.

After the types of TV images have been found and after each section of the corresponding photographs has been related to this or that type, we must determine which clouds are represented on the photograph. For this, we use direct calculation of the conditional probabilities of the different cloud patterns for the observed type of image and selection of the maximum of them

$$p(l/m) = \frac{p(l)\,p(m/l)}{\sum_l p(l)\,p(m/l)}, \qquad (3.54)$$

where $\mathbf{l}$ is the cloud pattern and m is the type of image.

The values of $p(\mathbf{l})$ and $p(m/\mathbf{l})$ depend on the geographic coordinates of the photographed region, the time of year, and the time of day. They are found by comparing the charts of the types of images with the analysis charts, carried out visually by the meteorologist interpreters. Such comparison must be made over a prolonged period in order to obtain stable estimates of a priori and conditional probabilities for all regions of the globe. Therefore, all the earth was divided into regions, uniform in the nature of their image on the TV photographs. Its own matrix of conditional probabilities was calculated for each type of region, no matter how large it was. With regard to the values of the a priori probabilities of the appearance of cloud patterns, they were calculated for each geographic region. /99

The TV photographs of the earth, obtained with the aid of the ESSA satellites, are matched with the terrain with rather large errors (of the order of 100 km). This creates additional difficulties in identification, because the cloud background may be a different underlying surface than follows from the data of geographic control matching. Therefore, instead of formula (3.54) to make a decision on the observed cloud pattern, the following expression is used.

$$\tilde{\tilde{p}}(\tilde{\mathbf{l}}) = \int_{\varphi} \int_{\lambda} f(\varphi, \lambda)\, p(\mathbf{l}/\mathbf{m})_{\varphi, \lambda}\, d\varphi\, d\lambda, \tag{3.55}$$

where $f(\phi, \lambda)$ is the probability of error in geographic control matching equal to ϕ by the range of latitude and λ by longitude, $p(\mathbf{l})$ is the a posteriori probability of the $\mathbf{l}$-th cloud pattern, and $p(\mathbf{l}/m)_{\phi,\lambda}$ is the probability of the $\mathbf{l}$-th cloud pattern provided that the m-th type of image is observed at a distance (ϕ, λ) from the considered point.

The results of automatic identification of clouds should be presented to meteorologists in the form of nephanalysis charts. For this a special program had been created for transforming the projections of the photographs into a stereographic projection of scale 1:15,000,000. In compiling this program it was taken into account that the coordinates of each identifiable section of the photograph are strictly defined, and the position of the satellite at the moment of surveying is known (latitude B, longitude L, azimuth A, and the altitude of the satellite as well as the orientation of the optical axis of the television camera with respect to the vertical of the satellite are known). The latitude and longitude of the center of each section of the photograph on the terrain may be found by the formulas of central projection and transformation of coordinates.

Conversion to rectangular coordinates (ξ, η) of the chart is accomplished by the formulas:

$$\xi = \frac{1{,}8R}{m} \frac{\cos B}{1 + \sin B} \sin L;$$
$$\eta = \frac{1{,}8R}{m} \frac{\cos B}{1 + \sin B} \cos L, \qquad (3.56)$$

where R is the earth's radius, and m is the scale of the chart.

The rectangular coordinates of the geographic grid are also calculated by the formulas for the meridians and parallels. The geographic grid is transmitted to the alphanumeric computer device, and the number of the cloud pattern, which was assigned to these sections during identification, is printed at the points corresponding to the position of the centers of the photograph section. /100

The experiments carried out on real TV images of the earth, obtained with the aid of the ESSA meteorological satellites, showed good agreement of automatic analysis with visual nephanalysis of those same photographs, as well as with the data of ground observations of clouds. One of the examples of this type is presented in Fig. 22. The original TV photograph of overcast, obtained on 13 February 1969 from the ESSA-6 satellite, is shown in it. The characteristic features of cloud cover visible on it are a mass of solid clouds in the right middle portion of the photograph (above central and southeastern Europe) and extensive clearing above the coast of western Europe and in the Baltic area (in the latter case snow-covered sections of land are visible on the photograph). Convective overcast has developed above the North Sea, variable cloudiness is observed in the region of the Mediterranean Sea, and slight clearing is visible above the Alps and in the upper parts of the Danube. The results of calculating the type of image for all sections of the photograph considered, transformed into a stereographic projection (the original is in a scale of 1:15,000,000), are shown in Fig. 22 b. The dimensions of each section on the terrain are about 50×50 km^2, which is in good agreement with the conditions of surveying clouds in ordinary ground observations. Each section is characterized by the type of image encoded on the chart by two octal numbers (from 01 to 10). A total of eight different types is distinguished.

It is easy to see upon comparison of Fig. 22 a and b that the configuration of the identified massifs of the image types is in good agreement with the configuration identified visually in Fig. 22 a. Even the cloudless sections of snow-covered land in the upper right corner of the photograph were distinguished from the adjacent cloud sections. A section of the photograph with an image

of the snow-covered peaks of the Alps was isolated into an individual contour. It was more difficult to distinguish the large tract of convective overcast over the North Sea, which is easily explainable. Clouds of this type are not typical for winter; therefore the covariational matrix of the video signal of the ground TV photographs is hardly suitable to describe the statistical structure of the image of convective clouds. The eigenvalues of those natural functions which describe the variations in the level of the video signal of these clouds in the TV photograph were too small, which led to their not being used as interpretation features.

The result of estimating the amount of clouds are three gradations (slight, variable, and solid) by formula (3.55) for each of the sections on the basis of data on the types of images recognized in the sections (Fig. 22 b) is shown in Fig. 22d . The characteristic feature of the given experiment was that, due to the small number of photographs processed, we were unable to obtain an estimate of the a priori probabilities of observation of all three gra- /101
dations of the amount of clouds for the considered area. Instead, the corresponding climatic values obtained from data of ground observations were used. The inadequacy of satellite and ground observations of clouds was apparently the reason, as can be seen in Fig. 22d we were unable to isolate the cloudless snow-covered region in the Baltic area. It was related to solid overcast, despite the fact that it was traced quite clearly on the chart of image types (Fig. 22 b). On the whole, the result of automatic identification of overcast is quite satisfactory, which may be seen by comparing Fig. 22 d and Fig. 22 c where nephanalysis of the photographs, carried out visually by the meteorologist interpreter, is shown, and the data of ground meteorological stations during the observation period nearest the moment of TV surveying are applied.

Of course these two types of analysis differ in details, but the good agreement of the overall configuration of the isolated cloud fields in the considered cases and in other cases which we analyzed permits us to conclude that the developed program is completely suitable for large-scale analysis of overcast from data of TV surveying of the ground with the aid of meteorological satellites. This conclusion is also supported by the data of quantitative comparison of machine and visual nephanalyses, presented in Table 10.

We note in conclusion that the procedure mentioned above of taking into account the inhomogeneity of brightness reproduction over the image field in realizing the program for automatic processing of television photographs on the Minsk-22 computer was not used because of the slow speed of this computer and because of the limited number of photographs which may be used for self-instruction of identification of image types.

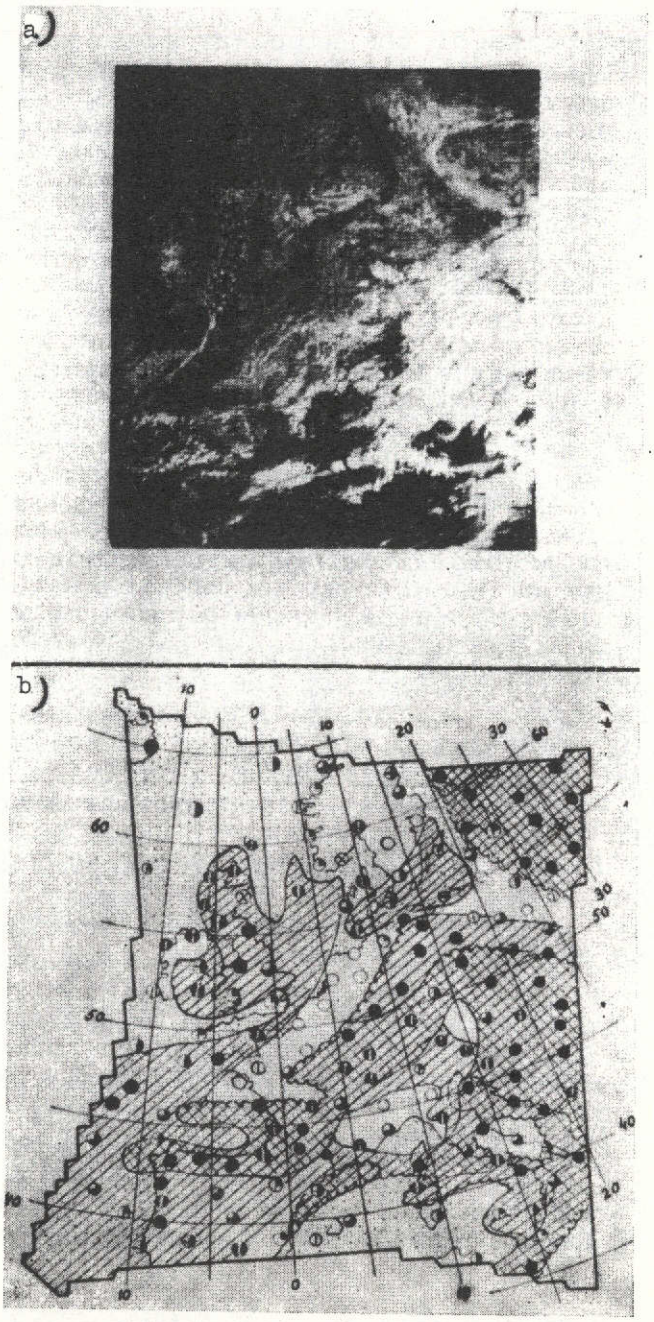

Fig. 22. Result of automatic processing and analysis of TV photographs in comparison to visual nephanalysis.

a) original television image, b) visual nephanalysis of the photograph and data on the total amount of clouds from ground observations during the nearest synoptic period, [continued on p. 107]

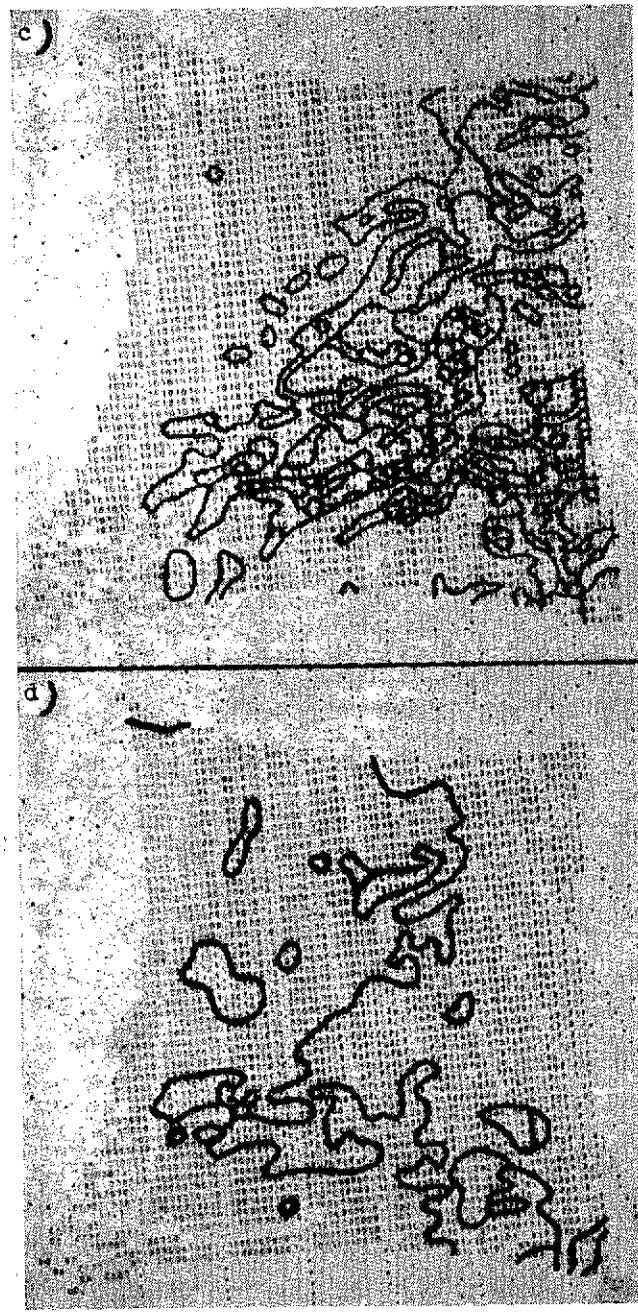

Fig. 22 (continued)

c) machine chart of the types of television image identified in photograph (a), d) machine nephanalysis of photograph (a) with isolation of three gradations of overcast (00- slight, 01- variable, 02- considerable). The original scale is 1:15,000,000.

Table 10. Results of comparing (number of cases and percent - in parentheses) automatic and visual nephanalysis of TV photographs of the earth, obtained with the aid of meteorological satellites.

Overcast according to visual nephanalysis	Overcast according to machine nephanalysis			Total
	Slight	Variable	Considerable	
Slight	712 (0.50)	73 (0.29)	120 (0.11)	905
Variable	559 (0.40)	148 (0.58)	254 (0.24)	961
Considerable	135 (0.10)	34 (0.13)	697 (0.65)	866
Total	1406 (1.00)	255 (1.00)	1071 (1.00)	2732

Comparatively high uniformity of brightness reproduction by the field of the photographs obtained from the ESSA satellites in the direct transmission mode made it possible to obtain the quite satisfactory results which are shown in Table 10. Let us look at Figs. 23-25 in order to more directly detect the errors which occur in this case. Four television photographs, obtained in two sequential passes of the ESSA-8 satellite above Europe, are shown in /110
Fig. 23. As can be seen by the grids of the geographic coordinates plotted on the photographs, the sections of terrain encompassing the photographs overlap. Charts of the image types, identified without taking into account distortions in the brightness of the image field in these photographs, are given in Fig. 24. It is obvious that in the overlapping zone the types of images identified in the different photographs sometimes differ rather considerably. The unconsidered inhomogeneity of brightness reproduction is manifested in this. However, the differences are not so great because, as can be seen in Fig. 25, where the cloud charts constructed from the data on the observed image types are presented, the configuration of the cloud fields in the different photographs are quite similar in the overlapping zones. In any case, the existing discrepancies do not exceed those which are usually the consequence of inaccuracies in geographic control matching of the images.

The program for automatic processing and analysis of overcast from data of television surveying of the earth from ESSA satellites carried out, as already mentioned, on the Minsk-22 computer is the first operational program of this type. Experiments carried out with it on processing and analysis of actual photographs indicated the essential solvability of the posed problem of automation of processing and objective analysis of overcast from data of television

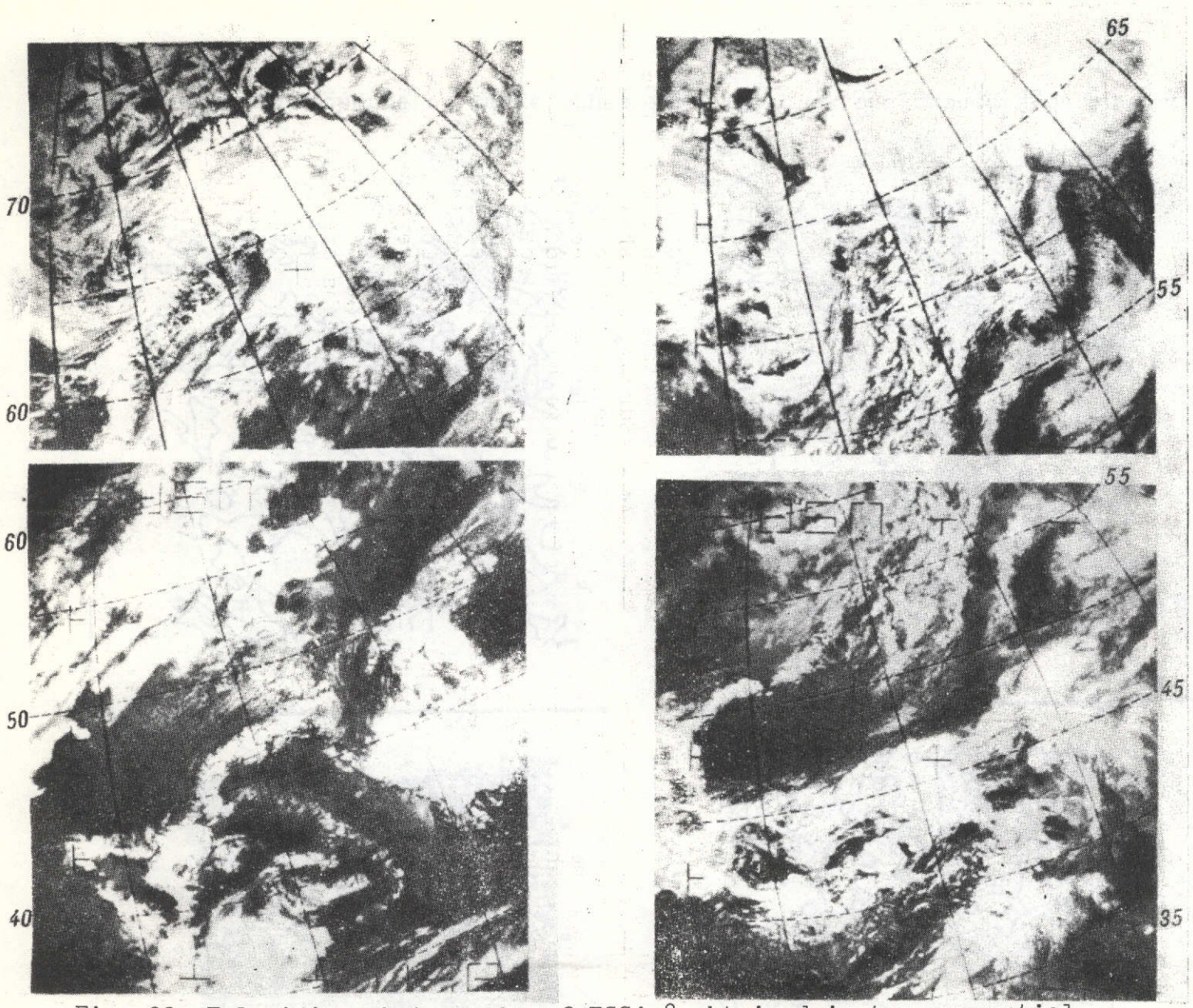

Fig. 23. Television photographs of ESSA-8 obtained in two sequential revolutions in the direct transmission mode.

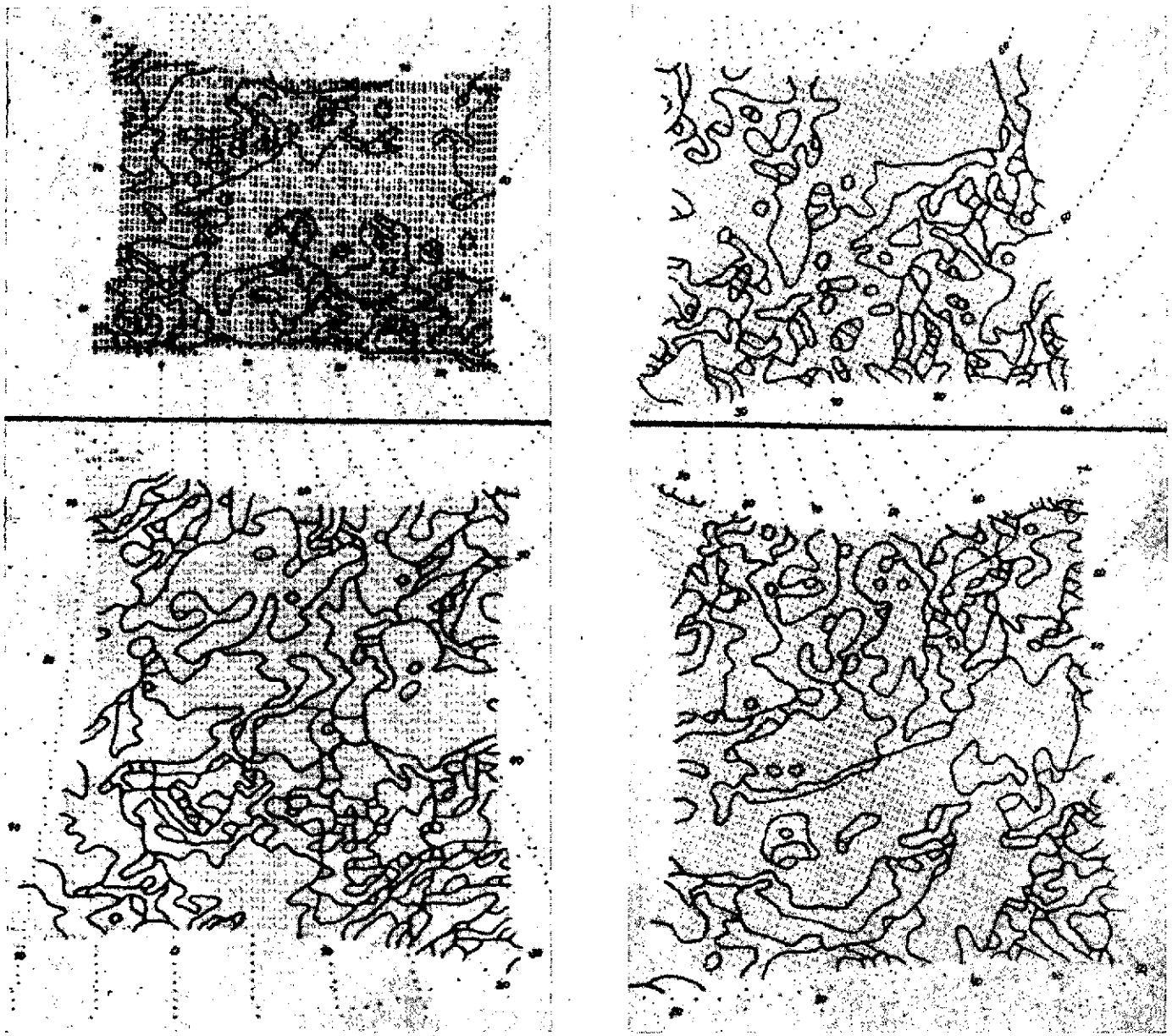

Fig. 24. Machine charts of image types identified by the photographs in Fig. 23.

Fig. 25. Machine nephanalysis of the photographs of Fig. 23.

surveying of the earth from satellites. However, the enormous volume of primary data describing the television image (~$1.5 \cdot 10^6$ bits per photograph) and the complexity of the algorithm itself makes it impossible to use this program in operational practice, since the time required for processing a single television frame comprises 30 minutes of machine time.

3. Automatic Processing and Analysis in Real Time of Infrared Photographs of the Earth Obtained from the Meteor Satellites

The experience accumulated in experiments with the above-described program for processing the ESSA television photographs is taken into account in creating a program for machine analysis of infrared images of the earth obtained with the aid of satellites of the Meteor system. The purpose of the investigation was, first, to determine the applicability of the developed method to low-resolution images obtained in a different (infrared rather than the visible) spectral range, and, second, taking into account the considerably smaller amount of primary infrared data, to achieve processing in real (or near-real) time.

Creation of a program for automatic processing and analysis of infrared photographs obtained from the Meteor satellites was facilitated by the fact that there were two finished programs for input of this data into the Minsk-22 computer and for its geographic control matching. These programs were created by V. I. Solov'yev in the Department of Analysis of Satellite Data of the Hydrometeorological Center of the USSR [38]. /111

The differences in the program developed here from that for the ESSA satellites are determined primarily by a different geometric structure for obtaining the infrared images. Instead of frame-by-frame surveying, single-element surveying is used with mechanical scanning of terrain along the flight path of a satellite in a strip approximately 1000 km wide. For automatic processing 68 measurements of the intensity of infrared emission in each scanning line were used. The intensity of infrared radiation has a latitudinal course, unrelated to the structure of overcast and at the same time complicating calculation of the features for cloud identification. Sliding averaging of the measured intensities on a scale comparable to the dimensions of large-scale cloud formations, i.e., of the order of 10^3 km, was carried out along the flight path of the satellite to eliminate it. The means obtained after some nonlinear filtration, which smooths out the extrema of the mean curve, were eliminated from each specific measurement. The measurements thus normalized also comprise the primary description of the infrared image, serving as the object of analysis. Besides the measurements themselves, data on the surveying time of each line of the orbital infrared photographs were stored in the computer memory.

A two-stage procedure, like that in the ESSA program described above, was employed for cloud identification. The orbital strip of infrared surveying was first divided into local sections of 8×8 scanning elements each (8 sections within the limits of the surveying strip) and the type of infrared image characterizing its pattern was determined for each section. To speed up processing time and to provide invariance to shifts and rotations of the image, instead of scanning coefficients of the eigenvectors of the covariational matrix of the infrared signal, single- and two-point moments of first and second order, which characterize the mean level of the normalized value of radiation, the range of values for individual scanning elements within the limits of the section, and also the predominant dimensions and spatial anisotropy of the inhomogeneities of the radiation field were used as the primary features. The specific type of these characteristics varied in different experiments while no satisfactory variant was found.

We note that in calculating the criteria it was essential to first eliminate pulse interference from the image, which is common for the digital transmission system employed in the IR system. A special algorithm for adapted filtration of the image was developed for this. This algorithm uses linear prediction of the signal level at the point of the image and coordinates (x_0, y_0) to detect the interference by interpolation of measurable values of the IR signal/112 in its neighborhood:

$$\overline{B(x_0, y_0)} = \frac{1}{\Omega_x \Omega_y} \int_{\Omega_x} \int_{\Omega_y} B(x_0 + \delta x, y_0 + \delta y)\, d\delta x\, d\delta y - B(x_0, y_0); \tag{3.57}$$

$$\Delta B(x_0, y_0) = B(x_0, y_0) - \overline{B(x_0, y_0)}. \tag{3.58}$$

If the considered point is not affected by interference, the prediction error may be assumed to be distributed normally with a zero average and dispersion $(\sigma_c[t])^2$, possibly dependent on time, because the overcasts observed from the satellite at different moments of time, for example above the equator and above the pole, have a different spatial structure. If there was interference, the error distribution in prediction is uniform within the range of the IR signal amplitude (b - a). Denoting the a priori probabilities of these events by $p_c[t]$ and $p_p[t]$, to obtain a solution on the presence or absence of interference, let us use the discriminant function

$$D(x_0, y_0) = \ln \frac{p\{c/\Delta B(x_0, y_0)\}}{p\{p/\Delta B(x_0, y_0)\}}. \tag{3.59}$$

Let us rewrite $z[t] = \Delta B(x_0, y_0)$ and write

$$D(z[t]) = \frac{1}{2}(z[t])^2/(\sigma_c[t])^2 - \ln\frac{p_c[t](b-a)}{p_p[t]\sqrt{2\pi}\sigma_c[t]} =$$
$$= (z[t])^2 - 2(\sigma_c[t])^2 \ln\frac{p_c[t](b-a)}{p[t]\sqrt{2\pi}\sigma_c[t]}. \qquad (3.60)$$

Since the prediction error in the presence of noise is much larger on the average than in its absence, the a priori probability of interference is

$$\frac{p_c[t](b-a)}{p_p[t]\sigma_c[t]\sqrt{2\pi}} > 1, \qquad (3.61)$$

then, by using the expansion of the logarithm of value (3.61) in a series and limiting ourselves to the first term of the series, we obtain

$$D(z[t]) \approx (z[t])^2 - 4(\sigma_c[t])^2 \frac{p_p[t]\sqrt{2\pi}\sigma_c[t]}{p_c[t](b-a)} =$$
$$= (z[t])^2 - n[t]. \qquad (3.62)$$

Thus, to detect the noise it is sufficient to compare the square of the error in linear prediction of the IR signal at the point of the image and coordinates (x_0, y_0) with some threshold, generally dependent on time. In the first approximation this dependence may be disregarded, having determined the threshold value for a number of values z[t] (t = 0, 1, 2, ..., T), for each of which it is known whether it corresponds to the presence or absence of noise. For this it is sufficient to find the estimates of the a priori probabilities of the presence and absence of noise by some "instruction" sample, as well as of the spread of the prediction error in the absence of noise. This solution of the problem is unnecessary, because the optimum threshold value, taking into account its time dependence, is very simply determined in the mode of normal operation of the program, i.e., without formulation of an "instruction" sample. For this, it is necessary to use a "self-instruction" algorithm of the following type. If it turns out in routine testing by exact formula (3.60) or by approximate formula (3.62) that there is no noise, "instruction" is carried out for adaptation to possible variations in the statistics of the real IR signal

/113

$$p_c[t+1] = p_c[t] + \Delta[1 - p_c[t]];$$
$$p_p[t+1] = 1 - p_c[t+1];$$
$$(\sigma_c[t+1])^2 = (\sigma_c[t])^2 + \Delta[(z[t+1])^2 - (\sigma_c[t])^2]. \qquad (3.63)$$

Moreover, the mean error in linear prediction of the IR signal is determined

$$\overline{z[t+1]}=\overline{z[t]}+\Delta[z[t+1]-\overline{z[t]}]. \tag{3.64}$$

In the reverse situation, i.e., when noise is detected, a signal equal to

$$z[t+1]^*=\overline{B[t+1]}+\operatorname{sign}(z[t+1])\,\overline{z[t]}, \tag{3.65}$$

is transmitted to the corresponding image point which prevents smoothing of the image, which is inevitable in linear filtration of noise. Moreover, "instruction" is carried out for adaptation to the possible altered noise statistics:

$$\begin{aligned} p_p[t+1]&=p_p[t]+\Delta[1-p_p[t]];\\ p_c[t+1]&=1-p_p[t+1]. \end{aligned} \tag{3.66}$$

Very rough estimates of approximation of several realizations of an IR signal with and without noise may be used as initial approximations for the values figuring in the discriminant function. The constant Δ in the formulas presented above for adaptation is positive and less than unity. Its value determines the effective "memory" of the adaptation system. The "memory" is of the exponential type. In order to prove this, let us assume that the estimate of the random value $\xi[t+1]$ of interest to us is found by means of

$$\xi[t+1]=\sum_{\tau=0}^{t+1}v_\tau\zeta[\tau]=\frac{\sum_{\tau=0}^{t+1}w_\tau\zeta[\tau]}{\sum_{\tau=0}^{t+1}w_\tau}, \tag{3.67}$$

where $v_\tau=w_\tau/\sum_{\tau=0}^{t+1}w_\tau$ are the normalized "weights" of the preceding observations of the random value. Rewriting (3.67) in recursion form /114 we obtain

$$\begin{aligned} \xi[t+1]&=\sum_{\tau=0}^{t+1}w_\tau\zeta[\tau]\Big/\sum_{\tau=0}^{t+1}w_\tau=\\ &=\Big\{\sum_{\tau=0}^{t}w_\tau\zeta[\tau]+w_{t+1}\zeta[t+1]\Big\}\Big/\sum_{\tau=0}^{t+1}w_\tau=\\ &=\Big\{\xi[t]\sum_{\tau=0}^{t}w_\tau+w_{t+1}\zeta[t+1]\Big\}\Big/\sum_{\tau=0}^{t+1}w_\tau= \end{aligned}$$

$$=\xi[t]+\left\{\xi[t]\left(\sum_{\tau=0}^{t}w_\tau-\sum_{\tau=0}^{t+1}w_\tau\right)+w_{t+1}\zeta[t+1]\right\}\Big/\sum_{\tau=0}^{t+1}w_\tau=$$

$$=\xi[t]+\frac{w_{t+1}}{\sum_{\tau=0}^{t+1}w_\tau}(\zeta[t+1]-\xi[t])=\xi[t]+\Delta[\zeta[t+1]-\xi[t]]. \qquad (3.68)$$

Thus, the adaptation constant is determined by the ratio of the "weight" of the last observation of random value to the "weights" of all past observations.

We note that the proposed algorithm works well when the basic assumption, assumed in derivation of the discriminant function (low noise probability), is fulfilled. Otherwise breaks in tracking the statistical characteristics of the signal are possible which are included in the fact that estimates of the statistical characteristics of noise are used as estimates of these statistical characteristics of the IR signal. This situation was observed in processing real-time IR photographs in those cases when the entire section of the IR image was completely obliterated by noise or when the synchronization of the lines of the IR photograph was considerably disrupted. As soon as the quality of the IR image improved, the normal working mode of the algorithm was restored due to adaptation.

After noise and slide omissions of the IR signal are eliminated, the described program for processing Meteor photographs provided for calculation of the primary features mentioned above, i.e., single- and two-point moments of first and second order. The clusters of points (types of IR image) were then found in the criterion space with the aid of the self-instruction program, described in the preceding section.

Subsequent investigation on calculation of the a priori and conditional probabilities was similar to that in identification of ESSA TV photographs. However, taking into account the global nature of IR surveying from the Meteor satellites, when estimating the a priori probabilities, we cannot limit ourselves to data from /115
climatic handbooks—the climatology of cloudiness is too poor. It is unrealistic to obtain estimates of the a priori probabilities of different types of overcast for all regions of the earth from data of the instruction sample of images. This requires an instruction sample consisting of many thousands of images. Hundreds of such images are required for correct estimation of the repeatability of five or six cloud patterns for an individual region. The number of such regions must be so great in order to detect all the characteristics of the very mottled pattern of the earth's cloud

cover (taking into account the capacity of the Minsk-22 machine memory, regionalization by sections 2×2° of the geographic grid of coordinates was used in the program). On the other hand, it was a desirable adaptation of the program to seasonal variations in the characteristics of overcast, which requires continuous recalculation of the conditional probabilities. Obviously, the meteorologist interpreter may not continuously "instruct" the machine. The latter must do this itself, for which a self-instruction algorithm must be introduced into it during normal operation.

The posed problem has been solved theoretically [114]. It reduces to performing the following operations in specific applications for cloud identification.

The earth is regionalized on the basis of climatological data. Each region includes in itself the areas identical in the nature of emission of visible or thermal radiation, for example a water surface with a temperature above zero or land with growing vegetation. Regionalization depends on the time year, for which a chart of the regions is compiled for each month. The list types of regions is identical for the entire year, i.e., each specific area is related to one or several alternately fixed types of regions throughout the year.

The matrices of the conditional probabilities are computed once and for all by a comparatively small instruction sample. With regard to the a priori probabilities, they are calculated for each moment of normal (operative) operation on cloud identification in the following manner. The values p(m), i.e., the recurrence of types of IR images, are calculated for each 2×2° of geographic region by the set of all IR photographs contained in it. In identification of a routine IR photograph of this geographic region, to find the a priori probabilities of the types of overcast, the following system of normal equations is solved.

$$p(\mathrm{m}) = \sum_{\mathrm{l}} p(\mathrm{l})\, p(\mathrm{m/l}),$$

$$(m = 1, 2, \ldots, M); \quad l = 1, 2, \ldots, L; \quad M \geqslant L) \tag{3.69}$$

with respect to the unknowns p(l).

The conditional probabilities $p(\mathrm{m/l})_{\varepsilon}$ are taken as those which correspond to the corresponding type of geographic regionalization. This type may change over the course of a year with the considered geographic area, it is clear that for each of the values of p(m) /116
should be replaced by storage with omission of very old observations, for which it is sufficient to correct the estimates of p(m) by the formulas:

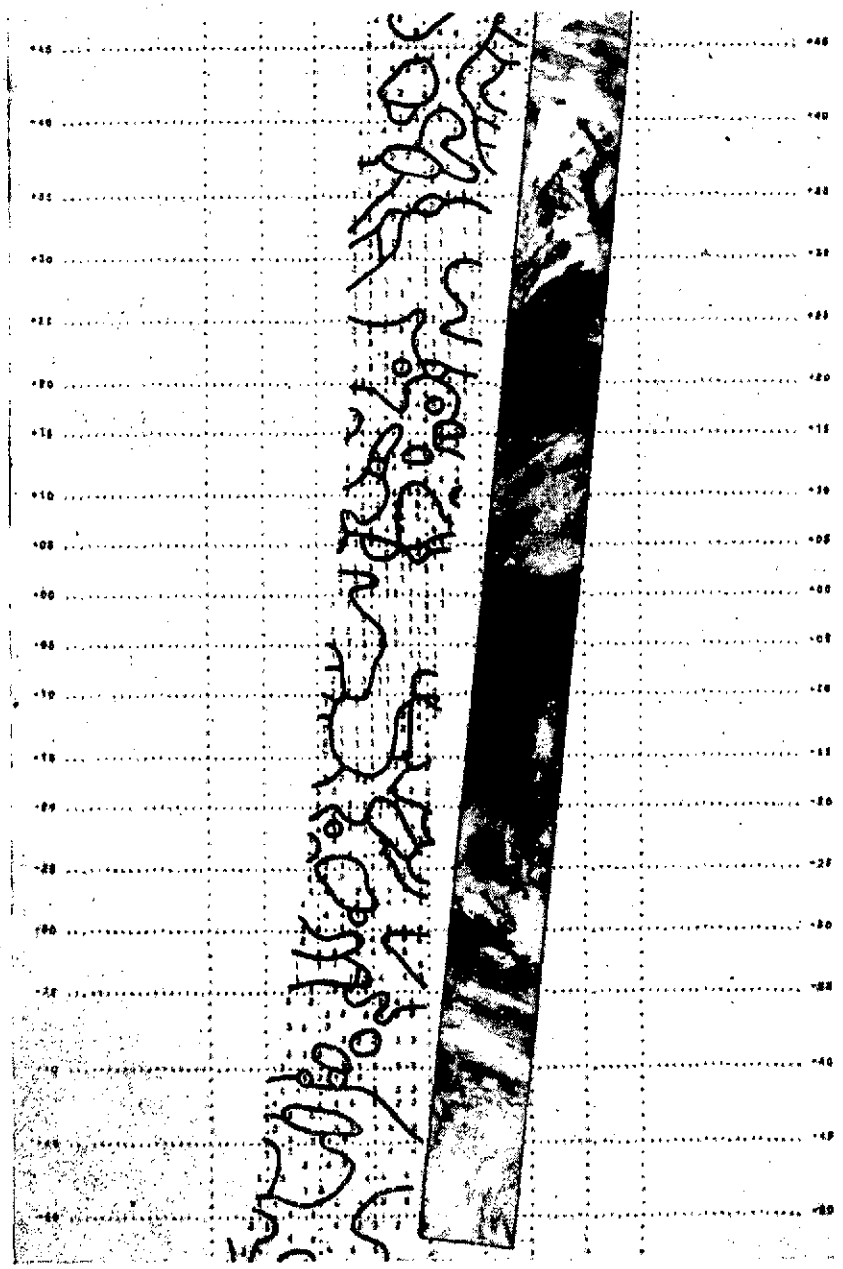

Fig. 26. Result of machine processing and analysis of orbital infrared photographs with identification of five types of overcast.

1- light low clouds or clear, 2- light, certainly with little or high clouds or with clouds of vertical development, 3- considerable or solid of only low clouds, 4- considerable, similar to the overcast of (2), 5- solid, of the same patterns.

$$p(m_i)_t = p(m_i)_{t-1} + \Delta[1 - p(m_i)_{t-1}];$$
$$p(m_j)_t = p(m_j)_{t-1} - \frac{\Delta}{M-1}[1 - p(m_j)_{t-1}]$$
$$(j = 1, 2, \ldots, M; \quad i \neq j), \tag{3.70}$$

if $\underline{m}_i$-th type of image is detected at the t-th moment of time for the area under consideration in the photograph.

The constant Δ determines the effective "memory" of the data storage system on the recurrence of different types of IR images. This value should be brought into agreement with the dynamics of replacing the diagrams of regionalization of the earth. Moreover, we note that in selecting the constant Δ such that the effective "memory" is equal, for example, to a month, we obtain the possibility of automatically issuing the mean monthly charts of overcast. They will be charts of calculated values of p(1).

The described program permits identification of the following six different types of overcast with gradations by the number and height of the upper boundary of the clouds: 1) clear or slight overcast of low clouds, 2) slight overcast of upper or middle clouds, vertical development or multilayered, 3) considerable or solid overcast of lower clouds, 4) considerable overcast of the type as in (2), 5) solid overcast of the same type, and 6) snow, ice, or clouds in Arctic and high-altitude regions. As a result of identification, that type of clouds is used to which corresponds the maximum a posteriori probability. It is calculated for each section of the IR photograph. The result is presented in the form of a chart in Mercator projection on a scale of 1:30,000,000. The processing time on the Minsk-22 computer for a full revolution of IR surveying comprises a little less than two hours with the time of about one and one-half hours that this information is received onboard the satellite. An example of processing is presented in Fig. 26.

Appendix

STATISTICAL CHARACTERISTICS OF THE SPACE-TIME VARIABILITY OF OVERCAST

We required the quantitative characteristics of the space-time variability of overcast to evaluate the information content of satellite nephanalysis in Chapter 2. /118

The basis for evaluating them were the hourly observations of the network of ground meteorological stations, located in Moscow and within a radius of 200 km from it, a total of about 40. The total amount of clouds according to observations at an individual station (Moscow) and the totals obtained on the observations of all stations located within squares of 100×100, 200×200, and 400×400 km^2 were considered as the parameter characterizing the state of the cloud cover. The squares were located concentrically around Moscow. More than 250,000 observations for the cold season (November-March) and approximately the same number of observations for the warm season (April-October) (1961-1966) was used.

The series of hourly observations obtained were used to calculate the temporal correlation functions and spectra of the total amount of clouds described in the literature [69]. The literature also contains the results of calculations of two-dimensional spatial correlation functions and spectra of the total amount of clouds from the data of observations of 324 meteorological stations obtained, uniformly scattered around the European USSR, for January, April, July, and October of 1961-1965.

Correlational-spectral analysis [69] made it possible to determine the main qualitative characteristics of the space-time variability of overcast in the considered area, consisting in the presence of the clearly defined hourly course of overcast during the warm season with the practical absence of this during the cold season. A four-day period of variations of the state of cloud cover (the natural synoptic period) was determined, especially during the cold season. This period is more clearly manifested the greater the spatial scale of averaging the data on overcast.

The basic characteristics of the spatial structure of overcast determined are its quasi-homogeneity and isotropism at a distance up to approximately 500 km. The data presented in [69] may also be used for certain quantitative calculations related to optimization of satellite systems for tracking cloud cover. However, the obvious abnormality of the distribution function for the total amount of clouds requires a type of calculating the more complicated characteristics of the space-time variability of overcast for correctness than the correlation functions and spectra. The required

Table I. Appearance (%) of different gradations of total amount of clouds (in points) with observations at a single station (Moscow) provided that a specific amount of clouds (first column - simultaneous observations, second column - with an interval of one hour, third column - with an interval of two hours) was observed in the neighborhod of this station (a square of 100×100 km^2 - first line, 200×200 km^2 - second line, 400×400 km^2 - third line). This was the warm season (April-September). The seasons were for 1964 and 1965. The total number of cases was 7344 for each range of asynchronism and for each square.

Amount of clouds in Moscow	Amount of clouds by squares															Unconditional recurrence
	10			9—7			6—4			3—1			0			
10	76.2	71.8	64.3	19.3	22.5	22.2	1.8	2.2	3.1	1.7	2.1	2.8	1.0	1.5	1.6	17.0
	49.6	48.9	40.0	22.5	23.1	33.7	10.8	11.4	12.0	12.1	10.8	9.7	5.0	5.8	4.6	10.6
	51.7	49.6	48.4	21.1	16.4	21.2	11.4	15.3	13.6	10.3	11.2	10.4	5.6	7.5	6.4	4.9
9—7	14.6	16.3	17.8	66.4	62.8	56.4	14.7	15.3	16.5	2.9	4.0	7.1	1.4	1.6	2.2	33.0
	23.4	22.8	22.5	49.5	48.9	44.7	13.8	14.2	16.8	7.5	8.4	9.7	5.8	5.7	6.3	35.9
	25.4	25.3	24.8	46.9	46.7	44.4	13.5	13.5	14.5	8.1	8.6	10.6	6.1	5.9	5.7	38.9
6—4	4.0	4.2	5.6	29.0	29.0	32.2	41.2	38.1	31.4	20.7	22.8	22.3	5.1	5.8	8.5	19.7
	12.5	12.1	13.6	31.8	31.6	32.9	28.1	26.1	23.0	18.5	19.6	19.3	9.0	10.7	11.2	21.7
	7.8	14.4	14.4	30.8	31.0	32.4	24.7	23.0	22.3	20.6	19.6	18.5	11.0	11.9	12.3	27.8
3—1	2.5	2.9	3.3	6.0	9.1	12.9	15.3	15.9	17.6	48.0	41.1	33.1	28.1	31.1	33.1	19.2
	9.2	10.2	9.2	18.7	19.0	21.7	14.9	14.8	18.3	28.6	28.6	25.7	28.5	27.3	25.1	22.7
	9.4	9.4	9.6	18.8	20.9	20.0	15.8	15.7	17.0	24.8	24.2	22.5	31.1	29.8	31.2	23.4
0	3.3	3.6	3.6	4.8	6.3	8.3	4.3	6.5	9.2	9.1	14.4	18.0	78.5	69.2	60.9	11.1
	8.0	7.4	6.0	14.1	14.4	13.1	10.2	10.5	9.5	11.7	16.8	18.9	55.9	50.9	52.5	9.1
	11.3	11.3	11.5	14.5	13.8	13.4	6.7	6.6	5.8	11.6	13.2	17.3	54.8	55.1	52.1	5.0
Unconditional recurrence		19.0			32.8			16.7			15.7			15.8		100.0

Table II. Recurrence (%) of different gradations of the total amount of clouds (in points) with observation at a single station (Moscow) provided that a specific amount of clouds (the first column - simultaneous observations, second column - with an interval of one hour, third column - with an interval of two hours) is observed in the neighborhood of this point (square of 100×100 km^2 - first line, 200×200 km^2 - second line, 400×400 km^2 - third line). This is the cold season (October-March). The seasons were for 1964-65 and 1966-66. The total number of cases was 7248 for each interval of asynchronism and for each square.

Amount of clouds in Moscow	Amount of clouds by squares															Unconditional recurrence
	10			9–7			6–4			3–1			0			
10	94,0	92,4	91,0	5,3	6,0	6,8	0,5	0,6	1,2	0,1	0,5	0,5	0,1	0,5	0,5	59,1
	93,3	92,5	91,0	5,7	5,8	6,6	0,5	0,7	0,9	0,4	0,5	0,6	0,1	0,5	1,0	52,7
	92,4	92,5	91,3	6,4	5,9	6,2	0,6	0,4	0,8	0,5	0,4	0,7	0,1	0,8	1,0	47,2
9–7	28,1	34,8	38,6	59,8	47,9	42,0	9,1	9,4	8,6	1,7	3,8	5,2	1,3	4,1	5,6	18,7
	42,7	44,4	45,9	44,2	42,1	39,2	8,0	7,2	6,6	2,8	3,3	3,7	2,3	3,0	4,6	24,5
	53,0	53,1	53,1	34,3	33,8	32,8	6,1	6,2	6,3	3,0	3,1	3,6	3,6	3,8	4,2	30,5
6–4	16,2	20,4	22,6	28,2	29,2	30,2	25,6	20,8	18,0	14,0	12,8	10,4	16,0	16,8	18,8	7,6
	16,5	20,5	22,7	27,0	29,0	29,0	23,7	18,8	17,7	15,7	13,8	11,0	17,1	17,9	19,6	8,9
	19,5	20,6	23,1	27,3	28,6	27,5	21,3	18,0	17,3	15,2	14,5	10,8	18,0	18,3	21,3	10,4
3–1	3,0	5,3	6,0	3,0	10,3	12,4	17,2	14,1	14,0	35,0	27,5	22,9	41,8	42,8	44,7	7,3
	5,0	6,0	6,3	5,3	9,2	10,2	11,5	10,9	11,5	25,6	21,3	19,1	52,6	52,6	52,9	8,6
	7,0	7,2	8,1	6,5	8,0	10,4	10,6	9,1	7,9	18,5	16,5	12,5	87,4	59,2	61,1	9,6
0	0,1	0,6	1,0	0,2	0,9	1,6	0,5	2,5	4,9	5,4	7,1	8,1	93,6	88,9	83,4	7,3
	0,2	0,6	1,7	0,6	0,6	1,1	1,0	2,8	2,5	6,0	7,0	7,2	92,2	88,0	87,5	5,3
	0,3	1,3	1,7	0,6	1,3	2,4	1,0	3,6	1,4	6,1	6,6	4,2	92,0	87,2	90,3	2,3
Unconditional recurrence	62,0			16,7			5,0			4,6			11,7			100,0

characteristics are primarily matrices of the transition probabilities of cloud cover from one fixed state to another for different scales of spatial averaging of the data and different temporal shifts. From transition probabilities, based on hourly observations in the Moscow area during the 1964-1966 seasons are presented in the Appendix (Tables I and II). The data of these tables were also used for evaluating the information content of satellite nephanalysis. They include the following conclusions.

The non-Gaussian property of the distribution function of the total amount of clouds is more strongly expressed during the cold season than during the warm. It is less appreciable the greater the spatial averaging of observations of overcast, so that it may apparently be disregarded for very large scales (of the order of $10^3 \times 10^3$ km^2). The interrelationship between simultaneous observations of clouds at an individual station and in its surrounding area is weaker the larger the territory considered. However, asynchronous relationships as the value of the shift in the time of observations at an individual station increases with respect to the areal observations become closer as the area increases, i.e., the large-scale characteristics of the structure of cloud cover are longer in duration. In all cases extremum states of cloud cover (overcast and clear) are more stable in space and time than intermediate states.

References

1. Ayzerman, M. A., E. M. Braverman, and L. I. Rozonoer, Metod potentsial'nykh funktsiy v teorii obucheniya mashin [Method of potential functions in the theory of teaching machines], Nauka, Moscow, 1970, 383 p. /122

2. Anderson, T. U., Vvedenye v mnogomernyy statisticheskiy analiz [Introduction to multidimensional statistical analysis]. Fizmatgiz, Moscow, 1963, 500 p.

3. Anekeyeva, L. A., Using data on overcast, obtained with the aid of artificial earth satellites, in objective analysis of the wind field. Transactions of the Hydrometeorological Center of the USSR, No. 36, 1968, p. 3-8.

4. Anekeyeva, L. A., On the problem of using satellite data on overcast in objective analysis of the wind field. Transactions of the Hydromet. Center of the USSR, No. 50, 1969, p. 31-36.

5. Aoki, M., Optimizatsya stokhasticheskikh sistem [Optimization of stochastic systems]. Nauka, Moscow, 1971, 424 p.

6. Barabash, L. L., et al, Voprosy statisticheskoy teorii raspoznavaniya [Problems of statistical recognition theory]. Sovetskoye radio, Moscow, 1967, 400 p.

7. Bakhtin, M. G., and D. M. Sonechkin, Evaluating the information content of nephanalyses carried out from data of television surveying from Tiros satellites. Transactions of the Hydrometeorological Center of the USSR, No. 11, 1967, p.103-110.

8. Bashkirov, O. A., E. M. Braverman, and I. B. Muchnik, Algorithms for teaching machines to recognize visual images based on use of potential functions. Avtomatika i telemekhanika, 1964, Vol. 25, No. 5., p. 692-695.

9. Bogomolov, O. S., On a method for restoring the pressure field from data of meteorological satellites. Transactions of LVIKA imeni A. F. Mozhayskiy, No. 507, 1967, p. 17-20.

10. Bratslavets, P. F., I. A. Rosselevich, and L. I. Khromov, Kosmicheskoye televideniye [Space television]. Svyaz', Moscow, 1967, 136 p.

11. Burtsev, A. I., et al, Molniya-1 transmits images of the earth from space. Meteorologiya i gidrologiya, 1966, No. 12, p. 3-9.

12. Vapnik, V. N., A. Ya. Lerner, and A. Ya. Chervonenkis, Teaching machines to recognize images by the method of generalized portraits. Transactions of the All-Union Congress on Automatic Control and Technical Cybernetics, Vol. 3, Nauka, Moscow, 1967, p. 112-118.

13. Vel'tishchev, N. F., The structure of overcast in atmospheric eddies, Meteorologiya i gidrologiya, 1965, No. 12, p. 11-19.

14. Vel'tishchev, N. F., Small perturbations of vertical velocity in an asymmetric atmospheric eddy. Transactions of the Hydrometeorological Center of the USSR, No. 20, 1968, No. 20, p. 35-41.

15. Vel'tishchev, N. F., The effect of stratification on formation of convective cells in the atmosphere. Transactions of the Hydrometeorological Center of the USSR, No. 30, 1968, p. 9-20.

16. Vel'tishchev, N. F., Cellular convection in the atmosphere. Transactions of the Hydrometeorological Center of the USSR, No. 50, 1969, p. 3-21.

17. Vel'tishchev, N. F. and A. A. Zhelnin, Meteorological conditions of formation of banks of convective overcast, Transactions of the Hydrometeorological Center of the USSR, No. 50, 1969, p. 22-30.

18. Vel'tishchev, N. F. and V. V. Ozerkinn, Restoration of the wind field in a cyclone with the aid of television images of overcast obtained from artificial earth satellites. Transactions of MMTs, 1966, No. 11, p. 15-25. /123

19. Vel'tishchev, N. F. and L. I. Silayeva, Convective cloud cells according to observations from artificial earth satellites. Transactions of the Hydrometeorological Center of the USSR, No. 20, 1968, p. 22-29.

20. Vetlov, I. P., Some results in comparison of satellite and ground observations of overcast. Transactions of MMTs, 1965, No. 8, p. 3-10.

21. Vetlov, I. P., Meteorological investigations with the aid of artificial earth satellites. In. Meteorologiya i gidrologiya za 50 let Sovetskoy vlasti [Meteorology and hydrology during 50 years of Soviet power]. Gidrometeoizdat, Leningrad, 1967, p. 27-50.

22. Vetlov, I. P., et al, Infrared equipment for satellites of the Meteor system, Meteorologiya i gidrologiya, 1970, No. 4, p. 80-91.

23. Galushkin, A. I., Mnogosloynyye sistemy raspoznavaniya oblakov [Multilayered systems of cloud identification]. MIIEM MV and SSO RSFSR, Moscow, 1970, 167 p.

24. Gandin, L. S., Some ways of utilizing satellite information in objective analysis of meteorological fields. Uchebnyy seminar po sputnikovoy meteorologii [Training seminar on satellite meteorology]. Gidromettsentr SSSR, Moscow, 1966, p. 1-21.

25. Gorbunov, G. V. and E. S. Moskalev, The use of Rademacher-Walsh polynomials in problems of approximating the functions of several variables. Kibernetika, 1971, No. 3, p. 19-22.

26. Dzyubenko, T. D. and A. M. Tsar'kova, Calculation of the position of the jetstream axis from data on overcast from meteorological satellites. Transactions of the Hydrometeorological Center of the USSR, 1968, No. 36, p. 40-46.

27. Dombkovskaya, Ye. P., The relationship between cloud masses visible from a satellite and the zones of precipitation falling from them. Transactions of the Hydrometeorological Center of the USSR, 1968, No. 36, p. 40-46.

28. Zhvalev, V. F., K. Ya. Kondrat'yev, and N. E. Ter-Markaryants, On calculating the spectral value of outgoing radiation and the contrasts between the radiation temperature of the underlying surface and clouds in relation to the problem of detecting overcast from artificial earth satellites. Transactions of the GGO, 1967, No. 203, p. 3-34.

29. Istomina, L. G., Determination of the statistical characteristics of the spatial structure of cloud fields from aerial photographs. Izzestiya AN SSSR, seriya fizika atmosfery i okeana 1966, Vol. II, No. 3, p. 263-271.

30. Istomina, L. G. and Ye. M. Kozlov, On the two-dimensional spatial structure of cloud field brightness. Izzestiya AN SSSR, seriya fizika atmosfery i okeana 1968, Vol. IV, No. 7, p. 717-727.

31. Istomina, L. G., M. S. Malkevich, and V. I. Syachinov, On the spatial structure of the earth's brightness field according to measurements from the Cosmos-149 satellite. Izvestia AN SSSR, seriya fizika atmosfery i okeana, 1970, Vol. VI, No. 5, p. 468-476.

32. Kachmazh, S. and G. Shteyngauz, Teoriya ortogonal'nikh ryadov. [The theory of orthogonal series]. Fizmatgiz, Moscow, 1958, 320 p.

33. Kondrat'yev, K. Ya., Luchistaya energiya Solntsa [The radiant energy of the sun]. Gidrometeoizdat, Leningrad, 1954, 599 p.

34. Kondrat'yev, K. Ya. and N. Ye. Ter-Markaryants, On the possibility of detecting overcast on the night side of the earth from data of measuring outgoing thermal radiation in the atmospheric window. Transactions of GGO, 1965, No. 170, p. 12-19.

35. Kol'bak, S., Teoriya informatsii i statistika [Information theory and statistics]. Nauka, Moscow, 1967, 408 p.

36. Latysheva, V. I., T. A. Mel'nikova, and D. M. Sonechkin, Using the statistical characteristics of a television signal to determine the amount and pattern of clouds in photographs obtained from meteorological satellites. Transactions of MMTs, 1966, No. 11, p. 42-59.

37. Lovanova, V. Ya., Characteristics of overcast distribution above the Northern Hemisphere. Transactions of NIIAK, 1967, No. 44, p. 55-65.

38. Mazina, L. G., et al, Machine analysis of infrared images of overcast obtained from the Cosmos-122 satellite. Transactions of the Hydrometeorological Center of the USSR, 1968, No. 20, p. 60-67.

39. Mazurin, N. I., Characteristics of the convective cloud fields/124 and the related precipitation zones. Transactions of the All-Union Scientific Meteorological Society, Vol. 5, Gidrometeoizdat, Leningrad, 1963, p. 29-37.

40. Mazurin, N. I., Some properties of solid overcast fields and precipitation zones above the Northern Hemisphere. Transactions of GGO, 1964, No. 161, p. 36-41.

41. Malkevich, M. S., et al, Calculation of the statistical characteristics of radiation fields above clouds. Kosmicheskiye issledovaniya, 1964, Vol. II, No. 2, p. 49-64.

42. Malkevich, M. S., A. S. Monin, and G. V. Rozenberg, The spatial structure of the radiation field as a source of meteorological data. Izvestiya AN SSSR, seriya geofizika, 1964, No. 3, p. 394-407.

43. Malkina, R. M., and A. A. Pervozvanskiy, Approximation by proximate points in problems on restoration of functions and pattern recognition. Izvestiya AN SSSR, seriya tekhnicheskaya kibernetika, 1969, No. 1, p. 133-137.

44. Markina, N. G. and L. A. Pakhomov, Statistical characteristics of the reflected radiation field. Transactions of TsAO, 1970, No. 86, p. 47-55.

45. Minina, L. S. Praktika nefanaliza [Techniques of nephanalysis]. Gidrometeoizdat, Leningrad, 1970, 336 p.

46. Musayelyan, Sh. A., Some problems of numerical interpretation of cloud data obtained from artificial earth satellites. Transactions of GGO, 1964, No. 166, p. 203-213.

47. Musayelyan, Sh. A. and N. N. Aprausheva, On joint utilization of the data of satellite observations and the sparse network of aerological stations for restoration of the fields of meteorological elements. Transactions of the Hydrometeorological Center of the USSR, 1968, No. 30, p. 93-99.

48. Musayelyan, Sh. A. and L. V. Belinskaya, On restoration of the fields of meteorological elements from data of satellite observations. Transactions of the Hydrometeorological Center of the USSR, 1968, No. 30, p. 100-110.

49. Musayelyan, Sh. A., N. S. Khazizova, and N. A. Shuzavkova, Some results of calculating vertical motion fields from overcast distribution. Transactions of MMTs, 1966, No. 11, p. 78-88.

50. Musayelyan, Sh. A., et al, Problems of using the data of meteorological satellites in numerical analysis and forecasting. Meteorologiya i gidrologiya, 1970, No. 12, p. 3-12.

51. Nad', J., Pattern recognition. Transactions of the Institute of Electrical Engineering and Radioelectronics Engineers, 1968, Vol. 56, No. 5, p. 57-85.

52. Nazirov, M., Shadows on satellite photographs as a source of information on the vertical extensions of the clouds. Transactions of the Hydrometeorological Center of the USSR, 1968, No. 36, p. 21-26.

53. Nayshuler, M. G., D. M. Sonechkin, and T. A. Yakovleva, Analysis of overcast from data of infrared surveying of the earth from satellites of the experimental Meteor system. Meteorologiya i gidrologiya, 1968, No. 11, p. 21-39.

54. Nil'son, N., Obuchayushchiyesya mashiny [Learning machines]. Mir, Moscow, 1967, 180 p.

55. Orlovskiy, Ye. L., et al, Teoreticheskiye osnovy elektricheskoy peredachy izobrazheniy [Theoretical bases of electrical

transmission of images]. Sovetskoye radio, Moscow, 1962, Vols. 1 and 2, 800 p.

56. Pratt, W. C., Yu. Keyn, and G. K. A. Andrews, Image coding by means of the Adamar transformation. Transactions of the Institute of Electrical Engineering and Radioelectronics Engineers, 1969, Vol. 57, No. 1, p. 66-76.

57. Purganskiy, V. S., The hydrodynamic model of the large-scale atmospheric vortex. Meterologiya i gidrologiya, 1968, No. 12, p. 14-23.

58. Purganskiy, V. S., Determination of the wind in a large-scale vortex in the "average" level of the atmosphere. Transactions of TsAO, 1970, No. 86, p. 56-70.

59. Rozenblat, F., Osnovy neyrodinamiki. Pertseptrony i teoriya mekhanizmov mozga [Fundamentals of neurodynamics. Perceptrons and the theory of mechanisms of the brain]. Mir, Moscow, 1965.

60. Sebestian, G. S., Protsessy prinyatiya resheniya pri raspoznavanii obrazov [Decision-making processes in pattern recognition]. Naukova dumka, Kiev, 1965, 135 p.

61. Smirnova, N. V., The billow clouds of barriers observed from artificial earth satellites. Transactions of the Hydrometeorological Center of the USSR, 1968, No. 20, p. 30-34.

62. Solov'yev, V. I. and I. S. Solov'yeva, Calculation of the angular elements of external orientation of photographs from meteorological satellites. Transactions of the Hydrometeorological Center of the USSR, 1967, No. 11, p. 111-117.

63. Solov'yev, V. I. and I. S. Solov'yeva, Mapping of overcast photographs obtained from the Molniya-1 satellite. Transactions of the Hydrometeorological Center of the USSR, 1968, No. 30, p. 61-67. /129

64. Sonechkin, D. M., On interpretation of television images of overcast obtained from artificial satellites. Meteorologiya i gidrologiya, 1962, No. 9, p. 30-33.

65. Sonechkin, D. M., On the comparability of satellite and ground data on the total amount of clouds. Transactions of the Hydrometeorological Center of the USSR, 1967, No. 11, p. 47-55.

66. Sonechkin, D. M., Classification of types of television images of overcast and of the earth's surface obtained from satellites

of the experimental Meteor system, Meteorologiya i gidrologiya, 1968, No. 9, p. 3-10.

67. Sonechkin, D. M., Objective methods of diagnosing overcast, Transactions of the Hydrometeorological Center of the USSR, 1968, No. 30, p. 39-49.

68. Sonechkin, D. M., Objective methods on diagnosing overcast, meteorological fields, Meteorologiya i gidrologiya, 1971, No. 3, p. 22-29.

69. Sonechkin, D. M. and I. S. Khandurova, Results of investigating the space-time variability of overcast in the European USSR, Transactions of the Hydrometeorological Center of the USSR, 1969, No. 50, p. 37-46.

70. Stratonovich, R. L., Optimum identification algorithms, Avtomatika i telemekhanika, 1968, No. 2, p. 110-113.

71. Stratonovich, R. L., The effectiveness of methods of mathematical statistics in problems of synthesizing algorithms for restoration of an unknown function, Izzestiya AN SSSR, seriya tekhnicheskaya kibernetika, 1969, No. 1, p. 32-46.

72. Stratonovich, R. L., Optimum expansion of the functional space in algorithms for restoration of distribution density and distribution function, Izzestiya AN SSSR, seriya tekhnicheskaya kibernetika, 1970, No. 2, p. 57-64.

73. Solov'yeva, I. S. and D. M. Sonechkin, Experiments on television surveying of the earth from the Molniya-1 satellite, Transactions of the Hydrometeorological Center of the USSR, 1968, No. 30, p. 50-60.

74. Wilkes, S., Matematicheskaya statistika [Mathematical statistics], Nauka, Moscow, 1967, 632 p.

75. Fadeyev, D. K. and V. N. Fadeyeva, Vychislitel'nyye metody lineynoy algebry [Computational methods of linear algebra], Fizmatgiz, Moscow, 1960, 656 p.

76. Feoktistov, K. P., et al, Some results of optical observations of the Voskhod spacecraft, In Issledovaniya kosmicheskogo prostranstva [Investigations of space], Nauka, Moscow, 1965, p. 62-63.

77. Fizika oblakov [Cloud physics], Edited by A. Kh. Khrgian, Gidrometeoizdat, Leningrad, 1961, 459 p.

78. Firsheyn, O. and M. Fishler, Automatic detection of sub-classes in problems of pattern recognition, In Avtomaticheskiya analiz slozhnykh izobrazheniy [Automatic analysis of complex images], Mir, Moscow, 1969, p. 235-238.

79. Fu, K., Posledovatel'nyye metody v raspoznavanii obrazov i obuchenii mashin [Sequential methods in pattern recognition and machine instruction], Nauka, Moscow, 1971, 256 p.

80. Ho, Yu-Tszi and A. K. Agravala, On algorithms for classification of images, Transactions of the Institute of Electrical Engineering and Radioelectronics Engineers, 1968, Vol. 56, No. 12, p. 5-19.

81. Tsypkin, Ya. Z., Adaptatsiya i obucheniya v avtomaticheskikh sistemach [Adaptation and instruction in automatic systems], Nauka, Moscow, 1968, 400 p.

82. Tsypkin, Ya. Z., Osnovy teorii obuchayushchikhsya sistem [Fundatmentals of the theory of teaching systems], Nauka, Moscow, 1970, 252 p.

83. Chapurskiya, L. I., On reliable detection of clouds in aerial photography, Aeros'yemka i yeye primeneniya [Aerial surveying and its applications], Nauka, Leningrad, 1967, p. 92-94.

84. Chapurskiya, L. I., The absolute spectral brightness of clouds and of the underlying surface in the near infrared region of the spectrum, Transactions of AANII, 1968, Vol. 284, p. 100-101.

85. Cahpurskiya, L. I., et al, The spectral brightness of clouds and landscape objects in the visible and near infrared regions of the spectrum. Transactions of GGO, 1968, No. 221, p. 185-197.

86. Chekirda, A. Z. and T. A. Yakovleva, Using satellite data on outgoing radiation for identification of precipitation zones, Meteorologiya i gidrologiya, 1967, No. 6, p. 13-20.

87. Chuzavkova, N. A., On the possibility of calculating the factor of the humidity according to cloud distribution, Trudy Gidromettsentra SSSR, 1967, No. 11, p. 65-73. /126

88. Shifrin, K. S. and Yu. S. Fridman, Geometric methods of processing television pictures of the earth's cloud cover, Trudy, GGO, 1970, No. 235, p. 24-41.

89. El'man, R. I., On the synthesis structure of an image analyizer, Izv. AN SSSR seriya tekh. kibernetika, 1968, No. 1, p. 135-150.

90. Yanko, Ya., Matematiko-statisticheskiye tablitsy [Mathematical-statistical tables], Moscow, Gosstatizdat, 1961, 243 p.

91. Adachi, T. and T. Kasai, Stereoscopic analysis of photographs taken by scopic analysis, J. Meteorol. Soc. of Japan, 1970, ser. II, Vol. 48, No. 3, p. 234-242.

92. Anderson, R. K., E. W. Ferguson, and V. J. Oliver, The use of satellite pictures in weather analysis and forecasting, Technical note no. 75, WMO, 1966, 187 p.

93. APT users guide, U. S. Department of Commerce, ESSA, Washington, 1965, 100 p.

94. Ausfesser, H. D., A. C. Johnson, and R. A. Kowalski, Computer correction of distortion in ATS-SSCC photographs, BAMS, 1969, Vol. 50, No. 2, p. 119-122.

95. Barr, S., M. B. Lawrence, and F. Sanders, Tiros vorticies and large scale vertical motion, Monthly Weather Review, 1966, Vol. 94, No. 12, p. 675-696.

96. Beran, D. W., Jet streams as observed by infrared satellites, Australian Meteorol. Magazine, 1968, Vol. 16, No. 2, p. 47-53.

97. Blackmer, R. H. and S. M. Serebreny, Dimensions and distributions of cumulus clouds as shown by U-2 photographs, Stanford Research Institute, Menlo Park, Calif., 1962, 17 p.

98. Blankenship, J. R., An approach to objective nephanalysis from an earth-oriented satellite, J. Appl. Meteorol., 1962, Vol. 1, No. 4, p. 319-326.

99. Blau, H. H., Cloud structure from infrared imagery, Appl. Optics, 1968, Vol. 7, No. 10, p. 1037-1039.

100. Booth, A. L. and V. R. Taylor, Meso-scale archive and computer products of digitized video data from ESSA satellites, BAMS, 1969, Vol. 50, No. 6, p. 431-438.

101. Boucher, R. J., Relationships between the size of satellite-observed cirrus shields and the severity of thunderstorm complexes, J. Appl. Meteorol., 1967, Vol. 6, No. 3, p. 564-572.

102. Bowley, C. J., et al, Satellite observations of wake formation beneath an inversion, J. Atmos. Sci., 1962, Vol. 19, No. 1, p. 31-35.

103. Bristor, C. L. and W. M. Callicott, Meteorological products from digitized satellite vidicon cloud pictures, MSL report 26, Washington, 1964, 19 p.

104. Bristor, C. L., W. M. Callicott, and R. E. Bradford, Operational processing of satellite cloud pictures by computer, Monthly Weather Review, 1966, Vol. 94, No. 8, p. 515-527.

105. Brodrick, H. J., E. P. McClain, and E. P. Ruzecki, Experimental use of satellite pictures in numerical prediction, MSL report 36, Washington, 1966, 25 p.

106. Chopra, K. P. and L. F. Hubert, Karman vortex streaks in earth's atmosphere, Nature, 1964, Vol. 23, No. 4952, p. 1114-1129.

107. Clapp, P. F., Global cloud cover for seasons using Tiros nephanalysis, Monthly Weather Review, 1964, Vol. 92, No. 11, p. 530-534.

108. Clauss, J. R., The relationship between total cloud amount and objectively defined synoptic parameters, Technical note no. 1, Meteorol. Abhandlungen, 1963, Vol. XXXII, No. 3, 77 p.

109. Conover, J. H., Cloud interpretation from satellite altitudes, C. R. Research Note 81, Air Force Cambridge Research Lab., 1962, 80 p.

110. Conover, J. H., The identification and significance of orographically induced clouds observed by Tiros satellites, J. Appl. Meteorol., 1964, Vol. 3, No. 3. p. 226-234.

111. Conover, J. H., Anomalus cloud lines, J. Atmos. Sci., 1966, Vol. 23, No. 11, p. 778-785.

112. Conover, J. H. and J. C. Sadler, Cloud patterns as seen from altitudes of 250-850 miles—preliminary results, BAMS, 1960, Vol. 41, No. 6, p. 291-297. /127

113. Cooper, P. W., Hyperplanes, hyperspheres, and hyperquadrics as decision boundaries. Computer and Information Sciences, R. H. Wilcox, Spartan Books, 1964, p. 111-138.

114. Cooper, D. B. and J. H. Freeman, On the asymptotic improvement in the outcome of supervised learning provided by additional nonsupervised learning, IEEE Transactions on Computers, 1970, Vol. 19, No. 11, p. 1055-1062.

115. Cover, T. M. and P. E. Hart, Nearest neighbor pattern classification. IEEE Transactions on Information Theory, 1967, Vol. 13, No. 1, p. 21-27.

116. Crowson, D. I., Cloud observations from rockets, BAMS, 1949, Vol. 30, No. 1, p. 17-22.

117. Darling, E. M. and R. D. Joseph, Pattern recognition from satellite altitudes. IEEE Transactions on System Sciences and Cybernetics, 1968, Vol. 4, No. 1, p. 38-46.

118. Doolitle, R. C., C. L. Bristor, and L. Lauritson, Mapping of geostationary satellite pictures—an operational experiment. ESSA Technical Memorandum NESCTM 20, Washington, 1970, 39 p.

119. Endlich, R. M., et al, Use of a pattern recognition technique for determining cloud motions sequences of satellite photographs, J. Appl. Meteorol., 1971, Vol. 10, No. 1, p. 105-117.

120. Erickson, C. O., Satellite photographs of convective clouds and their relation to the vertical wind shear, Monthly Weather Review, 1963, Vol. 92, No. 6, p. 283-296.

121. Erickson, C. O. and L. F. Hubert, Identification of cloud forms from Tiros-1 pictures, MSL report 7, Washington, 1961, 68 p.

122. Frankel, M. and C. L. Bristor, Perspective locator grids for Tiros pictures, MSL report 10, Washington, 1962, 19 p.

123. Fritz, S., The significance of mountain lee waves as seen from satellite pictures, J. Appl. Meteorol., 1965, Vol. 4, No. 1, p. 31-37.

124. Fujita, T., et al, Meteorological interpretation of convective nephsystems appearing in Tiros cloud photographs. Internat. Symposium on Rocket and Satellite Meteorology, Amst., Proceedings, 1963, p. 160-167.

125. Fukunaga, K. and W. L. G. Koontz, Application of the Karhunen-Loeve expansion to feature selection and ordering. IEEE Transactions on Computers, 1970, Vol. 19, No. 4, p. 311-318.

126. Fukunaga, K. and T. F. Krile, Calculation of Bayes' recognition error for two multivariate Gaussian distributions. IEEE Transactions on Computers, 1969, Vol. 18, No. 3, p. 220-229.

127. Greaves, J. R. and P. E. Sherr, The use of cloud-amount and cloud-type statistics in the design and operation of aerospace

systems. National Conference on Aerospace Meteorology, 4-th, Las Vegas, Nevada, Reports, 1970, p. 581-583.

128. Hanel, R., et al, The satellite Vangard II. Cloud cover experiment. IRE Transactions on Military Electronics, 1960, Vol. 4, No. 2-3, p. 303-304.

129. Hawkins, J. K., G. T. Elerding, K. W. Bixby, and P. A. Haworth, Automatic extraction of topographic map intelligence from aerial photos. 1966 IEEE Internat. Communs. Conference, Vol. 2, Lewis Winner, 1966, p. 1014-1019.

130. Hellman, M. E., The nearest neighbor classification rule with a reject option. IEEE Transactions on System Sciences and Cybernetics, 1970, Vol. 6, No. 3. p. 17-24.

131. Heydorn, R. P., An upper bound estimate on classification error. IEEE Transactions on Information Theory, 1968, Vol. 14, No. 9, p. 783-784.

132. Hubert, L. F. and O. A. Berg, A rocket portrait of a tropical storm, Monthly Weather Review, 1955, Vol. 83, No. 6, p. 119-125.

133. Hubert, L. F., Mesoscale cellular convection, MSL report 37, Washington, 1966, 68 p.

134. Hubert L. F. Accuracy of wind estimates from geostationary satellites. Scientific Discussions EC-XXII, ESSA, Washington, 1970, Appendix II, p. 1-19.

135. Hubert, L. F. and A. F. Krueger, Satellite pictures of mesoscale eddies, Monthly Weather Review, 1962, Vol. 90, No. 6, p. 481-494. /128

136. Hubert L. F. and A. Timchalk, Estimating Hurricane wind speeds from satellite pictures, Monthly Weather Review, 1969, Vol. 97, No. 5, p. 382-404.

137. Hubert, L. F., A. Timchalk, and S. Fritz, Estimating maximum wind speed of tropical storms from high resolution infrared data. ESSA Technical report NESC 50, Washington, 1969, 33 p.

138. Hunt, J. N. and P. E. Wickins, Vortex streaks in the earth's atmosphere. Pure and Applied Geophysics, 1967, Vol. 67, No. 2, p. 224-232.

139. Jones, G. D., D. T. Hilleary, and B. Fridovich, A diffuse light source for calibrating meteorological satellite television cameras, Appl. Optics, 1965, Vol. 4, No. 3, p. 861-870.

140. Kadota, T. T. and L. A. Shepp, On the best finite set of linear observables for discriminating two Gaussian signals. IEEE Transactions on Information Theory, 1967, Vol. 13, No. 2, p. 278-284.

141. Kailath, T., The divergence and Bhattacharyya distance measures in signal selection. IRE Transactions on Communication Technology, 1967, Vol. 15, No. 1, p. 52-60.

142. Kikuchi, K. and T. Kasai, Stereoscopic analysis of photographs by Nimbus II APT, J. Meteorol. Soc. of Japan, 1968, ser. II, Vol. 46, No. 1, p. 60-67.

143. Krueger, A. F. and S. Fritz, Cellular cloud patterns revealed by Tiros-1. Tellus, 1961, Vol. 13, No. 1, p. 1-8.

144. Leese, J. A., The role of advection in the formation of vortex cloud patterns. Tellus, 1962, Vol. 14, No. 4, p. 409-421.

145. Leese, J. A. and E. S. Epstein, Application of two-dimensional spectral analysis to the quantification of satellite cloud photographs, J. Appl. Meteorol., 1963, Vol. 2, No. 5, p. 317-341.

146. Leese, J. A., C. S. Novak, and B. B. Clark, An automated technique for obtaining cloud motion from geosynchronous satellite data using cross correlation, J. Appl. Meteorol., 1971, Vol. 10, No. 1, p. 118-132.

147. Lyons, W. A. and T. Fujita, Mesoscale motions in oceanic stratus as revealed by satellite, Monthly Weather Review, 1968, Vol. 96, No. 5, p. 304-314.

148. Malberg, H., Untersuchungen über die Auswertung von Satelliten-aufnahmen, insbesondere über die Abschätzung der troposphärischen Temperatur- Druck- and Feuchtigeverhältnisse [Investigations on analysis of satellite photographs, especially on the evaluation on troposphere temperature, pressure, and humidity relationships], Meteorol. Abhandlungen, 1969, Vol. 110, No. 2, 106 p.

149. Mancuso, R. L., An objective method for estimating wind-speed fields from wind-direction fields, QJRMS, 1970, Vol. 96, No. 410, p. 601-609.

150. Marill, T. and D. M. Green, On the effectiveness of receptors in recognition systems. IRE Transactions on Information Theory, 1963, Vol. 13, No. 1, p. 11-17.

151. Mattson, R. and J. E. Dammaun, A technique for determining and coding sub-classes in pattern recognition problems, IBM J. Research and Development, 1966, Vol. 9, No. 4, p. 410-426.

152. Maykut, E. S., An experiment in objective nephanalysis using proposed HRIR satellite infrared radiation data, J. Appl. Meteorol., 1964, Vol. 3, No. 3, p. 215-225.

153. McClain, E. P., On the relation of satellite-viewed cloud conditions to vertically integrated moisture fields, Monthly Weather Review, 1966, Vol. 94, No. 8, p. 509-514.

154. McClure, J. H., Motions in the upper troposphere as revealed by satellite-observed cirrus formations, MSL 39, Washington, 1966, 89 p.

155. McLean, G. S., Cloud distributions in the vicinity of jet streams, BAMS, 1957, Vol. 38, No. 10, p. 579-583.

156. Miller, F. R., An application of Tiros cloud observations in sparse data regions, Monthly Weather Review, 1963, Vol. 91, No. 9, p. 433-451.

157. Oliver, V. J., R. K. Anderson, and E. W. Ferguson, Some examples of the detection of jet streams from Tiros photographs, Monthly Weather Review, 1964, Vol. 92, No. 10, p. 441-448.

158. Oliver, V. J. and M. B. Oliver, Cloud patterns. Part I. Some aspects of the organization of cloud patterns, Monthly Weather Review, 1963, Vol. 91, No. 10-12, p. 621-629.

159. Peterson, D. W., Some convergence properties of a nearest neighbor decision rule. IEEE Transactions on Information Theory, 1970, Vol. 16, No. 1, p. 24-31. /129

160. Roy H. Blackmer and S. M. Serebreny, Analysis of maritime precipitation using radar data and satellite cloud photographs, J. Appl. Meteorol., 1968, Vol. 7, No. 1, p. 122-131.

161. Ruzecki, M. A., Use of satellite cloud photographs in numerical weather prediction, MSL report 23, Washington, 1963, 22 p.

162. Rao, P. K., Estimating cloud amount and height from satellite infrared radiation data. ESSA Technical report NESC 54, Washington,, 1970, 11 p.

163. Schwalb, A. and J. Gross, Vidicon data limitations. ESSA Technical Memorandum NESCTM 17, Washington, 1969, 22 p.

164. Senn, H. V. and P. J. Davies, Optical rectification and gridding of satellite photographs, J. Appl. Meteorol., 1966, Vol. 5, No. 3, p. 334-342.

165. Shenk, W. E., Meteorological satellite infrared view of cloud growth associated with the development of secondary cyclones, Monthly Weather Review, 1970, Vol. 98, No. 11, p. 861-868.

166. Shenk, W. E. and E. R. Kreins, A comparison between observed winds and cloud motions derived from satellite infrared measurements, J. Appl. Meteorol., 1970, Vol. 9, No. 4, p. 702-710.

167. Smigielski, F. J. and L. M. Mace, Estimating mean relative humidity from the surface to 500 millibars by use of satellite pictures. ESSA Technical Memorandum NESCTM 23, Washington, 1970, 13 p.

168. Spragins, J., Learning without a teacher. IEEE Transactions on Information Theory, 1966, Vol. 12, No. 2, p. 223-229.

169. Taylor, H., ATS-1 offers improvement in air safety, Technology Week, 1966, Vol. 19, No. 25, p. 14.

170. Taylor, V. R., Operational brightness normalization of ATS-1 cloud pictures. ESSA Technical Memorandum NESCTM 24, Washington, 1970, 15 p.

171. Timchalk, A. I., L. F. Hubert, and S. Fritz, Wind speeds from Tiros pictures of storms in the tropics, MSL report 38, Washington, 1965, 24 p.

172. Whitney, M. B., R. C. Doolitle, and B. Goddard, Processing and display experiments using digitized ATS-1 spin scan camera data. ESSA Technical report NESC 44, Washington, 1968, 60 p.

173. Whitney, L. F. and L. D. Herman, The nature of intermediate-scale cloud spirals. ESSA Technical report NESC 45, Washington, 1968, 69 p.

174. Whitney, L. F., A. Timchalk, and T. I. Gray, On locating jet streams from Tiros photographs, Monthly Weather Review, 1966, Vol. 94, No. 3, p. 127-138.

175. Winston, J. S., Global distribution of cloudiness and radiation for seasons as measured from weather satellites, Climate of the Free Atmosphere, Vol. III, World Survey of Climatology, Elsevier Publishing Co., Amst., p. 288-314.

☆ U.S. GOVERNMENT PRINTING OFFICE: 1975—635-048/56